TOWARDS INTRA-ARTICULAR APPLICATION OF BIOLOGICAL THERAPEUTICS FOR OSTEOARTHRITIS

Sohrab Khatab

TOWARDS INTRA-ARTICULAR APPLICATION OF BIOLOGICAL THERAPEUTICS FOR OSTEOARTHRITIS

Sohrab Khatab

Towards intra-articular application of biological therapeutics for osteoarthritis

Intra-articulaire toepasbaarheid van biotherapeutica voor artrose

Proefschrift

ter verkrijging van de graad van doctor aan de
Erasmus Universiteit Rotterdam
op gezag van de
rector magnificus

Prof.dr.ir. A.J. Schuit

en volgens besluit van het College voor Promoties.
De openbare verdediging zal plaatsvinden op

dinsdag 24 februari 2026 om 13.00 uur

door

Sohrab Khatab
geboren te Kabul, Afghanistan

Printing: Proefschriftspecialist | proefschriftspecialist.nl
Layout: Britt de Kroon, persoonlijkproefschrift.nl
Coverdesign: Sodaba Khatab

Financial support for publication and dissemination of this thesis was provided by:
• Department of Orthopedics, Erasmus MC University Medical Center, Rotterdam
• Nederlandse Orthopaedische Vereniging (NOV), 's Hertogenbosch
• Erasmus University Rotterdam, Rotterdam
• Sportskliniek, Admiraal de Ruyter Ziekenhuis

The research described in this thesis was financially supported by the Dutch Organisation for Science, division Applied and Engineering Sciences (technical foundation STW, grant number 12898).

Erasmus University Rotterdam

Promotiecommissie:

Promotor:	prof. dr. G.J.V.M. van Osch
Overige leden:	dr. M.J. Hoogduijn prof.dr. F. Jenner prof.dr. T. Gosens
Copromotoren:	dr. M.R. Bernsen dr. G.M. van Buul

Table of Contents

CHAPTER 1

General Introduction
Aim and outline of this thesis

Osteoarthritis

Osteoarthritis (OA) is a progressive disabling joint disease, in 2019 there were 528 million people living with osteoarthritis worldwide [1]. In 2021 over 1.5 million people suffered from OA in the Netherlands alone. The prevalence in women is higher than in men (1.8 : 1), with the hip and knee being the most affected joints. In 2019 the total medical costs for OA in the Netherlands were 1.1 billion euro, 1.1% of the total healthcare costs [2]. The prevalence of the disease - and with it the healthcare costs - is increasing. The prevalence increased by 123.2% in the last 30 years and is projected to double by 2050, mainly due to factors such as an aging population and the obesity endemic [2-4]. OA is characterised by loss of cartilage integrity, subchondral bone changes, formation of osteophytes and inflammation of the synovial membrane [5]. The interplay between these processes and tissues and their exact role in the etiology and progression of the disease is yet unclear. These processes together result in pain and functional disability, which are the main reasons for patients to seek medical treatment.

Yet, to this date, no curative treatment for OA exists. Current treatments mainly aim at alleviation of disease symptoms and do not provide a durable solution by modifying pathological osteoarthritic processes. Current therapeutic options include life-style changes, physical therapy, pain medication, injection therapy with for instance corticosteroids and – for end-stage OA – joint replacement. Since joint arthroplasties have a limited lifespan, the need for disease-modifying drugs or therapies is high. Ideally, such a therapy would inhibit or repair damage to the joint tissues and simultaneously reduce pain and disability.

Role of synovial inflammation in OA

To inhibit or even repair damage in the joint, one must have a better understanding of the etiology of OA. This is necessary to develop disease modifying osteoarthritis drugs (DMOADs) that target one or multiple pathological pathways. The more our knowledge expands on this matter, the more specific DMOADs we can aim to develop. It has become evident that OA pathology includes an inflammatory component [6]. Tumour necrosis factor (TNF)α and interleukin (IL)-1β are known to play a pivotal role in the etiology of OA [7]. Especially in post-traumatic joints there is a high concentration of proinflammatory cytokines, including, but not limited to TNFα and IL-1β, together with matrix metalloproteinases (MMPs) [8, 9]. Peak concentration is reached 24 hours after trauma, but even after a year, the concentration of inflammatory cytokines is higher than in normal knee joints [10]. Aside from direct damage to the joint, these increased levels of cytokines could play a pivotal role in the development of OA later in

life in a post-traumatic joint [11-13]. The inflammatory cytokines in OA can be produced by all tissues in the OA joint, including synovial membrane, cartilage and subchondral bone [14]. Synovial membrane inflammation is attributed to be a major feature of OA and it's progression [15-17]. This synovitis presents as thickening of the synovial membrane, and within this membrane an increased presence of immune cells such as macrophages [7, 18]. Macrophages have been demonstrated to play an important role in the mediation of synovial inflammation and pathophysiological changes of cartilage and bone, by producing cytokines (like IL-8 and IL-10) and MMPs [7, 18].

Once OA is developed, a situation with a persistent and chronic low grade inflammation establishes, which some compare with a chronic wound environment[19]. Unlike a normal wound healing process, where the inflammation caused by damage associated molecular patterns (DAMPs) is followed by regeneration and tissue modulation of the diseased site, in OA the inflammation persists. This causes a sustained imbalance in catabolic and anabolic processes, causing production of more DAMPs leading to more inflammation. Thus, causing an vicious cycle of inflammation and ongoing tissue destruction in this situation of disturbed joint homeostasis [18].

Although a certain amount of inflammation is essential to initiate tissue repair, problems arise when the level in inflammation gets out of control [20]. Balancing on this line of just the right amount of inflammation dosed at the right time, is an important challenge in tackling inflammation in OA. In the current symptomatic treatment of OA there is already a role for non-steroidal anti-inflammatory drugs (NSAIDs) and intra-articular injected steroids to counter synovial inflammation, hereby relieving the pain. Although short-term use of NSAID can temporarily improve pain and decrease the concentration of cytokines such as IL-6 and TNFα in knee OA, long term use is associated with gastro-intestinal problems and kidney failure [21, 22]. Similar to NSAIDs, intra articular injection of steroids can achieve short-term pain relief. They can, however, have a detrimental effect on cartilage and can accelerate the progression of OA on the long term [23].

Thus, to this day, no disease-modifying osteoarthritis drug (DMOAD), specifically countering the inflammatory pathway of OA, is on the market. Two promising therapeutic options with so-called biologicals with anti-inflammatory capacities are mesenchymal stromal/stem cells and platelet rich plasma.

Mesenchymal stromal/stem cells

Mesenchymal stromal/stem cells (MSC) were first introduced by A.I. Caplan in 1991. He described a group of cells, isolated from human bone marrow, with great proliferation and differentiation capacity. These cells could differentiate into multiple skeletal lineages, both *in vitro* and *in vivo*. Earning them the title of "stem cells". Mesenchymal was a reference to the mesoderm, which is the middle embryonic layer, and progenitor

of the body's skeletal elements [24]. In the following years the title stem cells was challenged and other names where proposed such as mesenchymal stromal cells (MSC) and medicinal signalling cells (MSC). Mostly because these cells can be isolated from almost every vascularized tissue in the human body and their multi-lineage differentiation potential appears of less importance in their working mechanism, than previously thought [25]. Independent of their nomenclature, MSC play a pivotal role in physiological tissue homeostasis, inflammation and regeneration after tissue injury [26].

Several (pre)clinical studies have shown promising results for intra-articular MSC injection as a treatment for OA [27-32]. Murphy *et al.* were the first to show amelioration of degenerative changes after intra-articular injection of bone marrow-derived MSC in a caprine OA model [29]. Others have found diminishment of OA-associated pain or synovial inflammation and cartilage degradation in pre-clinical studies [31, 32]. Initial reports from clinical studies have indicated that intra-articular application of MSC is safe for OA and possibly results in amelioration/improvement of clinical symptoms [27, 30].

Next to their potential to differentiate into several lineages, MSC can influence their (micro)environment by secreting trophic mediators [33-38]. Previously, it was demonstrated that although injection of MSC has beneficial effects, cells exhibiting a classic MSC profile are no longer detectable 3 to 4 weeks after intra-articular injection [39, 40] even more so when they had been systemically applied [41]. Thus, although long-term engraftment is very low, intra-articular injection of MSC can have a prolonged beneficial effect. This led Prockop (2009) and von Bahr *et al.* (2012) to postulate the 'hit-and-run' mechanism, in which MSC-secreted factors play an important role [36, 42]. They hypothesized that the main working mechanism of the MSC is not via their differentiation capacity, but due to their capacity to activate or inhibit endogenous cascades or cells, without the need of long term engraftment of the MSC themselves. Different studies have shown that MSC-secreted factors alone could possibly counteract inflammatory and catabolic processes and simultaneously attract endogenous repair cells in various pathological conditions [38, 43-45].

Thus, the MSC-secreted factors provide the interesting option of possibly basing future therapies on this secretome. There are two ways to harness this capacity. For one, we could prolong the local presence of MSC, enabling a prolonged interplay with the inflamed and/or diseased tissue and the MSC. This could lead to situation specific, tailored production of cytokines and growth factors by the MSC. Another way is to stimulate the MSC *in vitro* by exposing them to inflammatory factors, causing them to produce and secrete these cytokines and growth factors on a supra-physiological scale. Subsequently, this "secretome" can be harvested and made ready for amongst others intra articular injection.

MSC encapsulation in alginate

Cell encapsulation retains cells at the desired location by acting as a mechanical barrier for cell migration and additionally provides protection of the encapsulated cells against the host's immune system. The increased cell retention and cell survival can result in an enhanced therapeutic efficacy at the local site of the disease [46, 47]. Alginate is a polymer widely used in tissue engineering and drug delivery because of its biocompatibility, stability, non-antigenicity, and chelating ability [48, 49]. It can be processed into 3D structures for cell encapsulation. Besides providing a barrier for cells, alginate allows for the release of growth factors and cytokines produced by the encapsulated cells to the microenvironment and vice versa. Cytokines from the microenvironment can thus reach the encapsulated cells. This provides a setting for dynamic cross talk between cells and their environment [48, 50, 51]. Furthermore, by encapsulating cells in alginate, we may create a safer way for using allogeneic cells as an alternative to autologous grafts by shielding them from the host's immune system [52-54]. This could greatly enhance the clinical translatability of MSC-based therapies.

MSC-secretome

During homeostasis, MSC are quiescent and are only activated when needed. MSC are continuously communicating with their environment via cell-cell contact, cytokines and growth factors [45, 55, 56]. Under inflammatory conditions, with typically high concentrations of interferon γ (IFNγ), TNFα and interleukin 6 (IL-6), MSC respond by changing to their immunomodulatory function [56, 57]. *In vivo* activation of MSC is difficult to control or influence and, thereby, likely to be subject to large variability. *In vitro* stimulation of MSC with, for instance, inflammatory factors as TNF-α and IFN-γ, provides an option to further optimise the use of the MSC immunomodulatory abilities. Because MSC secretome is a cell free product it is likely to have less regulatory issues for clinical application and thus more practical, especially when using allogeneic MSC. Although generally considered immune-privileged, MSC do maintain a degree of immunogenicity [58]. And since the concentration of immune complexes in the secretome is lower than with cells, this could lead to a minimized host inflammatory response [57]. Thus the use of secreted factors of stimulated MSC, instead of the cells themselves, provides options to enhance standardisation, affordability and efficacy of this therapeutic approach. Therefore, the use of MSC secretome could improve MSC-based therapeutic efficacy and would greatly enhance the clinical applicability of this biological treatment as a true DMOAD.

Platelet rich plasma

Another option for biological therapy for tissue injury is platelet rich plasma (PRP). PRP is a plasma product extracted from whole blood that contains at least 1.0 ^{3} x 10^{6} platelets per microliter [59]. When the platelets undergo degranulation, they release cytokines and growth factors such as transforming growth factor b (TGF-B) and platelet-derived growth factor (PDGF), two important factors in tissue healing [59-61]. This activation of platelets can happen *in vivo* or *in vitro*. When PRP is activated *in vitro*, this results in PRP releasate (PRPr), a product without leukocytes, yet possessing high concentrations of growth factors [62].

From preclinical studies we know that PRP can promote the proliferation of cells derived from human synovium and cartilage and that PRP-treated chondrocytes repair cartilage better than nontreated chondrocytes in focal cartilage defects[63-65]. The anti-inflammatory effects of PRP have been demonstrated both in a co-culture system of osteoarthritic cartilage and synovium and in human osteoarthritic chondrocytes, where it reduced multiple proinflammatory processes induced by IL-1β [64, 66]. Several clinical trials in OA patients have led to the conclusion that multiple PRP injections are safe and have a beneficial effect for up to 12 months on OA symptoms, such as pain [67-72]. However, there is an ongoing discussion about the true efficacy of PRP [73, 74].

Although the use of PRP products seems promising for the treatment of OA, the wide variability in outcome parameters evaluated, as well as PRP and PRPr production protocols, makes interpretation of results between studies difficult [75-77]. This may be one of the reasons why the exact working mechanisms of intra-articular injected PRP products, and thus their effect on pain, cartilage damage and synovial inflammation, are not fully understood. Unravelling this mechanism, could provide an opportunity to further improve the therapeutic efficacy of PRP products.

Aim and outline of this thesis

Knowledge on the role of inflammation in the pathophysiology of OA is increasing. This knowledge about disease processes provides new options for intervention to tackle the development and progression of OA. As stated before, an anti-inflammatory therapy for OA would ideally reduce symptoms such as pain and simultaneously inhibit or repair cartilage damage.

The aim of this thesis is to investigate the use of paracrine factors of MSC and platelets, as a disease modifying therapy for osteoarthritis. To pursue the goal of developing an allogeneic off-the-shelf therapeutic. I have used either an approach in which the cells are encapsulated as an injectable therapeutic, or a cell free approach; this to minimize safety concerns and regulatory issues when using allogeneic cell sources and to increase clinical translatability.

The first objective is to improve the therapeutic efficacy of allogeneic MSC by prolonging their longevity *in vivo* after intra-articular injection. In **Chapter 2**, MSC are encapsulated in alginate beads to protect them for the host's immune system and to reduce migration out of the desired location, in this case the diseased OA joint. Although cell-cell contact is not possible, there is still an interplay via paracrine factors of the diseased joint and the encapsulated MSC. The integrity of the MSC-alginate beads *in vivo* is followed non-invasively with magnetic resonance imaging (MRI) and the longevity of the MSC with bioluminescence imaging (BLI). In this chapter the therapeutic efficacy of these MSC-alginate beads in osteoarthritic rat joints is also evaluated, by assessing their effects on pain, synovial inflammation, and cartilage damage.

To develop a true cell-free biological therapeutic, the therapeutic capacity of MSC secretome is examined in **Chapter 3**. We stimulated MSC *in vitro* with pro-inflammatory cytokines to induce the production of paracrine anti-inflammatory factors, after which the MSC secretome was injected intra-articularly in a murine knee OA model. Outcome parameters such as synovial inflammation, but also subchondral bone alterations, cartilage damage and pain were assessed. In an effort to improve the translatability of the MSC-secretome as a potential therapeutic for OA, a bigger animal model is used in **Chapter 4.** This equine LPS-induced inflammation model is used to examine the possible anti-inflammatory capacity of MSC secretome. Clinical outcome parameters such as joint effusion and lameness are assessed, together with synovial fluid analysis and joint histology.

The promising results from MSC-derived paracrine factors, aroused my interest in platelets as a possible source of paracrine factors with possible anti-inflammatory effects. Platelets are easier to attain, and do not need extensive culture procedures. PRP, a plasma product with high concentration of platelets, can be activated *in vitro*

with use of $CaCl_2$. This causes the platelets to burst and release their paracrine factors. This PRPr can be harvested for further use as a cell free product. In **Chapter 5**, I study the anti-inflammatory therapeutic effect of PRPr in a murine OA model. Outcome parameters such as synovial inflammation, presence of macrophage subtypes as well as pain and cartilage damage are assessed.

In **Chapters 6 and 7**, I discuss and summarize my findings and provide potential directions for future research aimed at improving the paracrine based anti-inflammatory biological therapeutics and their translation to human clinical studies as true disease modifying osteoarthritis drugs (DMOADs).

CHAPTER 2

MSC encapsulation prolongs MSC survival after intra-articular injection in a rat OA model

Published as:

MSC encapsulation in alginate microcapsules prolongs survival after intra-articular injection, a longitudinal in vivo cell and bead integrity tracking study

Sohrab Khatab, Maarten J. Leijs, Gerben van Buul, Joost Haeck, Nicole Kops, Michael Nieboer, P. Koen Bos, Jan A.N. Verhaar, Monique Bernsen, Gerjo J.V.M. van Osch

in Cell Biology and Toxicology, 2020

Sohrab Khatab designed and conducted the experiments, performed data collection and analysis and drafted, edited and reviewed the manuscript.

Abstract

Mesenchymal Stem Cells (MSC) are promising candidates for use as a biological therapeutic. Since locally injected MSC disappear within a few weeks, we hypothesize that efficacy of MSC can be enhanced by prolonging their presence. Previously, encapsulation in alginate was suggested a suitable approach for this purpose. Using alginate high in mannuronic acid (High M) and alginate high in guluronic acid (High G), we found no differences between the two alginate types regarding MSC viability, MSC immunomodulatory capability or retention of capsule integrity after subcutaneous implantation in immune competent rats. High G proved to be more suitable for production of injectable beads. Firefly luciferase-expressing rat MSC were used to track MSC viability. Encapsulation in high G alginate prolonged the presence of metabolically active allogenic MSC in immune competent rats with monoiodoacetate induced osteoarthritis for at least 8 weeks. Encapsulation of human MSC for local treatment by intra-articular injection did not significantly influence the effect on pain, synovial inflammation or cartilage damage in this disease model. MSC encapsulation in alginate allows for an injectable approach which prolongs the presence of viable cells subcutaneously or in an osteoarthritic joint. Further fine tuning of alginate formulation and effective dosage for might be required in order to improve therapeutic efficacy depending on the target disease.

Statement of Significance

We describe the evaluation of a method to encapsulate human mesenchymal stem cells in small, injectable hydrogel beads. Alginate hydrogel is used as a carrier and protective barrier for stem cells, thus improving the therapeutic use of (allogeneic) stem cells — based on their known capacity to secrete factors that modulate the diseased environment. The work contains extensive *in vitro* and *in vivo* evaluations of survival and functionality of the encapsulated cells. With a novel *in vivo* imaging approach we longitudinally followed the fate of the beads. Next to their use in osteoarthritis, which we evaluated in our final tests, this can be used for other local degenerative diseases such as myocardial infarction, macular degeneration or diabetic ulcers.

Introduction

Application of Mesenchymal Stem Cells (MSC) is promising due to their ability to influence their (micro) environment by secreting trophic mediators [33-38]. These secreted factors have been demonstrated to counteract inflammatory and catabolic processes and attract endogenous repair cells in various pathological conditions [38, 43-45]. MSC secreted factors have been shown to improve cardiac function after myocardial infarction in pigs [38], ischemia in mice [78] and reduce pain in a murine osteoarthritis (OA) model [79]. Previously it was demonstrated that although injection of MSC has beneficial effects, the MSC themselves are no longer detectable 3 weeks after intra-articular injection [39, 40]. We hypothesize that the efficacy of MSC can be enhanced by prolonging their local presence by enabling longevity through encapsulation in a biomaterial.

Alginate is widely used in tissue engineering and drug delivery, because of its biocompatibility, stability, non-antigenicity and chelating ability (Reviewed in [48, 49]). This commonly used gel for cell encapsulation provides protection of the encapsulated cells against the host's immune system and at the same time retains cells at the desired location, by acting as a mechanical barrier. The increased cell retention and cell survival can result in an enhanced therapeutic efficacy at the local site of the disease [46, 47]. Besides providing a barrier for cells, alginate allows for the release of growth factors and cytokines produced by the encapsulated cells to the microenvironment and vice versa. Cytokines from the microenvironment can reach the encapsulated cells. This provides a setting for dynamic cross talk between cells and their environment [48, 50, 51]. Furthermore, by encapsulating cells in alginate, we may create a safer way for using allogeneic cells as an alternative to autologous grafts by shielding them from the host's immune system [52-54]. This would greatly enhance the clinical translatability of MSC-based therapies. We have previously shown that allogenic MSC encapsulated in alginate could survive locally after subcutaneous implantation *in vivo* and could act as an interactive immunomodulatory release system for at least 5 weeks *in vitro*, hereby emphasizing the possible advantages of this approach [52].

The variety in composition and production methods of different alginates has a major effect on its biocompatibility, stability, non-antigenicity and chelating ability [49]. Therefore, the first objective of this work was to find the most suitable clinical grade alginate for MSC encapsulation to enable their longevity *in vivo*, while maintaining anti-inflammatory and tissue modulating capacities. Alginate consists of a combination of β-D-mannuronic acid and α-L-guluronic acid. We compared two alginates, one consisting of a high concentration of β-D-mannuronic acid (High M alginate) and the other with high concentration of α-L-guluronic acid (High G alginate). The alginates were evaluated regarding their effect on cell survival, preservation of

immunomodulatory function of the MSC and histocompatibility using a set of *in vitro* assays and *in vivo* tests. One alginate formulation was selected to reproducibly produce small beads of injectable size. Then, we tested the prolonged presence of MSC and alginate microcapsules as well as their therapeutic efficacy in a local disease model.

Injection of MSC has been shown to diminish several features of osteoarthritis (OA) in pre-clinical and some initial clinical studies [28, 29, 32, 80-82]. OA is a degenerative disabling joint disease, characterized by loss of cartilage integrity, subchondral bone changes, formation of osteophytes and inflammation of the synovial membrane [83]. Unfortunately to this date, no curative treatment for OA exists, while OA is a growing problem in society, already affecting over 10% of individuals aged 60 years or older [83]. We evaluated whether encapsulation in alginate could prolong the local presence of allogeneic MSC in an immunocompetent rat OA model, using longitudinal bioluminescence imaging (BLI) and we followed the structural integrity of the alginate beads after injection in the knee of rats via longitudinal MRI. Since pain and functional disability are the main reasons for patients to seek medical treatment, we evaluated the efficacy of encapsulation of MSC in alginate beads to reduce pain as well as cartilage damage and synovial inflammation in a rat model of OA.

Materials and methods

Expansion of rat and human mesenchymal stem cells

Allogeneic rat MSC (rMSC) were used for cell tracking experiments *in vivo*. rMSC were isolated (with ethical approval under animal ethical # EMC 116-12-08) from three to four months old male Lewis rats (Janvier labs) as described elsewhere and expanded up to passage 3 [84], to be used for subcutaneous *in vivo* experiments. For *in vivo* cell tracking experiment in the joint we used allogeneic F344 rat MSC (Millipore, Billerica, MA) that were transduced to express firefly luciferase (r(Fluc)MSCs) as described before. [85, 86].

Human bone marrow MSC (hMSC) were used to evaluate therapeutic efficacy *in vitro* and *in vivo*. Cells were derived from 6 patients undergoing total hip replacement (mean age 49 ±11.2 years; F:M ratio 1:1) by needle aspiration after written informed consent and approval by the medical ethical committee (Erasmus MC protocol METC-2004-142 and Albert Schweizer Hospital protocol 2011-07). Bone marrow cells were plated at 50,000 cells/cm^2 and after 24 hours flasks were washed to remove non-adherent cells and cells were further cultured and expanded as described below for a maximum of 4 passages.

For cell expansion, both rat and human MSC were seeded at a density of 2300 cells/cm^2 in cell culturing flasks, in expansion medium consisting of Minimal Essential Medium Alpha (αMem; Gibco, Rockville, USA), 10% heat-inactivated Fetal Calf Serum

(FCS; Gibco, Rockville, USA), 1.5 µg/mL fungizone (Invitrogen, Carlsbad, USA), 50 µg/mL gentamicin (Invitrogen, Carlsbad, USA), 25 µg/mL ascorbic acid-2-phosphate (Sigma-Aldrich, Saint Louis, USA) and 1 ng/mL Fibroblast Growth Factor 2 (FGF2; AbD Serotec, Oxford, U.K.). Cells were cultured in an incubator at 37°C, 5% CO2 and 90% humidity. Medium was renewed twice a week. When MSCs were approximately 70% confluent they were passaged by trypsinisation of cells with a 0.25% trypsin/EDTA solution (Life Technologies, Waltham, USA).

Preparation of MSC-alginate constructs

Clinical grade High mannuronate (M) alginate *(L. Pallida)* and High guluronate (G) alginate *(L. Hyperborean)* (respectively; Lot # E01 AAL-070912 and Lot # C01 AAL-110808 both kind gifts of BTG/CellMed AG, Alzenau, Germany) were used. Both alginates were diluted in a 0.5%, 1.1% and 2.5% concentration in NaCl 0.9% and filter-sterilized afterwards. The shear-dependent viscosity of the solutions was measured by a rheometer Physica MCR301 (Anton Paar GmbH, Ostfildern, Germany) at room temperature (20 ^{0}C). The viscosity was measured in a shear rate range of 1-5000 s-1 by increasing the shear rate each 5 seconds for a duration of 2 min and 45 sec. Data were analysed with Rheoplus Software version 3.4 (Anton Paar GmbH, Ostfildern, Germany). For 1.1% High M alginate the low-shear viscosity at 20 ^{0}C was found to be 1,320 mPa*s and for 1.1% High G alginate the low-shear viscosity at 20 ^{0}C was 274 mPa*s. The effect of shear stress on the viscosity was similar for both alginates.

Prior to encapsulation, MSC were washed with saline. A homogeneous solution of 4.0x10^6 MSC per 1 ml filter-sterilized 1.1% High M alginate or 1.1% High G alginate was prepared. This cell density was selected after a series of tests comparing 0.4, 4 and 20 million cells per ml, indicating that 4 million cells/ml was the most efficient cell number in terms of cell viability and immunomodulatory properties during 2 weeks encapsulation in alginate *in vitro* (data not shown).

Beads of approximately 2 mm in diameter were created by manually dripping the MSC-alginate mixture through a 23 gauge needle in a 102 mM $CaCl_2$ solution for 10 minutes. After incubation, beads were washed two times for 5 min with saline before further use in *in vitro* experiments.

For subcutaneous implantation, alginate disks were created by polymerisation of the rMSC-alginate solution took place in a sterilized, custom-designed mold consisting of two durapore membranes (5 µm pore size, Millipore) at both sides of a 3 mm thick metal ring [87]. After 30 min in 102 mM $CaCl_2$ the construct was washed two times in saline and 8 mm diameter constructs were made with sterile dermal punches (Spengler, Hannover, Germany).

To produce smaller beads in a more reproducible way, we used the Buchi Encapsulator B-395 Pro (Buchi Labortechnik AG, Flawil, Switzerland). After optimizing

the settings, beads of approximately 300 µm in diameter were made from 1.1% High G alginate with the following machine settings: flow rate 3 mL/min, nozzle size 150 um, frequency 1600 Hz, voltage 730 V, stir-rate 30% speed. To be able to track the alginate beads using MRI *in vivo*, we solidified the alginate solution with 102 mM $CaCl_2$ with 20 mM Gadolinium(III) chloride hexahydrate (Lot #MKBJ3153V, Sigma-Aldrich, St. Louis, USA). Beads were kept in this solution for 10 minutes, then washed twice with saline solution, and kept for a maximum of 4 hours in saline prior to injection.

In vitro characterisation of MSC-alginate constructs

Three hMSC-alginate beads were placed in 24 well plates in 900 ul of medium consisting of αMem with fungizone (1.5 µg/mL), gentamicin (50 µg/mL), 1% Insulin-Transferrin-Selenium (ITS; Biosciences, New Jersey, USA) and 0.1 mM vitamin C (Sigma, St. Louis, MO). Medium was refreshed twice a week. Beads were harvested directly after encapsulation and washing with saline (T=0), after one week (T=1) and two weeks of culture (T=2) to determine cell viability and immunomodulatory capacity.

Cell viability

Survival of encapsulated hMSC was measured by the amount of DNA and LIVE/DEAD® assay at T=0 and T=2 weeks (using cells from 2 different bone marrow donors). For DNA analyses, six beads were harvested at each time point and dissolved in 150 µl/bead. Sodium-citrate buffer (150 mM NaCl (Sigma-Aldrich, St. Louis, USA), 55 mM Na-citrate (Sigma-Aldrich), 20 mM EDTA (Sigma-Aldrich)) for half an hour at 4°C. Samples were centrifuged at 180xG for 8 min and pellets were stored at -80°C. Standard curves were made with DNA of hMSC of the same donor before encapsulation. DNA was determined with the CyQUANT® Cell Proliferation Assay Kit (Invitrogen, Carlsbad, CA, USA) following the manufacturer's instructions. The fluorescence measurements were performed on a microplate reader with excitation at 480 nm and emission detection at 520 nm (Spectramax Gemini, Molecular Devices, Sunnyvale, CA, USA).

LIVE/DEAD® assay (Invitrogen, Carlsbad, CA, USA) was performed by incubating MSC-alginate beads for 30 minutes in 100 µl labelling solution with 1.0 µl/ml green-fluorescent calcein-AM and 1.5 µl/ml red fluorescent ethidium homodimer-1, at 37°C. Z-stacks were made using an Axiovert 200 MOT fluorescent microscope (Carl Zeiss microscopy, Thornwood, NY, USA) with a thickness of 200 µm per slide. Viable and dead cells were counted in two Z-stacks on two areas of 0.25 mm^2 per z-stack using ImageJ 1.48 (Java, Redwood Shores, California, United States).

Immunomodulatory capacity

First, immunomodulatory capacity of the encapsulated hMSC (using cells from 2 different bone marrow donors) was determined by measuring interleukin-6 (IL-6)

protein levels and IDO activity. After two weeks of culture hMSC were stimulated with 50 ng/ml IFNγ and 50 ng/ml TNFα (Peprotech, Londen, UK). For control, medium without IFNγ and TNFα was added to encapsulated hMSC. After 24 hours, conditioned medium was harvested and stored at -80°C until analyses. IL-6 levels in the stimulated and non-stimulated hMSC conditioned media were measured by ELISA (R&D systems, Abingdon, UK) according to the manufacturer's instructions. IDO activity was determined in the stimulated and non-stimulated MSC conditioned media by the level of its metabolite L-kynurenine. This was measured spectrophotometrically as described previously [88].

The immunosuppressive capacity of encapsulated hMSC was determined in a co-culture with activated lymphocytes. The MSC-Alginate beads (using MSC from 1 bone marrow donor) were cultured for 2 days and 29 days and then were stimulated with 50 ng/ml IFNγ and 50 ng/ml TNFα for 24 h. The MSC-alginate beads were washed two times with saline and 4, 2 or 1 bead (approx. $3.0x10^4$ hMSC per bead) was transferred in a 48-wells plate to obtain a 1:2.5, 1:5 and 1:10 MSC/peripheral blood mononuclear cells (PBMCs) ratio. PBMCs were isolated with Ficoll-Paque™ PLUS (density 1.077 g/ml; GE Healthcare, Uppsala, Sweden) from buffy coats of healthy blood donors (Sanquin, Rotterdam, The Netherlands) and frozen at -150 ^{0}C until further use. $1.0x10^6$ PBMCs/ml were labelled with 1 µM carboxyfluorescein succinimidyl ester (CFSE) and activated with antibodies against CD3 and CD28 (1 µl per $1x10^6$ cells in 1 ml, BD Biosciences). As positive and negative lymphocyte proliferation control, activated and non-activated CFSE-PBMCs were used. As a positive control for immunomodulatory capacity of hMSC, 1.2×10^5 hMSC in monolayer were used. After five days of co-culture, PBMCs were retrieved, incubated with CD4 (APC-A; BD Biosciences) and CD8 (PE-CY7-A; BD Biosciences). Proliferation was determined from dilution of CFSE (FITC) staining using 8 colors FACSCANTO-II with FACSDIVA Software (BD Biosciences) and FlowJo Software (Tree Star Inc. Palo Alto, CA).

Animal experiments

We performed three separate animal experiments to assess influence of MSC encapsulation on cell longevity and effect of encapsulation on treatment efficacy. These experiments were carried out in accordance with the EU Directive 2010/63/EU for animal experiments. First we implanted rMSC-alginate (High G and High M) constructs subcutaneously in rats to asses construct integrity and rMSC survival *in vivo* (Experiment A, Figure 1). In the second *in vivo* experiment we moved to the joint and traced intra-articularly injected r(Fluc)MSC and r(Fluc)MSC-alginate High G beads crosslinked in the presence of Gadolinium, over time to prove that we can prolong the presence of rMSC at the desired location (Experiment B, Figure 1). In the third experiment we studied the therapeutic efficacy of intra-articularly injected hMSC

either free or encapsulated in beads (Experiment C, Figure 1). All experiments are explained in further detail below. All experiments were performed on 16 weeks old, male Wistar rats, weighing 250-300 gram (Harlan Netherlands BV, The Netherlands), with approval of the animal ethics committee (protocol # EMC116-15-02). Rats were housed in groups of two per cage, under 12 hours light-dark cycle at a temperature of 24°C degrees Celsius, and had access to water and food ad libitum at the animal testing facilities of the Erasmus MC, University Medical Center. Before the start of the experiments, rats were allowed to acclimatize for a week. All procedures involving subcutaneous implantations, intra-articular injections or scanning were applied under 2.5% isoflurane anesthesia.

The constructs of High G alginate and High M alginate with rMSC were placed in saline and subcutaneously implanted on the back of three rats. Each rat received two constructs of High G alginate with rMSC and one without cells and two constructs of High M alginate with rMSC and one without cells. Directly and 12 hours after the operation the rat got a subcutaneous injection with buprenorphine (Temgesic) 0.01 mg/kg bodyweight. To track the subcutaneously implanted rMSC, they were labelled one day prior to encapsulation in alginate with superparamagnetic iron oxide (SPIO) using ferumoxides 100 ug/mL medium (Endorem™, Guerbet S.A., Paris, France) complexed to protamine sulphate 5 ug/mL medium (LEO Pharma N.V., Wilrijk, Belgium) as described previously [89]. Imaging of the MSC constructs was done by MR imaging directly after implantation and thereafter weekly up to 5 weeks. Five weeks after implantation the rats were euthanized. The subcutaneous implantation regions were harvested, fixed in 0.05 M Tris buffered saline with 10 % formalin and 15 mM CaCl for 24 h and embedded in paraffin.

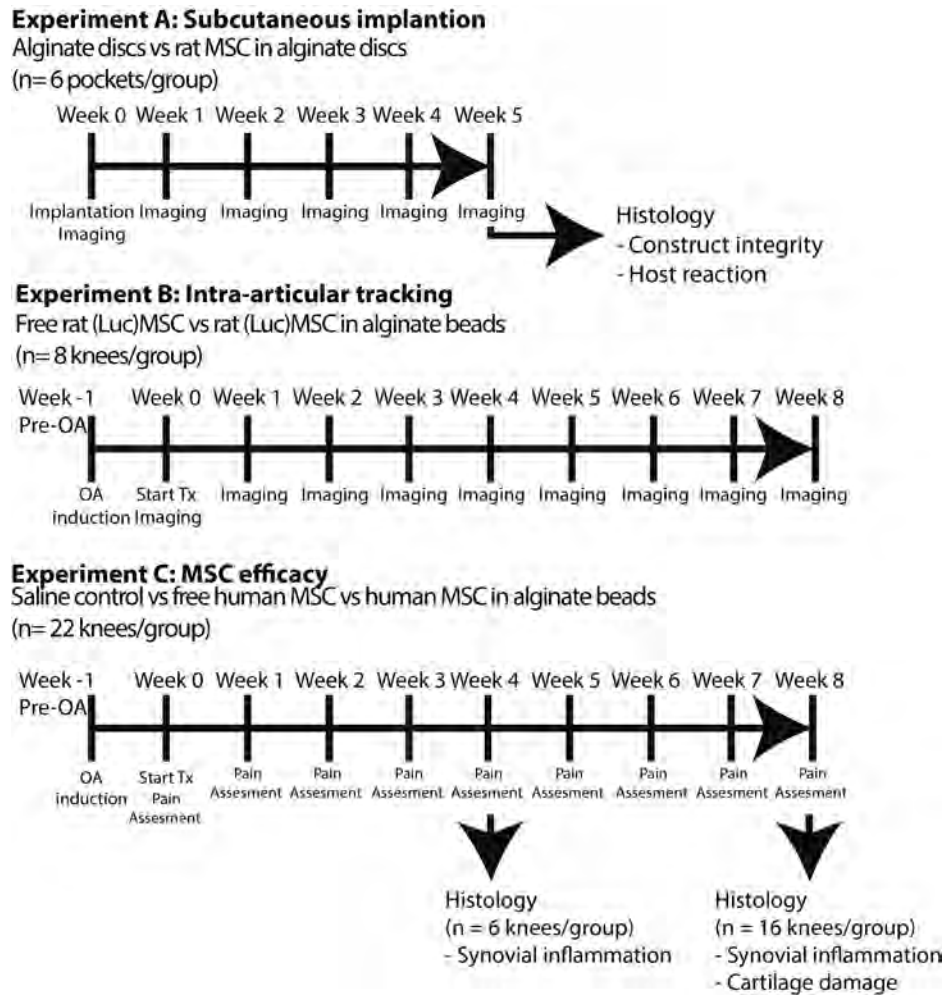

Subcutaneous implantation

Figure 1. Experimental set up of in vivo experiments to evaluate the effect of encapsulation of MSC in alginate on cell viability and efficacy to treat OA

In experiment A, rMSC-alginate constructs and empty alginate constructs were implanted subcutaneously in rats to asses construct integrity and MSC survival *in vivo*. In experiment B, longevity of MSC in an OA knee joint was tested using allogenic r(Fluc)MSC either free or encapsulated in alginate beads. Weekly imaging with MRI for construct integrity and BLI for cell viability followed till the end of the experiment at week 8. In experiment C, the therapeutic efficacy of hMSC in an OA knee joint was studied. hMSC were injected intra-articularly either free or encapsulated in alginate beads and compared to saline control. The effect on pain was measured weekly and knees were harvested for histology at week 4 (synovial inflammation) and week 8 (synovial inflammation and cartilage damage).

Intra-articular hMSC efficacy experiment

Bilateral OA was induced as described above. One week after OA induction (referred to as day 0), rats were randomly divided into three treatment groups, rats received in both knees the same treatment, except one animal which received free hMSC in one knee and saline control in the contra-lateral knee resulting in three groups: A. Saline control (n=19) B. 1.0 x10^5 freely injected hMSC (n=19); and C. 0.8 x 10^5 ±0.1 x 10^5 hMSC encapsulated in alginate beads (n=22). MSC from 3 human donors were pooled to take into account the inter-donor variability. Four weeks after treatment, the animals were euthanized to assess the effects of our treatments on synovial inflammation and knee joints were prepared for histological evaluation (n=6 knees/group). The remaining animals were euthanized week 8 after start of treatment and knee joints were harvested for histological analysis (n=16 knees/group). In the latter group, pain was evaluated weekly with mechanical allodynia tests (method see below).

Imaging

Bioluminescence Imaging (BLI)

To evaluate the presence of living cells over time, luciferase activity of injected r(Fluc)-MSC was measured using the Xenogen IVIS Spectrum (PerkinElmer, Hopkington, MA), 15 min after intra-peritoneal injection of 50 µg Beetle luciferin in 150 µL saline (Promega Benelux B.V., Leiden, the Netherlands). Optical intensity is reported as arbitrary units. Data were analyzed using the software Living Image version 3.2 (Caliper LS).

Magnetic Resonance Imaging (MRI)

MR imaging was performed on a preclinical 7.0T MRI scanner (MR 901 Discovery, Agilent/GE Healthcare, Milwaukee, Wisconsin). For imaging SPIO labelled rMSC, a 72 mm transmit/receive body coil was used. Image acquisition was performed using a fast spoiled gradient echo sequence with the following parameter settings: TE/TR= 1.1/7.3 ms, NEX= 4, FOV 8x6 cm2, acquisition matrix 256x192, slice thickness = 1 mm, bandwidth = 60 kHz, flip angle= 0150. Sagittal and coronal scans were performed to localize the hypo-intense SPIO deposits.

For intra-articular localization of alginate beads and to follow up the presence of these beads *in vivo* we used gadolinium in the alginate beads and scanned with a 150 mm body coil for transmission, and a four-channel cardiac coil (Rapid Biomededical GmbH, Rimpar, Germany) for signal reception. A 3D - fast spoiled gradient echo sequence was used to scan the injected rat knees (TE/TR 10.0/30.0 ms, NEX 2, FOV 6.00 x 4.50 cm2, acquisition matrix 512 x 512, Slice thickness 0.50 mm, Bandwidth 31.25 kHz, Flipangle 16°). The number of beads per knee was counted manually using the built-

in dicom viewer on the scanner (Software build 1094.1, General Electric Healthcare, Milwaukee, Wisconsin).

Pain assessment

Hind paw withdrawal reflex was measured with von Frey filaments (Bioseb, France) as an indicator of pain [90]. Animals were habituated to measuring cages and handling by the examiner starting two weeks prior to OA induction. The hind paws of the rats were stimulated using a series of von Frey filaments, increasing in strength starting at 0.2 grams to a maximum of 26 grams. If the paw was withdrawn after the administration of the von Frey filament for a minimum of 4/5 times, the strength of the filament was noted. If no reaction was seen after 5 attempts, for a maximum of 3 seconds each, a stronger filament was used, until a response was measured. A baseline measurement was performed after the rats were habituated and just before OA induction. Follow up measurements were performed 7 days after OA induction, which was just before therapy administration, and thereafter once weekly till the end of the experiment at 8 weeks. All measurements were performed by the same examiner, blinded for the treatment groups, in the same room, with temperature set at 18-20 degrees Celsius and the same background noises present at time of measurement. Measurements were performed at the same time of day.

Histology

Evaluation of subcutaneously implanted MSC-alginate constructs

6 µm paraffin sections were deparaffinised and stained for Perls' iron according to the manufacturer's protocol (Klinipath BVBA, Duiven, The Netherlands) to locate the SPIO-rMSC. SPIO- labeled rMSC which stain blue with Perls'. CD68 and CD3 staining was performed to identify macrophages and T lymphocytes as an indication of a local inflammatory response. Antigen retrieval for CD68 and CD3 was performed through incubation in citrate buffer (10 mM citric acid, 0.05 % Tween 20, pH 6.0) for 20 minutes at 90-95 ^{0}C. Sections were incubated for one hour with primary antibodies for CD68 (BM4000 5 ug/mL; OriGene Technologies, Herford) or CD3 (Ab16669, dilution 1:100; Abcam Cambridge, UK) diluted in PBS/1 %BSA (Sigma #A7284) after blocking of non-specific binding sites with 10 % goat serum (Southern Biotech #0060-01) in PBS/1%BSA. A secondary antibody biotinylated goat-anti-mouse 1:50 (Biogenex, HK-325-UM) was used, followed by incubation with streptavidin-AP 1:50 (Biogenex, HK-321-UK). Staining was then visualized using an alkaline-phosphatase substrate followed by counterstaining with haematoxylin.

Evaluation of knee joints after MSC-alginate bead injection

Knees were fixed in formalin 4% (v/v) for one week, decalcified in 10% EDTA for 2 weeks and embedded in paraffin and coronal sections of 6 µm were cut. Sections were collected anterior to posterior every 300 µm to give a good overview of the damage throughout the entire knee. Cartilage damage was evaluated on Safranin O-stained sections, with a scoring system described by Pritzker *et al.* [91]. Scoring was done on three sections aiming around the mid portion of the joint. The Pritzker score ranges from 0-6 for structural damage and 0-4 for GAG-staining intensity. These scores were multiplied with a factor 1-4 to account for the percentage of surface affected (factor 1= 0-25%, 2=26-50%, 3=51-75% and 4=76-100% surface area). This led to a maximum score of 24 for structural damage and a maximum of 16 for GAG loss, as described previously by van Buul *et al.* [85] The scoring of two blinded observers was averaged and used for data analyses.

Synovial inflammation was evaluated on sections stained with hematoxylin eosin. The sections were imaged using NanoZoomer Digital Pathology program (Hamamatsu Photonics, Herrsching am Ammersee, Germany) and synovial thickness was measured from the capsule to the superficial layer of the synovial membrane in the parapatellar recesses at the medial and the lateral side at three positions per section, as previously described [79, 92]. These measurements were performed on three sections per knee, with 300 µm between the sections. The thickness measurements were averaged to obtain a single value per knee joint.

Statistical Analysis

Data was analyzed with IBM SPSS statistics 24 *(SPSS, Chicago, IL)*. . To evaluate the *in vitro* data of DNA, live/dead cell count, IL-6 secretion, IDO activity and lymphocyte proliferation of MSC alginate beads, Mann-Whitney U tests were performed. To evaluate the number of alginate beads on MRI scans of rat joints over time, a Wilcoxon Signed Ranks Test was performed, since data did not met requirement for normality with the Shapiro-Wilk test. To compare fluorescence intensity of r(Flu)MSCs in the free MSC group versus the MSC-alginate group, a Mann-Whitney U test was performed, since data did not met the requirement of equal distribution and normality with the Shapiro-Wilk test. To evaluate the fluorescence intensity within groups over time, a Wilcoxon signed ranks test was performed. For treatment effects on pain, all groups were compared using a linear mixed model in which measurement time point and treatment were considered fixed factors and withdrawal threshold a dependent factor. After significance was confirmed, a One-way ANOVA was performed to determine differences between groups. To determine differences over time per treatment, a linear mixed model analysis was performed in which measurement time point was

considered a fixed and withdrawal threshold a dependent factor. Post-hoc analysis using Bonferroni correction was performed.

For synovial inflammation, homogeneity of variances and normality was confirmed with a Shapiro-Wilk test and a One-way ANOVA was performed, post-hoc analyses were performed by Bonferroni correction was applied.

For non-parametric cartilage scoring data, Mann-Whitney U tests were used to assess MIA or measurement time point effects. Kruskal Wallis tests were used for treatment effects within time points. Post-hoc analyses were performed by Bonferroni correction. For all tests, *P* values <0.05 were considered statistically significant.

Results

MSC remain viable and immunomodulatory active in both clinical grade High M alginate and High G alginate

The amount of DNA measured in the beads after two weeks was 45.4% in High M alginate (p=0.01) and 57.4%% in High G alginate (p=0.04) of the amount at the moment of encapsulation (Figure 2A). No significant difference was found in the amount of DNA between High M alginate or high G alginate constructs. The number of viable cells was not significantly different between High M and High G alginate directly after encapsulation or after 2 weeks in culture (Figure 2B).

hMSC encapsulated in either alginate retained their immunomodulatory capacities when stimulated with IFNγ and TNFα. This stimulation induced IL-6 secretion (Figure 2C) and IDO activity (Figure 1D) from the encapsulated MSC irrespective of the type of alginate used. Alginate-encapsulated hMSC significantly inhibited proliferation of stimulated CD4+ and CD8+ T lymphocytes. Three days after encapsulation hMSC encapsulated in High G and High M alginate (Figure 2E&F) significantly inhibit T lymphocyte proliferation in a dose dependent manner (all p=0.024). Thirty days after encapsulation, inhibition was reduced but in particular still present in High G alginate when four and two beads were used (p=0.024) (Figure 2F). Empty constructs of alginate had no effect on T-cell proliferation. The inhibition by 1.2×10^5 hMSC in monolayer was similar to the inhibition of 4 alginate constructs, containing a similar number of MSC on day 0.

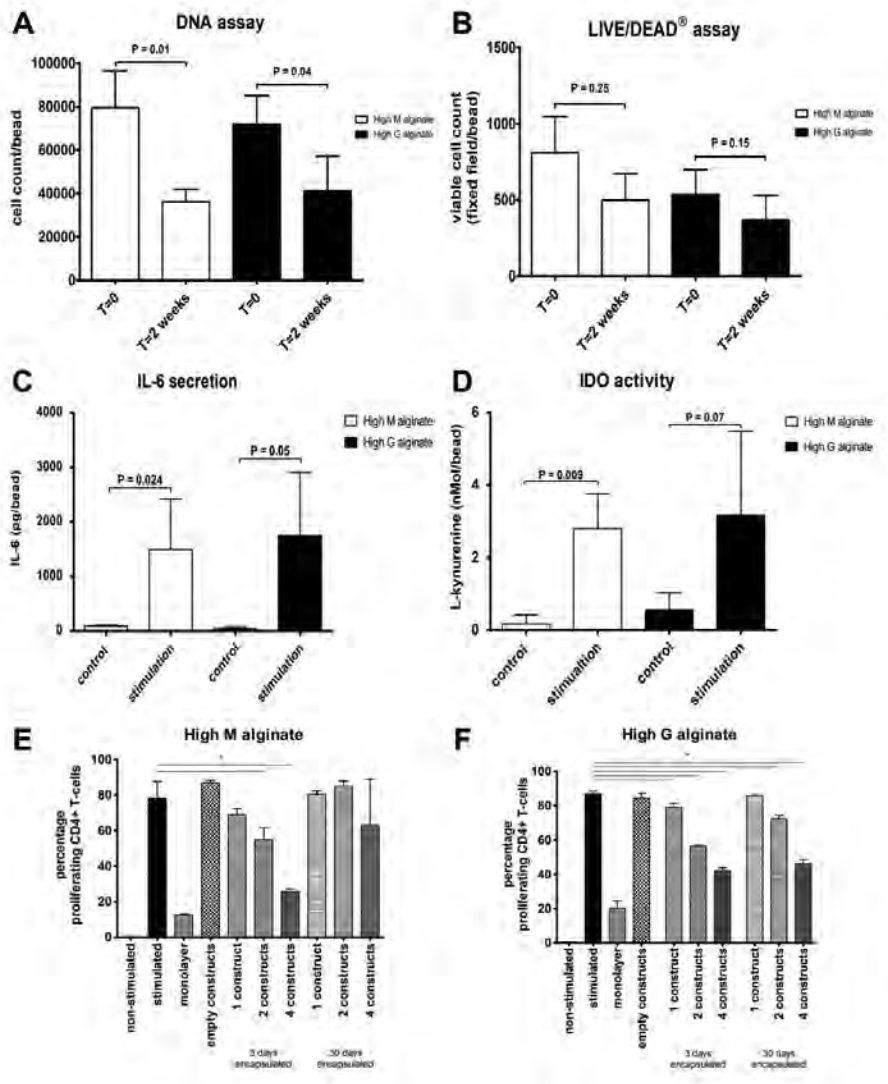

Figure 2. Viability and immunomodulatory capacity of encapsulated MSC in High G alginate and High M alginate.

(A) DNA amount directly after encapsulation or after two weeks (**B**) number of viable cells directly after encapsulation and after two weeks. (**C**) IL-6 secretion and (**D**) IDO activity measured as concentration of l-kynurenine in the medium after stimulation with IFNγ/TNFα (a-d all performed with hMSC of 2 different donors with 3 samples per donor).

Activated CD4+/CD8+ T lymphocytes co-cultured with one, two and four hMSC-alginate constructs with (**E**) High M or (**F**) High G alginate, 3 d and 30 d after encapsulation of hMSC (performed in triplicate with samples of 1 hMSC donor and 1 PBMC donor). First bar: non-stimulated PBMCs; positive control: Second bar: stimulated PBMCs without alginate constructs; Third bar: stimulated PBMCs in presence of 1.2×10^5 hMSC in monolayer; Fourth bar: stimulated PBMCs in presence of empty alginate constructs.

Mean ± SD is shown * indicates statistical significance

No difference in construct integrity and MSC retention after in vivo implantation of encapsulated allogeneic MSC in High M alginate and High G alginate

Subcutaneously implanted alginate-encapsulated SPIO-MSC remained clearly visible on MR images over 5 weeks (Figure 3A-B) and where clearly visible macroscopically upon explantation (Figure 3C) without noticeable differences between high M and high G alginate constructs. As observed in histological sections, there was good integrity of the constructs (Figure 3D-G) and a homogenous distribution of SPIO labelled cells in alginate constructs (Figure 3H-K). The rat tissue surrounding the constructs showed very limited foreign body reaction without cell infiltration of macrophages (CD68; Figure 3H-K) or T lymphocytes (CD3; Figure 3L-O). No differences in construct morphology or foreign body reaction were observed between High M alginate and High G alginate.

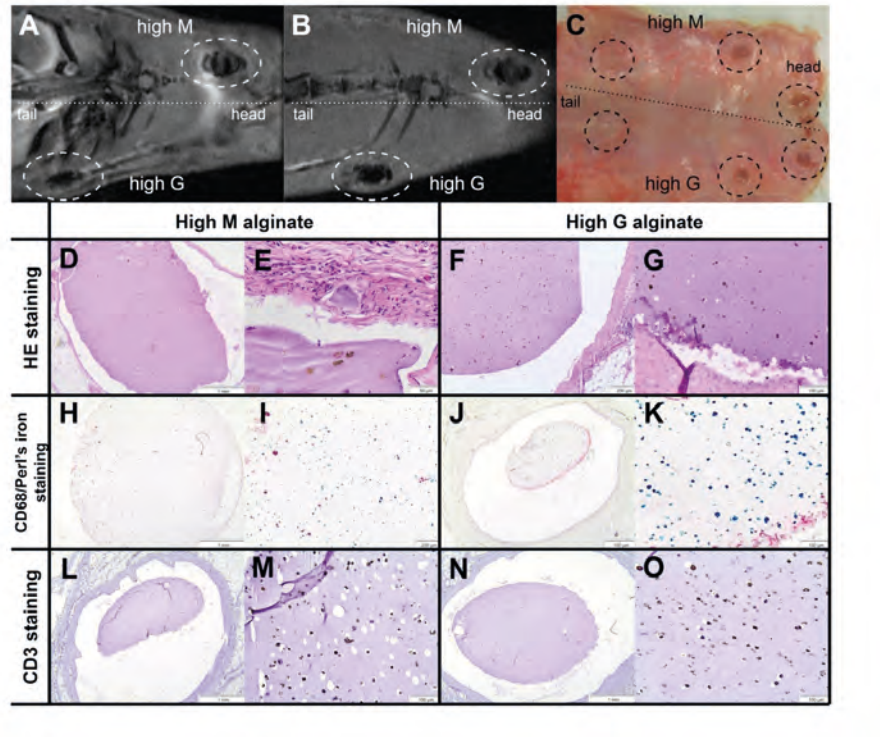

Figure 3. Subcutaneous implanted allogeneic rMSC in immunocompetent rats.

(A) MRI image directly after implantation and **(B)** MRI image 5 weeks after implantation, Alginate constructs are visible due to the labelled SPIO cells in the constructs. **(C)** After 5 weeks, the constructs were clearly visible after removal of the skin. **(D-G)** Histology of the constructs with Hematoxylin and Eosin staining of high M and high G alginate constructs. **(H-K)** Perl's iron staining (blue), which stains SPIO combined with CD68 staining (red) to stain macrophages. **(L-O)** CD3 staining (red) to stain T lymphocytes (black dots in cells represent SPIO particles).

Alginate encapsulation using a micro-encapsulator results in small injectable beads with vital MSC.

After optimizing the settings of the encapsulator device we were able to produce homogenous beads of 0.3 mm using High G alginate. With the more viscous High M alginate, the beads were larger and the size was less homogenous. We decided to continue with High G alginate. The average bead size produced with High G alginate was 284 ±28µm, with each bead containing 112±32 MSC (Figure 4A,B). To confirm that the anti-inflammatory capacity of the hMSC was not affected by the procedure with the micro-encapsulator, we performed an IDO assay on the secretome of the stimulated hMSC. We compared hMSC in monolayer versus hMSC-encapsulated in alginate beads (n=3 donors). Encapsulated hMSC displayed similar IDO activity compared to hMSC in monolayer (L-kynurenine concentration; 48.91 ±10.67 µM vs 45.63 ±1.17 µM respectively using equivalent numbers of cells) (Figure 4C). This indicates that after cell encapsulation, hMSC maintained anti-inflammatory capacities.

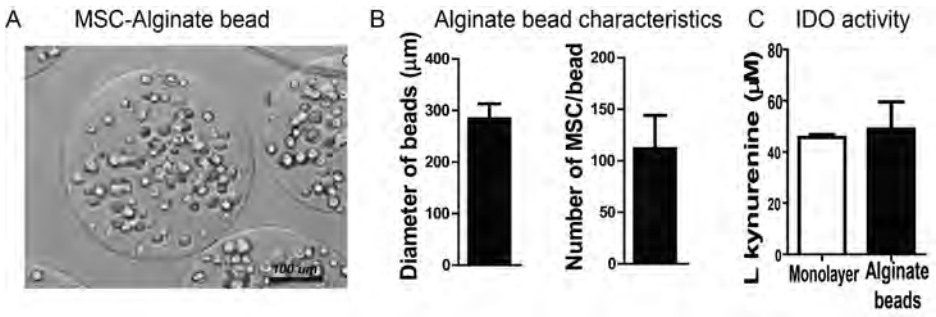

Figure 4. Characteristics of MSC-alginate beads produced with micro-encapsulator device.
(**A**) hMSC-alginate beads prepared with the micro-encapsulator. (**B**) The average diameter of the alginate beads and number of hMSC/bead. (**C**) Concentration of L-kynurenine as measure of IDO activity corrected for the number of cells in the secretome of MSC stimulated with TNFα/IFNγ.

Intra-articularly injected MSC-alginate beads remain present and metabolically active in the joint for at least 8 weeks in vivo

Unfortunately, one rat of the group with alginate died during imaging at day 0 probably due to anesthesia-related issue and the results of these knees were excluded from analyses. The other animals were longitudinally followed by imaging in MRI and BLI during 8 weeks.

To track the MSC-alginate beads *in vivo*, alginate was crosslinked with Gadolinium ions which are visible on MRI. At baseline, the number of alginate beads per knee was 73 ±36 (Figure 5A-B). The majority of the alginate beads were located in the suprapatellar pouch. On follow-up scans the alginate beads appeared more dispersed throughout the joint. The number of beads decreased to 46 ±34 per knee at week

4 (p=0.028 compared to week 0), and remained stable afterwards till the end of the experiment at week 8 (37±20). To track long-term cell activity after intra-articular injection, we used bioluminescence (BLI) scanning of allogeneic r(Fluc)MSC that were either encapsulated in alginate beads before injection (n=6 knees) or freely injected in the knee (n=8). The first scan was preformed immediately after injection (Figure 5C) and subsequently scanned repeatedly until week 8. The BLI signal in the r(Fluc)MSC-alginate group was lower than expected based on cell number at day 0, most likely due to impaired metabolic activity of the cells shortly after encapsulation in alginate which is supported by a higher BLI signal after 2 weeks. BLI signal decreased significantly from week 2 to week 3 (p =0.028) but remained stable hereafter (p > 0.293). From week 3 on, the fluorescence in the r(Fluc)MSC-alginate group was significantly stronger than in the free r(Fluc)MSC group (p< 0.04 for all time points; Figure 5C-D).

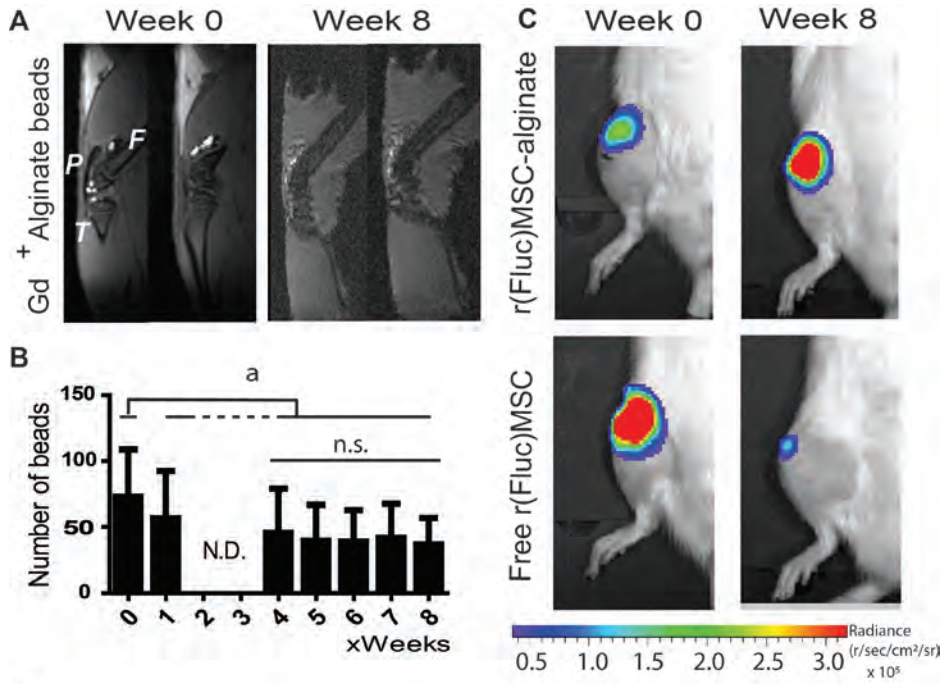

Figure 5. In vivo cell tracking
(A) MRI of rat knee joints injected with gadolinium labeled alginate beads, directly after intra-articular injection and after 8 weeks. (**B**) Quantification of number of alginate beads per joint over time (Due to technical problems with the MRI scanner, week 2 and 3 scans were not available). (**C**) BLI of free r(Fluc) MSC and r(Fluc)MSCs-alginate bead directly after injections and after 8 weeks**.**

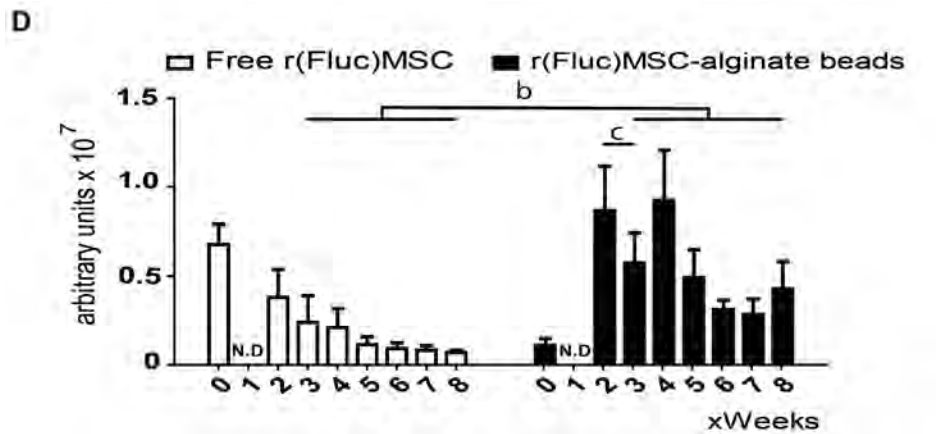

Figure 5. In vivo cell tracking
(**D**) Quantification of BLI signal over time (due to technical problems with the IVIS, week 1scans were not available). The images shown in **A** and **C** are representative animals for each group. In **A**; P = patella, F= femur, T = tibia. In **D**; white bars = free (Fluc)MSC and black bars = r(Fluc)MSC-alginate beads. (b, p< 0.04; c, p=0.028). n=8 knees for free r(Fluc)MSC and n=6 knees for r(Fluc)MSC-alginate group. N.D. = not determined due to technical error. n.s. = not significant.

Encapculation in alginate did not improve effect of hMSC on pain, cartilage damage or synovial inflammation.

To test the efficacy of the hMSC-alginate beads as therapy for osteoarthritis, we assessed the effect on pain reduction, cartilage damage and synovial inflammation in a rat OA model. Pain was assessed by means of tactile allodynia using the von Frey filaments. Prior to MIA injection, all the animals had comparable withdrawal thresholds. One week after MIA injection and before treatment, all three treatment groups (saline control, free hMSC and hMSC-alginate beads) showed a significant decrease in withdrawal threshold ($p < 0.02$), indicating pain as a result of MIA injection. One week after treatment, only the animals in the saline control group showed an additional significant decrease in withdrawal threshold compared to the time point just before treatment (p=0.001), indicating exacerbating pain over time. No increase in sensitivity to pain stimulus was observed in the free hMSC or hMSC-alginate beads group. Although rats in the free hMSC group showed a trend towards less pain in time, significant difference compared to the saline treated group was only reached at the end of the experiment at week 8 (saline control vs free hMSC, p=0.036). The hMSC-alginate beads group was not significantly different from saline control or free hMSC at week 8 (resp. p= 0.404 and p=0.722), or any other week. (Figure 6A,B).

Cartilage damage was scored 8 weeks after treatment on the femorotibial compartment of the joint as well as the patella using a modified Pritzker score method.

Mild osteoarthritic changes were present in all groups. There were no significant differences in cartilage damage or GAG loss between treatment groups (Figure 6C-F).

As an indicator of inflammation we performed thickness measurements of the synovial membrane at the para-patellar recesses at 4 and 8 weeks after start of treatment. (Figure 6G,H). No significant differences between groups were found at week 4 (p=0.198) The hMSC-alginate group showed a trend towards a thicker membrane at week 8 (p=0.058) and more infiltration of inflammatory cells next to encapsulation of alginate remnants (Black arrows in Figure. 6I,J) compared to the saline control and free hMSC group. To examine if alginate would induce inflammation in the joint, we injected empty alginate beads intra-articularly in 2 additional healthy rat knees. One week after injection, synovial inflammation was seen on histology, characterized by synovial hypercellularity and encapsulation of the alginate beads, indicating a mild foreign body reaction against the alginate (figure 7).

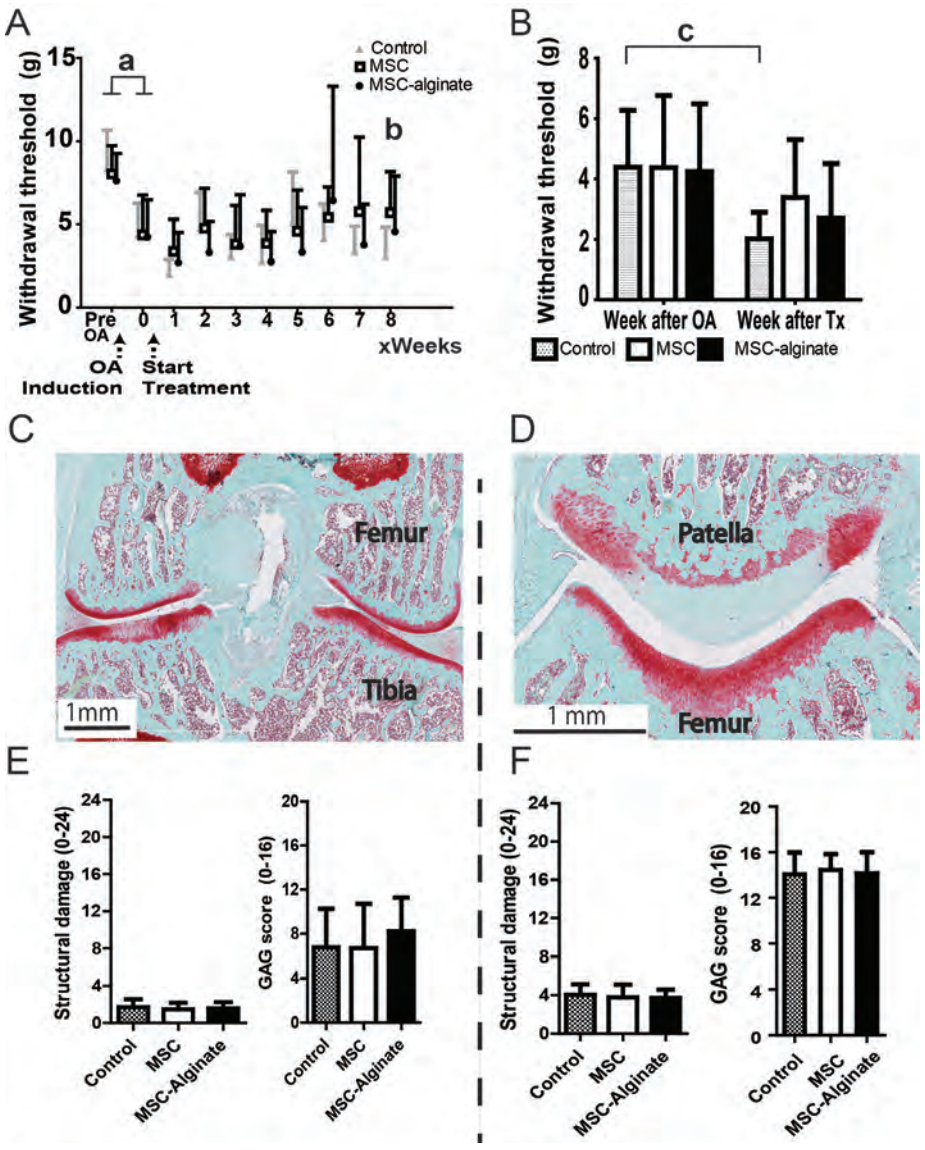

Figure 6. Therapeutic efficacy of MSC-alginate beads in a rat OA model.
(A) hind limb withdrawal threshold as measure of pain over time. **(B)** withdrawal threshold 1 week after treatment. **(C)** A representative example of the Safarin-O staining at the femorotibial compartment (D) and at the patellofemoral compartment. **(E)** The structural damage according to the Prizker score and GAG loss for femorotibial **(F)** structural damage and GAG loss in patella. The maximum score for structural damage was 24 and for GAG loss 16, in which a higher score represents more damage.

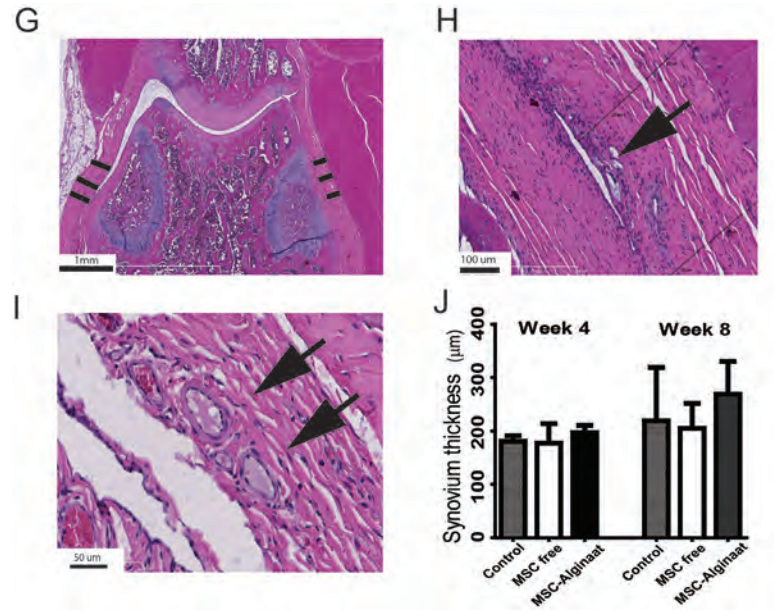

Figure 6. Therapeutic efficacy of MSC-alginate beads in a rat OA model.
(G) HE staining of parapatellar recesses and indication of synovial membrane thickness. **(H-I)** some degradation and encapsulation of alginate was observed (Black arrows). **(J)** Quantification of synovial thickness over time (a; $p < 0.02$, b; $p=0.036$ and c; $p =0.001$) All data shown as mean ±SD. At week 4, n=5 knees/group; week 8, n=16 knees/group.

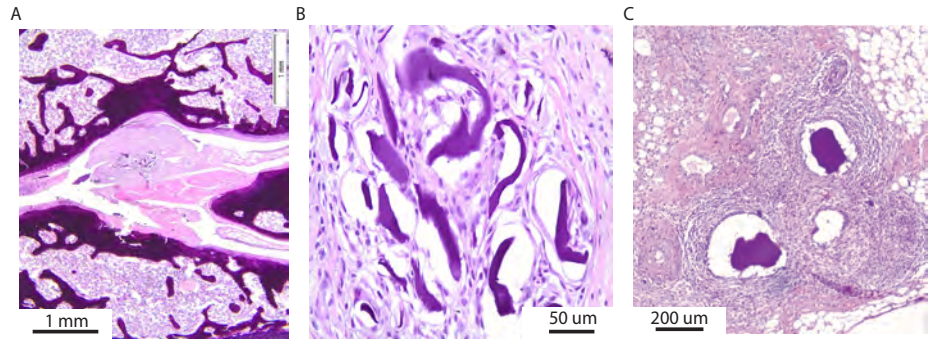

Figure 7. Empty alginate microbeads in healthy rat knees.
HE stainings one week after injection. (**A+B**)synovial thickening, encapsulation of the alginate beads. **(C)** hyper cellularity in the synovium. The form of the beads can have changed due to the histological process.

Discussion

MSC have previously been described to have a beneficial effect in regenerative medicine, both in pre-clinical and some initial clinical studies, although evidence for long-term engraftment is low [36, 39, 40, 42, 85]. This led Prockop *et al.* and von Bahr *et al.* to postulate the 'hit-and-run' mechanism [36, 42] which proposes the cells to only have a short interaction with the micro-environment. The design of the current study is based on the idea that the therapeutic efficacy of MSC could be enhanced by prolonging the local presence of MSC and their secreted factors at the desired location. To achieve this purpose we encapsulated MSC in alginate and demonstrate that the cells remained viable in this carrier, are protected against the allogeneic immune system and retained immunomodulatory capacity when stimulated by external cytokines or immune cells. Moreover, we demonstrate retention of construct integrity *in vivo* over time by longitudinal MRI. For this purpose gadolinium was used to crosslink the alginate. By combining MRI with BLI of constructs that contained luciferase transfected cells, we showed that encapsulation of MSC is beneficial for *in vivo* cell survival and that it prolonged their local presence in a diseased and inflamed environment.

We used two types of alginate to encapsulate cells, both were clinical grade but differed in composition with respect to the ratio of guluronate and mannuronate. With both alginate types, MSC retained their immunomodulatory capacity *in vitro*. The results are similar to our previous study where we used a different type of alginate that had a low viscosity and less well defined composition [52]. As there is a great variability in the ratio of mannuronate and guluronate between different types of alginate that are (commercially) available, our work in which we used high quality GLP produced High G and High M alginate demonstrates that a wide range of alginates might be suitable for encapsulation. Different alginates have different viscosities which can greatly influence the mechanical properties of the construct and thus its integrity and the infiltration of cells. After subcutaneous implantation in immune competent rats, constructs of High G and High M alginate remained intact with a thin capsule formed around the construct. There was no infiltration of immune cells in the alginate. We took the alginate-encapsulated MSC a step further by evaluating them in a diseased situation, in our case in rat knees after induction of osteoarthritis. To provide an injectable therapy, we optimized a protocol using a machine for encapsulation , that enabled reproducible generation of a homogeneous population of MSC-alginate microbeads, with an average diameter below 300 µm. The size of these constructs contributes to easy clinical application, since they are small enough to pass through a 23G needle that can be used for most clinical applications.

The use of Gadolinium, with its contrast properties in MR imaging [93], made it possible to monitor localization and integrity of the alginate constructs over time. Gadolinium was incorporated in the guluronate or mannuronate molecules upon polymerization and loss of Gadolinium signal was attributed to loss of construct integrity. Quantification with MRI of the Gd-labelled beads indicated an initial loss of some beads with subsequent retained visible presence of approximately half of the alginate beads up to the end of the experiments at 8 weeks post-injection. Although we cannot exclude that the loss of Gadolinium signal is caused partly by diffusion of Gadolinium out of the bead, under *in vitro* conditions leakage of Gadolinium out of the alginate beads was not seen at all during a three week follow-up period (data not shown). Therefore, we assume that lessening of the number of visible beads is due to disintegration of the beads with concomitant release and loss of hMSC. The latter is confirmed by the BLI data that showed a matching decrease in cell signal over time. A substantial part of the cells, however, remained present till the end of the study. Possibly, some beads are lost due to mechanical forces in the joint during movement of the animal. We speculate that this problem might be less in a larger joint where the beads have more space to be distributed to a relatively sheltered position, such as in the suprapatellar pouch, where high loading that occurs between cartilage surfaces can be avoided. The unique option to follow bead integrity on MRI, while having the anatomy of the joint visible in the same image, provides a safe and helpful tool to follow alginate constructs, also in a clinical setting in human, equine or canine patients. The method might be useful for *in vivo* tracking of other materials that polymerize with divalent cations such as fibrin.

Besides bead- and cell tracking to demonstrate prolonged cell presence, we tested therapeutic efficacy of the encapsulated MSC in a rat model for OA. Although we have previously shown MSCs retain osteogenic and adipogenic differentiation capacity after 30 days of alginate encapsulation (Leijs *et al.*, 2017), we hypothesize that therapeutic effect of MSCs is mainly by secretion of factors. In previous work we have shown that multiple intra-articular injections of MSC-secretome can inhibit pain and have a protective effect on cartilage damage in a mouse OA model [79]. This confirms that MSC based treatments can exert their effects *in vivo* by their secretome and do not rely solely on cell-cell contact or their differentiation capacity. In this study we quantified the stimulation induced IL-6 secretion and IDO activity from the encapsulated hMSC. This is, however, only a small fraction of the biologically active factors that are secreted by MSC, either soluble or in extracellular vesicles. It is, therefore, important to test the functionality of the secreted factors, which we did by demonstrating that these encapsulated hMSC significantly inhibited proliferation of stimulated CD4+ and CD8+ T lymphocytes in a dose dependent manner.

Preferably, a continuous interaction and feedback loop between the diseased tissue and the exogenous MSC is created, in order to produce cytokines and growth factors at the right time and in the right concentration. Based on the longer presence we choose to inject $1x10^5$ cells per joint. This number is ten times lower than what we injected previously in the same rat OA model [32]. Possibly as a consequence of that, in our study a therapeutic effect of freely injected human MSC was not detectable. The encapsulated MSC, however, did not do better than the freely injected MSC. This absence of improved therapeutic effect by encapsulation could be due to an insufficient number of cells. Maybe, initially a larger cell number is needed to reduce the inflammation. The small size of the rat joint, however, did not allow injection of more beads. Because preliminary experiments had indicated the density of 4 million cells/ml to be a good balance between concentration of secreted factors and stability of the gel construct, we have not considered using higher cell numbers per bead. Furthermore, we have chosen to use human MSC for this study to increase the clinical translatability of a human allogeneic MSC-alginate construct. A disadvantage of the use of xenogeneic MSC in this set up could be that some important factors and cytokines might not be interspecies conserved. This can cause *in vivo* miscommunication between xenogeneic MSC and the diseased environment. Since we and others have seen anti-inflammatory effects of xenogeneic MSC secretome alone, we can conclude that the secreted factors of xenogeneic MSC are capable to at least achieve anti-inflammatory and chondroprotective effects in OA[79]. Nevertheless, it is still possible that the use of xenogeneic MSC depreciates the full potential of MSC therapy, an issue that could be tackled by using allogenic MSC. The use of xenogeneic MSC could also explain the discrepancy between our work and the recently published work of Choi *et al.*, showing promising results using allogenic encapsulated MSC in a rabbit OA model, although in that study no cell or construct tracking was performed [50].

Although the use of alginate encapsulation is promising in the field of regenerative medicine, it might bring safety and regulatory issues. Although the fibrous capsule formed around the alginate implants when implanted subcutaneously was very thin and the constructs remained completely intact, upon injection in the joint we noticed a trend to synovial thickening and the alginate beads were encapsulated in the synovial membrane. This reaction, even though it was not a strong foreign body response, might have dampened the anti-inflammatory effect of MSC and in extension its effect on pain. Since this reaction seemed less strong after subcutaneous implantation of MSC-alginate or empty alginate constructs, it might be caused by mechanical damage to the constructs or the presence of local inflammation in the osteoarthritic joint. If the alginate is compromised and starts to slowly release the xenogeneic hMSC, an adaptive immune response can be initiated, further reducing the therapeutic potential. Although immune privileged, MSC do maintain a degree

of immunogenicity [58]. This foreign body reaction leading possibly to a slow release of xenogenic MSC out of the alginate, possibly causing a chronic local inflammation. Thus, to limit this reaction, two factors play an important role: the biomaterial (the alginate) and the MSC. Focusing on the biomaterial, it is possible that a different type of alginate could be more resistant to damage in the osteoarthritic joint. This would prevent the release of xenogeneic hMSC, thus the adaptive immune response and decrease the fibrous tissue formation as seen in our experiments. Another way to decrease this reaction is to use autologous MSC, this would further inhibit the graft versus host disease. Of course extensive *in vitro* and *in vivo* experiments are needed to investigate these hypotheses.

In conclusion, we have provided a method to produce a homogenous gadolinium labeled cell-alginate construct combined with imaging techniques that are suitable for minimal invasive longitudinal follow-up studies in patients. We showed that non-autologous MSC can survive longer and remain metabolically active *in vivo* up to at least 8 weeks, when encapsulated in alginate. The possibility to retain non-autologous cells and the production of standardized small beads, greatly increased the feasibility of producing cell-alginate micro capsules in a standardized safe way and on a large scale, giving it the potential of an 'off-the-shelf' biological therapeutic option. These are both important additional steps towards clinical applicability. Unfortunately the overall treatment effect on pain, synovial inflammation and cartilage quality in this study could not be confirmed in our *in vivo* OA model, possibly due to specific local tissue responses to the alginate beads or a suboptimal cell number. Our results encourage further development of this strategy to provide an injectable therapy by cell encapsulation that greatly prolongs the interplay between the therapeutic cells and their diseased target tissues, taking into account specific local and disease requirements.

CHAPTER 3

MSC secretome reduces pain and prevents cartilage damage in murine OA model

Published as

Mesenchymal stem cell secretome reduces paijn and prevents cartilage damage in a murine osteoarthritis model.

Sohrab Khatab, Gerjo J.V.M. van Osch, Nicole Kops, Yvonne M. Bastiaansen-Jenniskens, P.Koen Bos, Jan A.N. Verhaar[1], Monique R. Bernsen[2], Gerben M. van Buul

in European Cells and Materials, 2018

Sohrab Khatab designed and conducted the experiments, performed data collection and analysis and drafted, edited and reviewed the manuscript.

Abstract

Mesenchymal stem cells (MSCs) represent a promising biological therapeutic option as an osteoarthritis (OA) modifying treatment. MSCs secrete factors that can counteract inflammatory and catabolic processes and attract endogenous repair cells. We studied the effects of intra-articular injection of MSC secretome on OA-related pain, cartilage damage, subchondral bone alterations and synovial inflammation in a mouse collagenase induced OA model. MSC secretome was generated by stimulating human bone marrow derived MSCs from end-stage OA donors with IFNγ and TNFα. Mice (N=54) were randomly assigned to injections with MSC secretome from 20.000 MSCs, 20.000 MSCs or medium (control). Pain was assessed by hind limb weight distribution. Cartilage damage, subchondral bone volume and synovial inflammation were evaluated by histology. MSC secretome injected mice showed pain reduction at day 7 compared to control mice. Cartilage damage was more abundant in the control group compared to healthy knees, a difference which was not found in knees treated with MSC secretome or MSCs. No effects were found regarding synovial inflammation, subchondral bone volume or the presence of different macrophage subtypes. Injection of MSC secretome or MSCs derived from end stage human OA donors resulted in early pain reduction and had a protective effect on the development of cartilage damage in a murine OA model. By using the regenerative capacities of MSCs via their secreted factors, it is possible to greatly enhance the standardization, affordability and clinical translatability of this approach. This way, we can evolve this biological therapy towards a true disease modifying anti-osteoarthritic drug.

What is known about the subject: Intra-articular MSC injection can ameliorate OA related pain and processes. It appears that the trophic effects of MSCs are important for their regenerative capacities. Several factors are known to play a role, but the exact mechanism is unclear.

What this study adds to existing knowledge: MSC secretome is at least as effective as MSCs in reducing OA-related pain and cartilage damage. We are the first to present anti-osteoarthritic effects *in vivo* of MSC secretome from aged human donors with end-stage OA, thereby emphasizing the clinical relevance of these findings.

Introduction

Osteoarthritis (OA) is a disabling joint disease affecting over 10 % of individuals from the age of 60 [83]. OA is characterised by loss of cartilage integrity, subchondral bone changes, formation of osteophytes and inflammation of the synovial membrane [5]. The interplay between these processes and tissues and their exact role in the etiology and progression of the disease is yet unclear. These processes together result in pain and functional disability, which are the main reasons for patients to seek medical treatment. To this date, no curative treatment for OA exists. Current treatments mainly aim at the treatment of the disease symptoms and not at a durable way of modifying pathological osteoarthritic processes. Current therapeutic options include life-style changes, physical therapy, pain medication and – for end-stage OA – joint replacement. Since joint arthroplasties have a limited life-span, the need for disease-modifying drugs or therapies is high. Ideally, such a therapy would inhibit or repair damage to the joint tissues and simultaneously reduce pain and disability.

Mesenchymal stem cells (MSCs) represent a promising biological therapeutic option as an OA modifying treatment. Stem cells play a pivotal role in physiological tissue homeostasis and regeneration after tissue injury [26]. Next to their differentiation potential into several lineages, including the chondrogenic lineage, MSCs can influence their (micro)environment by secreting trophic mediators [33-38]. These secreted factors could possibly counteract inflammatory and catabolic processes and attract endogenous repair cells [36, 38, 43, 45]. Several (pre)clinical studies show promising results for intra-articular stem cell injection as a treatment for OA [28, 29, 31, 32, 82, 94]. Murphy *et al.* are the first to show amelioration of degenerative changes after intra-articular injection of bone marrow-derived MSCs in a caprine OA model [29]. Others find diminishment of OA-derived pain [32] or synovial inflammation and cartilage degradation in pre-clinical studies [31]. Initial reports from clinical studies indicate that intra-articular application of MSCs is safe for OA and possibly results in clinical improvement [30, 94].

The MSC trophic capacities provide the interesting option of possibly basing future therapies on the secreted factors rather than on the MSCs themselves. The importance of the endocrine MSC function is further endorsed by the fact that locally [32] or systemically [41] applied MSCs show very limited long-term engraftment, for which a 'hit and run' mechanism is postulated [36, 42]. In addition, the MSCs need to be activated to exert their trophic effects [45, 55, 56]. Such an in vivo activation is difficult to control or influence and, thereby, likely to be subject to large variability. In vitro stimulation with, for instance, inflammatory factors provides an option to further optimise the use of the MSC immunomodulatory abilities.

The use of the MSC secretome could improve the therapeutic efficacy and would greatly enhance the clinical applicability of this biological treatment as a true disease-modifying anti-osteoarthritic drug. The aim of the present study was to explore the anti-osteoarthritic effects of the human MSC secretome, compared to the MSCs, on various outcome measures in a collagenase mouse OA model. Injection of human MSC secretome was hypothesised to be at least as effective as MSCs in reducing OA-related pain, cartilage damage, subchondral bone alterations and synovial inflammation.

Materials and Methods

Expansion of MSC

Human bone marrow MSCs were derived from heparinised femoral-shaft marrow aspirate of six patients undergoing total hip replacement (mean age 55.3 ± 10.0 years; female : male ratio 1 : 2) using previously described procedures [95], after written informed consent and approval by the medical ethical committee (protocol METC-2004-142). Briefly, bone marrow cells were plated at 50,000 cells/ cm2 and, after 24 h, the flasks were washed to remove non-adherent cells. Then, MSCs were trypsinised [0.25 % trypsin/ethylenediaminetetraacetic acid (EDTA) solution (Life Technologies)] and seeded in cell culturing flasks at a density of 2,300 cells/ cm2 in expansion medium consisting of minimal essential medium alpha (αMEM; Gibco), 10 % heat inactivated foetal calf serum (FCS; Gibco), 1.5 µg/ mL fungizone (Invitrogen), 50 µg/ mL gentamicin (Invitrogen), 25 µg/mL ascorbic acid-2-phosphate (Sigma-Aldrich) and 1 ng/mL fibroblast growth factor 2 (FGF2; AbD Serotec, Oxford, UK). Cells were cultured in an incubator at 37 °C, 5 % CO2 and 90 % humidity. Medium was refreshed twice a week. MSCs were passaged at approximately 70 % confluency. MSCs used for in vivo experiments were characterised by fluorescence-activated cell sorting (FACS) analysis and resulted positive for CD73, CD90, CD105 and CD166 and negative for CD11C, CD31 and CD45 (data not shown). de Mos *et al.* show tri-lineage differentiation of cells isolated following this procedure[95]. The viability of the MSCs was evaluated after trypsinisation and before being injected or seeded for obtaining the secretome: less than 5 % of the cells were dead, as indicated by trypan blue positive staining. Human MSCs from end stage OA donors were used to increase the clinical translatability of the study.

Preparation of MSC secretome

To produce the MSC secretome, passage 3 MSCs were plated at a density of 3.5 × 104 cells/cm2 and cultured for 24 h in expansion medium. After 24 h, cells were activated to secrete immunomodulatory factors by culturing for 24 h in stimulating medium (van Buul *et al.*, 2012). This stimulating medium consisted of αMEM supplemented

with 1.5 µg/mL fungizone, 50 µg/mL gentamicin, 1 % insulin-transferrin selenium (ITS; Biosciences), 50 ng/mL interferon gamma (IFNγ; PeproTech) and 50 ng/mL tumour necrosis factor alpha (TNFα; PeproTech). After 24 h of stimulation, MSCs were washed five times with phosphate-buffered saline (PBS; Gibco). To collect the paracrine factors, collecting medium was added, consisting of only αMEM with 0.05 % bovine serum albumin (BSA; Sigma-Aldrich) – to stabilise the secreted factors and as an adhesive for smaller molecules to bind to and to be retained after the concentration step – and without phenol red – which can mimic an oestrogen and, therefore, influence cell behaviour in vivo. 1 mL of collecting medium was added per 2.0 × 105 MSCs. MSC secretome was collected after 24 h and centrifuged at 700 ×g for 8 min to remove cell debris. The secretome equivalent of 20,000 MSCs, a number of cells previously used in a mouse collagenase OA model [31], was planned to be injected in a murine knee joint. To achieve this in an end volume of 6 µL, suitable for injection in a mouse knee joint, the MSC secretome was concentrated by loading on a 3 kDa cut-off filter (Amicon Ultra-4 Centrifugal Filter Unit, UFC800324, Merck Millipore B.V.) and spinning down for 20 min at 4000 ×g. Molecules above 3 kDa were retained. The concentrated MSC secretome was collected, aliquoted and stored at – 80 °C for further use. Concentrated secretome was checked for indoleamine 2,3-dioxygenase (IDO) activity by measuring the metabolite L-kynurenine concentration, as described before (van Buul *et al.*, 2012). Briefly, the concentrated secretome was diluted 10 times and 200 µL of the diluted sample were mixed with 30 % trichloroacetic acid (Sigma-Aldrich), incubated at 50 °C for 30 min and spun down at 10,000 ×g for 5 min. 75 µL of supernatant were added together with 75 µL of 7,12-dimethylbenzanthracene (DMBA; Sigma-Aldrich) (20 mg/ mL in acetic acid). The extinction was measured at 490 nm in a Versamax microplate reader (Molecular Devices, LLC, San Jose, CA, USA). A L-kynurenine concentration of 33.7 ± 4.5 µM was calculated considering the dilution factor, indicating substantial immunomodulatory MSC activity. To develop the concentrated secretome production protocol, the secretomes of three MSC donors were used. Increased IDO activity confirmed the anti-inflammatory capacity of the donors. A minimum of 0.05 % of BSA was needed in the secretome to maintain the secreted cytokines and growth factors, based on the concentrations of interleukin 6 (IL-6). The concentration of IL-6 in the concentrated secretome was measured by enzyme-linked immunosorbent assay (ELISA; R&D systems) according to the protocol supplied by the manufacturer. In the obtained batch of secretome, the concentration of IL-6 was 238 ± 42 ng/mL if 0.05 % BSA was present and lower and below the detection limit if no BSA was present (data not shown). Later, this developed protocol was used to produce concentrated secretomes of three new donors, in which the IDO activity was tested to confirm the donors' anti-inflammatory capacity. The MSC secretomes of these donors were pooled and used for in vivo experiments. Control medium was subjected to the same handling

as the MSC secretome, including 24 h incubation and concentration, except for the exposure to the MSCs, and stored at – 80 °C for further use.

Animal experimental design

Experiments were performed on 54 male C57/Bl6 mice, age 12 weeks (Harlan Netherlands B.V., Horst, the Netherlands), with approval of the animal ethical committee (#EMC 116-14-03). Mice were housed in groups of three or four mice per cage, under 12 h light-dark cycle at a temperature of 24 °C and had access to water and food ad libitum at the animal testing facilities of the Erasmus MC, University Medical Centre, Rotterdam, the Netherlands. Before the start of the experiments, mice were allowed to acclimatise for a week. OA was induced unilaterally in the knee of all mice by 2 intra-articular injections of 3 units collagenase type VII (Sigma-Aldrich) at days – 7 and – 5. All intra-articular injections were applied with an injection volume of 6 µL and under 2.5 % isoflurane anaesthesia, using a 50 µL glass syringe (Hamilton Company, Ghiroda, Romania) and a 30 G needle (BD). Contralateral control knees were kept naïve and were not injected. Mice were randomly assigned to either treatment group A, which was injected with 20,000 passage 3 MSCs in 6 µL concentrated medium, treatment group B, injected with MSC-secretome from 20,0 00 MSCs concentrated in 6 µL medium or control group C, injected with 6 µL control medium (n = 11 mice per group, 1 mouse in the control group was not assessed by histology due to technical problems). MSCs used in group A were not activated by stimulating medium prior to injection, since in vivo activation by the osteoarthritic environment was considered to be more clinically relevant. All groups received three consecutive injections: the first injection (referred to as day 0) was given 7 d after the first collagenase injection and repeated at day 2 and 4. Once weekly, weight distribution over the left and right hind limbs was evaluated as an indicator of pain (for the method see below). Animals were euthanised at day 21 after start of treatment and knee joints were harvested for histological analysis. To assess the early effects of the treatments – especially on synovial inflammation – an additional experiment was performed consisting of 7 mice in each group (same 3 treatment groups as mentioned previously, n = 7 mice per group). These animals underwent identical OA induction and treatment protocols. They were euthanised at day 5 after the treatment start and knee joints were prepared for histological evaluation.

Measurement of hind limb weight distribution

Hind limb weight distribution, as an indicator of pain, was monitored by an Incapacitance Tester (Linton Instrumentation, Norfolk, UK), as previously described [32]. Mice were positioned on the Incapacitance Tester with each hind limb resting on a separate force plate. Animals were habituated to the apparatus, starting 2 weeks prior

to the experiments. The examiner performing the measurements was blinded to the data registration. Measurements were automatically stored in a computer database. A baseline measurement was performed at day – 7, just before the induction of the OA. Follow up measurements were performed 1 week after OA induction at day 0, just before therapy administration and at day 7, 14 and 21. After the 3 weeks of data collection, upon data analyses, measurements with a registration below 3 g (< 10 % of total body weight) per hind limb or less than 10 g (< 30 % of total body weight) in total over both hind limbs were excluded. 30-45 measurements were recorded per time point, 15 measurements per time point per animal were available on average. For each time point per mouse, the average of these measurements was used to calculate the percentage of weight on the affected limb as an indication of pain in the affected limb. The average value per measurement time point was used for statistical analyses.

Histology

Knees were fixed in 4 % formalin (v/v) for 1 week, decalcified in 10 % EDTA for 2 weeks and embedded in paraffin. Coronal sections of 6 µm were cut for analysis of synovial inflammation and cartilage damage.

Cartilage damage

Cartilage damage was evaluated on thionine-stained sections by two observers blinded to the treatment groups using the scoring system described by Glasson *et al.* [96]. Briefly, this score ranges from 0, for normal cartilage, to 6, for cartilage with clefts and erosion to the calcified cartilage in > 75 % of the articular surface. For each knee, cartilage quality in the lateral and medial compartment – both femur and tibia – of the knee was scored on 3 sections at standardised locations in the knee with 180 µm between the sections, leading to a maximum score of 12 per compartment and a total summed score of 36 per compartment. For each compartment, the maximum and summed score assigned by the two blinded observers was averaged. Since OA damage was most pronounced in the lateral compartment (data not shown), these data were considered for further analyses.

Subchondral bone changes

The percentage of subchondral bone per total volume of subchondral space between calcified cartilage and growth plate was calculated. Measurements were performed using ImageJ software (NIH). For each knee, a region of interest was drawn in a standardised way on 3 sections at standardised locations in the knee, with 180 µm between the sections. The region of interest was drawn between the calcified cartilage on the top and the growth plate on the bottom. The insertion of the cruciate ligaments was used as medial boundary and the lateral side of the growth plate as

lateral boundary, taking care not to include osteophytes. Since the largest amount of remodelling was found in the medial compartment (data not shown), these data were considered for further analyses.

Synovial inflammation

Sections were stained with haematoxylin and eosin for synovial inflammation assessment. Images were acquired using the NanoZoomer Digital Pathology program (Hamamatsu Photonics, Ammersee, Germany). Synovial thickness was measured from the capsule to the superficial layer of the synovial membrane at the medial and lateral sides of the parapatellar recesses (three positions per section). These measurements were performed on three sections per knee, with 180 µm between the sections. The thickness measurements were averaged to obtain a single value per knee joint. To evaluate macrophage subtypes in the synovial membrane, inducible nitric oxide (iNOS) was used as a marker of pro-inflammatory macrophages, CD163 as a marker of anti-inflammatory macrophages and CD206 as a marker of tissue repair macrophages [97, 98]. For this purpose, sections were deparaffinised, washed and heat-mediated antigen retrieval was performed for CD163 and CD206, by placing the slides in 95 °C citrate buffer (pH 6) for 20 min. Antigen retrieval for iNOS was performed by placing the slides in 95 °C Tris-EDTA buffer (pH 9) for 20 min. Blocking of specific binding was performed with 10 % goat serum (Southern Biotech, Birmingham, AL, USA) for 30 min. Hereafter, sections were incubated for 1 h with the primary antibodies iNOS (2.0 µg/mL, #15323, Abcam), CD163 (0.34 µg/mL, #182422, Abcam) and CD206 (2.5 µg/mL, #64693, Abcam), followed by 30 min incubation with a biotinylated anti-rabbit Ig link (HK-326-UR, Biogenex, Fremont, CA, USA), diluted 1 : 50 in PBS/1 % BSA. Thereafter, sections were incubated with an alkaline-phosphatase conjugated streptavidin label (HK-321-UK, Biogenex) diluted 1 : 50 in PBS/1 % BSA. To reduce background, endogenous alkaline phosphatase activity was inhibited with levamisole (Sigma-Aldrich Chemie). New Fuchsin (Fisher Scientific) and Napthol AS-MX phosphate (Sigma-Aldrich Chemie) substrates were used for colour development and counterstaining was performed with haematoxylin. As a negative control, rabbit IgG antibody (DakoCytomation, Glostrup, Denmark) was used. The sections were ranked from the weakest to strongest staining for iNOS, CD163 and CD206 by two observers blinded to the treatment groups. When multiple sections had similar staining strength, i.e. amount of positive cells, the rank mean was assigned to each section. The average of the ranks assigned by the two observers to the knee for a certain staining was used for further analyses.

Statistical analysis

Data were analysed with IBM SPSS statistics 24 (SPSS, Chicago, IL, USA). For the effect on weight distribution, normality per measurement time point was confirmed with a

Shapiro Wilk test. For pain measurements, the collagenase effect was analysed using a two-tailed paired t-test before and after OA induction. For treatment effects, all groups were compared using a linear mixed model in which measurement time point and treatment were considered fixed factors and weight-bearing a dependent factor. Post-hoc analyses were performed by Bonferroni correction. Quantitative histology data were analysed by means of a univariate general linear model where measurement time point and treatment were considered fixed factors and subchondral bone volume percentage a dependent variable. Semi quantitative histology scores were compared using a non-parametric Mann-Whitney test, to assess collagenase or measurement time point effects, and Kruskal Wallis test, to assess treatment effects within different time points. Binominal histology data were analysed by means of $\chi 2$ test for multiple group testing and Fisher's exact test for comparing separate groups. For all tests, $p < 0.05$ was considered statistically significant. Correlation analysis was performed by means of a Spearman's ρ test. For the interpretation of the correlation coefficient, the absolute value of rs was used, classifying the correlations as weak (< 0.39), moderate (0.40-0.59), strong (0.60-0.79) and very strong (> 0.80). Correlations were regarded significant if $p < 0.05$.

Results

Injection with MSC secretome resulted in early pain reduction

Weight distribution over the hind limbs was determined as an indicator of pain (Fig. 1). On day – 7, just before induction of OA, the average weight on the right hind limb for all groups was 49.9 ± 1.7 %, indicating no difference between left and right hind limbs. 7 d after induction of OA (day 0, before treatment), 41.2 ± 6.3 % of the weight was distributed on the OA-affected limb, indicating pain when compared to before OA induction (Fig. 1, $p < 0.001$). No differences between treatment groups were found before both OA induction and treatment. At day 7, significantly more weight was put on the OA-affected limb by MSC-secretome- (49.5 ± 2.2 %) and MSC- (47.7 ± 2.9 %) injected animals at day 7, compared to control animals (43.6 ± 4.2 %; $p = 0.001$ and $p = 0.023$ respectively). Furthermore, the MSC-secretome- and MSC-injected animals put significantly more weight on their OA-affected limb on day 7 as compared to day 0 ($p = 0.013$ and $p = 0.032$ respectively, not shown in graph) whereas control animals did not, indicating early normalisation in weight bearing and pain reduction in treated animals. At day 14 and day 21, all groups showed less pain when compared to day 0, whereas no significant difference between groups was observed.

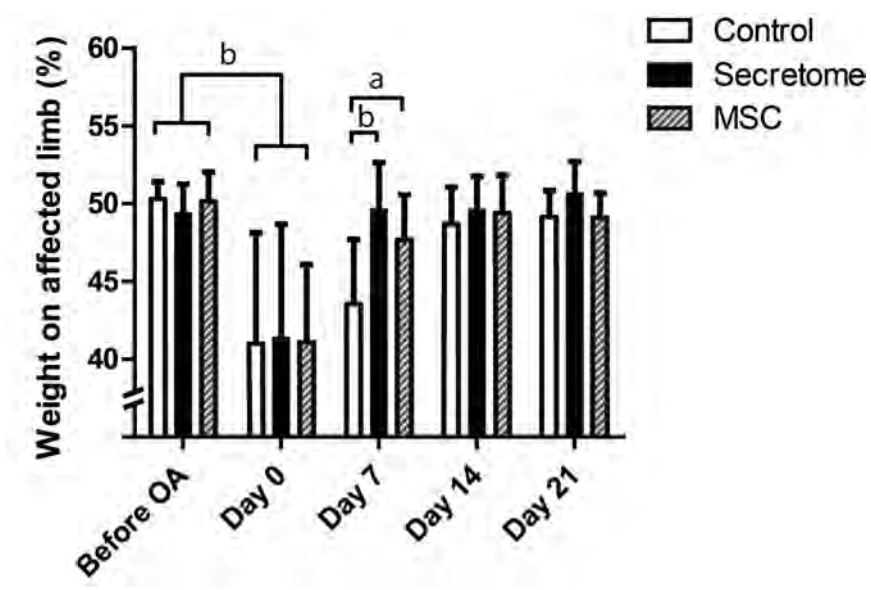

Figure 1. Assessment of hind limb weight distribution. Hind limb weight distribution was measured as an index of joint pain. OA induction by collagenase induced significant pain. MSC secretome and MSC injection resulted in normalization of weight bearing at day 7, at which time point pain was significantly reduced compared to the control group as well as to time point day 0. At day 14 and day 21, all groups showed significantly less pain compared to day 0. Data shown as mean ±SD, N=11/group, [a] $P<0.05$;[b] $P<0.001$

MSC secretome had a protective effect on cartilage damage but not on subchondral bone remodeling

To evaluate cartilage damage, all knees were scored 21 d after treatment (Fig. 2a,b, score range 0-12 for max score and 0-36 for sum score). Due to a high variability in the development of OA, no significant differences were found by non-parametric tests when comparing OA scores between knees treated with collagenase and healthy knees or among any of the treatment groups (Fig. 2a,b). Since some animals showed a clear OA development whereas others did not, binominal data were generated, where a max OA score of > 2 was considered as having OA and a score of ≤ 2 as not having OA (Table 1). A significant difference when comparing all groups was found using $\chi 2$ test ($p = 0.044$), after which separate groups were tested using Fisher's exact test. In the control group, where collagenase was injected but no MSC treatment was applied, more knees had OA than in the healthy group ($p = 0.012$). OA development was prevented in knees that were treated with MSC secretome or MSCs, in which no significant difference was found between healthy knees ($p = 0.238$ for both). No significant effect was observed when directly comparing MSC-secretome- or MSC-injected knees to control knees ($p = 0.183$ for both).

Identical analyses were performed for the sum OA scores (Fig. 2b), where a sum OA score of > 3 was considered as having OA and a sum score of ≤ 3 as not having OA (data not shown). Although the control group contained most animals with OA, no significant difference among all groups regarding sum OA scores was found by $\chi 2$ test; consequently, no further analyses were performed to evaluate treatment effects.

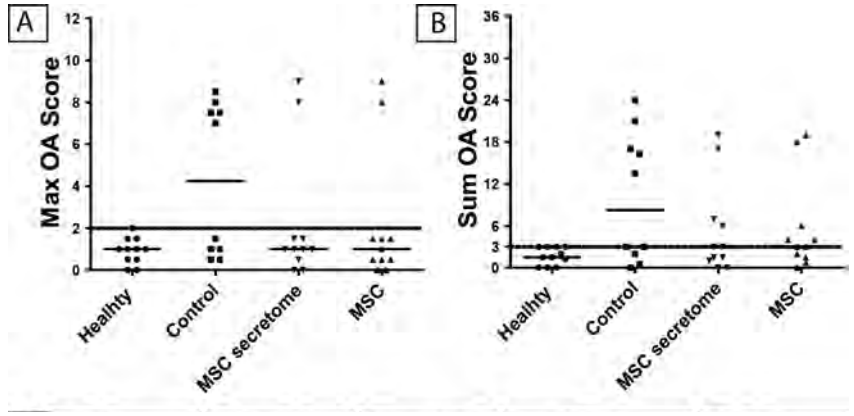

Figure 2. Maximum and sum OA scores for the lateral compartment were not significantly different between any of the groups **(A, B)**. Individual values are shown, solid lines represent median values, dotted line represents cut-off value for definition of OA development or not. For binominal data regarding max OA score, a significant difference was found when comparing OA incidence in control knees versus healthy knees (C, [a] $P < 0.05$). In MSC secretome or MSC treated knees, development of OA was prevented and no significant difference was found between these groups and healthy knees.

Table 1. OA incidence in healthy and treated knees. A maximum OA score of 2 was used as cut-off. A significant difference was found when comparing the binominal data of OA incidence in control *versus* healthy knees. No significant difference was found between MSC-secretome or MSC-treated knees as compared to healthy knees, indicating a chondroprotective effect. $^{a}p < 0.05$.

OA incidence	Healthy	Control	MSC secretome	MSC
AO	0	5	2	2
Non-OA	11	5	9	9
Percentage AO	0.0 %	50.0 %	18.2 %	18.2 %

To further appraise the influence of MSC secretome on OA processes, the effects on subchondral bone remodelling at day 5 and day 21 after treatment were determined (Fig. 3a,b). Although subchondral bone volume appeared to be slightly decreased in knees with induced OA, no significant difference between any of the groups was found.

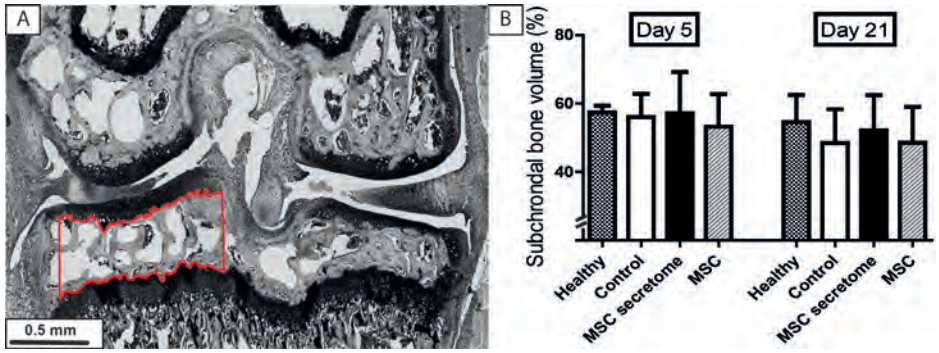

Figure 3. Subchondral bone volume percentage of total volume of subchondral space between calcified cartilage and growth plate was calculated as depicted in A. No differences were found between healthy and OA induced knees or any of the treatment groups. Data shown as mean ±SD for medial tibial plateau, N=7/group at day 5 and N=11 at day 21; healthy knees N = 5 at day 5 and N = 6 at day 21.

MSC secretome had no effect on synovial membrane inflammation

All collagenase-injected knees displayed a significantly thickened synovial membrane when compared to healthy knees at 5 and 21 d after treatment (Fig. 4a,b; $p < 0.001$ for both time points). No significant difference was observed between treatment groups within each time point. Overall, synovial membrane thickness was largely reduced over time between day 5 and day 21 for all groups ($p < 0.001$).

To further analyse the synovial inflammation processes, the presence of different macrophage subtypes was assessed by the presence of iNOS+ (pro-inflammatory), CD163+ (anti-inflammatory) and CD206+ (tissue repair) cells in the different treatment groups. The presence of iNOS+ cells was not significantly different between the treatment groups at each time points individually or between both time points (Fig.

4c). A trend was observed towards a lower presence of iNOS+ cells in the control vs. MSC group at day 5 ($p = 0.053$). A significant increase in the presence of CD163+ and CD206+ cells was found in all groups at day 21 vs. day 5 ($p < 0.001$ and $p = 0.004$, respectively), but no differences in the presence of CD163+ or CD206+ cells were observed between treatment groups at both time points.

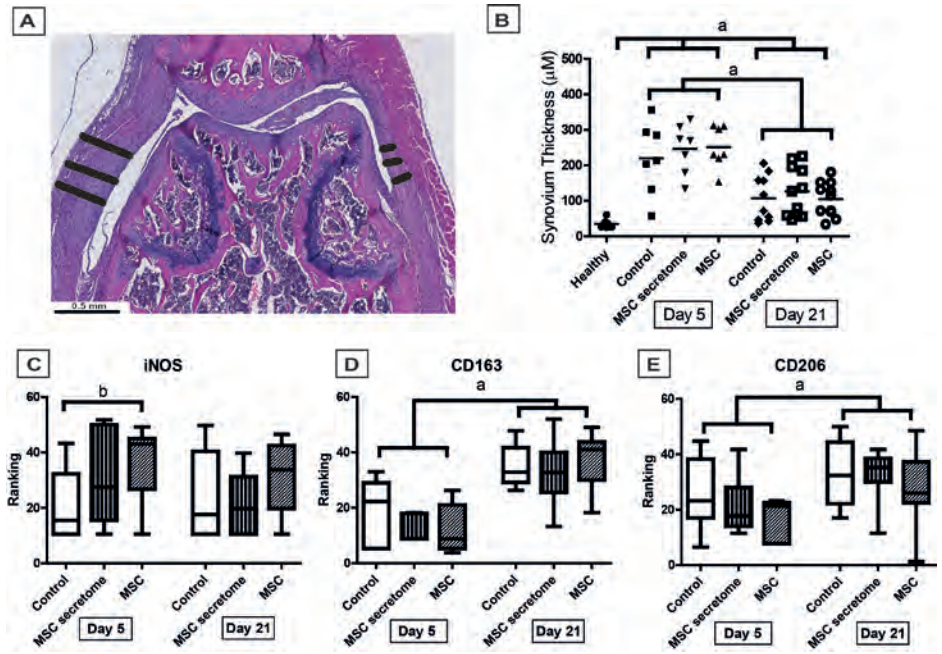

Figure 4. Synovial membrane thickness decreases in time, no effect of treatment groups is seen. Individual values are shown, lines represent mean values **(A, B)**. A trend towards more iNOS positive staining is seen in the MSC group at day 5. The amount of CD163 and CD206 staining increases in time. Box and whiskers plots are shown, lines represent median values **(C)**.

To further unravel the inflammatory processes and their relation to pain and structural damage, these aspects were correlated to the presence of the different macrophage subtypes (Table 2). An increased staining for CD163+ cells (anti-inflammatory macrophages) was moderately associated with a thinner synovial membrane [correlation coefficient (CC) = – 0.397, $p = 0.003$, all treatment groups combined], but not with cartilage damage. This could indicate that more staining for anti-inflammatory macrophages was related to less synovial inflammation. In addition, the amount of CD163+ staining was moderately associated with less pain at day 14 (CC = – 0.394; $p = 0.026$), possibly pointing towards pain reduction in the presence of anti-inflammatory macrophages. CD163+ staining was weakly associated with the intensity of CD206+ staining (CC = 0.281; $p = 0.042$), representing the co-presence of

anti-inflammatory and repair-related macrophages. CD206+ staining was moderately associated with both lateral (CC = 0.465; p = 0.007) and medial OA damage (CC = 0.412; p = 0.028), but not with synovial thickness. This could indicate a higher presence of tissue-repair-associated macrophages in the situation of more cartilage damage. Lastly, a moderate association between subchondral bone volume and synovial thickness was found (CC = 0.496, p < 0.001), possibly indicating an increased bone remodelling with increased synovial inflammation. No significant associations were found between iNOS+ staining and pain, synovial thickness or cartilage damage. There were no associations between pain and synovial thickness, OA score or subchondral bone volume.

Table 2. Selection of correlations coefficients between the parameters tested. Associations between $CD163^+$ and $CD206^+$ staining and various OA aspects as reported in previous figures. * Weight distribution on the affected limb was measured as an indicator of pain; the higher the percentage of weight on the affected limb the less pain, thus giving a negative association with $CD163^+$ cells. Synovial thickness, subchondral bone volume and macrophage data based on day 5 and day 21 time points, OA score based on day 21 time point only.

Parameters tested by Spearman ρ		Correlation coefficient	Strength	*p*-value	Interpretation
CD163 + cells	Synovial membrane thickness	− 0.397	Moderate	0.003	Higher CD163 staining intensity associated with thinner synovial membrane
CD163 + cells	Pain day 14	− 0.394	Moderate	0.026	Higher CD163 staining intensity associated with less pain at day 14*
CD163 + cells	$CD206^+$ cells	0.281	Weak	0.042	Higher CD163 staining intensity associated with more repair macrophages
CD206 + cells	Lateral OA score	0.465	Moderate	0.007	Higher CD206 staining intensity associated with more lateral OA damage
CD206 + cells	Medial OA score	0.412	Moderate	0.019	Higher CD206 staining intensity associated with more medial OA damage
Subchondral bone volume	Synovial membrane thickness	0.496	Moderate	< 0.001	Larger subchondal bone volume associated with thicker synovial membrane

Discussion

Injection of human MSCs secretome resulted in an early pain reduction and had a protective effect on the development of cartilage damage in a mouse collagenase-induced OA (CIOA) model. No clear treatment effects were observed on subchondral bone remodelling or synovial inflammation, although several significant moderate correlations between macrophage phenotypes and OA characteristics were found. These correlations enhanced the understanding of the inflammation role in the mouse CIOA model. MSC secretome injections were at least as effective as MSCs in

the amelioration of OA related pain or morphological changes, endorsing the potential of this cell-free approach.

MSCs diminish several OA characteristics, as demonstrated in pre-clinical and some initial clinical studies [28, 29, 31, 32, 82, 94]. Although intra-articular injection of MSCs does benefit the joint after OA induction, the MSCs themselves are not detectable 3 weeks after injection [32]. This limited presence of the MSCs in the joint is also observed by Diekman *et al.* [39] and Mak et. al. [40], the latter suggesting that this is due to differentiation, migration or cell death. Thus, although long-term engraftment is not present, intra articular injection of MSCs can have a beneficial effect, leading Prockop [36] and von Bahr [42] to postulate the 'hit-and-run' mechanism, in which the MSC-secreted factors play an important role. The use of the therapeutic MSC secretome without actual employment of cells originates from the cardiovascular field [99]. Although the longevity of the secreted factors is expected to be even lower than that of the MSCs, they seem to have an effect in vivo, possibly by activating a cascade of reactions.

It is not known which factor(s) in the MSC secretome is responsible for the anti-osteoarthritic effect. Next to IL-6, prostaglandin E2 (PGE2), TNF stimulated gene 6 (TSG-6) and hepatocyte growth factor (HGF), which are partly responsible for some effects in various disease models (reviewed by Madrigal *et al.,* [100]), extracellular vesicles secreted by the MSCs are speculated to be important for injury reduction and repair in, for example, experimental myocardial infarction, stroke or endotoxin-induced lung injury, as reviewed by Konala *et al.* [101] and Rani *et al.* [57]. In the orthopaedic field, Platas *et al.* (2013) demonstrate protective effects of adipose tissue-derived MSC secretome in an inflammatory in vitro chondrocyte model [102]. Other groups show beneficial effects of MSC-derived exosomes and/or particles in various pre-clinical OA models in vivo, as reviewed by Toh *et al.* [103]. Although the extracellular vesicle content in the MSC secretome was not quantified, a large proportion of the extracellular vesicles, mainly the exosomes (10-100 nm) and microvesicles (100 1000 nm), was most likely retained [104]. The retention of the extracellular vesicles is described by the manufacturer when using the Amicon Ultra-4 Centrifugal Filter Unit, even with a larger 10 kDa cut-off. Therefore, the observed effects were due, possibly, to the MSC extracellular vesicles, which provide a controlled microenvironment and protect their content from degradation in vivo thanks to their bilayer membrane [105]. These in vivo effects were promising and encourage the further unravelling of the MSC therapeutic function. Nevertheless, these cited studies are based on extracellular vesicles isolated from the secretome of young animals, human embryonic stem cells or genetically modified cells. To our knowledge, this was the first evidence of in vivo anti-osteoarthritic effects of MSC secretome isolated from aged human donors with end-stage OA.

Although promising, the MSC secretome could also contain components causing an adverse effect. Additional proteomic studies are needed to examine the exact components of the secretome, to further elucidate its working mechanism. The secretome use would greatly reduce problems linked to safety and legal issues related to cell-based therapies, thereby emphasising the clinical relevance of these findings. If the MSC secretome could be used in OA therapies as an alternative to MSCs, the possibilities to provide a more standardised and affordable therapeutic option would be largely increased. Good manufacturing practice (GMP) facilities could become more centralised and large quantities of MSC secretome could be generated from well-defined, selected batches of MSCs. The secretome could be checked for predetermined concentrations of cytokines and growth factors. These could either be preferable or non-preferable cytokines depending on the application. Simultaneously, problems raised by legal and safety issues regarding the use of cell therapy would be decreased. Nevertheless, such an approach might bring new safety and regulatory issues, such as finding suitable MSCs donors for maintaining a large scale secretome production in vitro.

The pain reduction by treatment with MSC secretome or MSCs, as seen in the present study, lasted for the entire experiment. Interestingly, the control group showed a pain reduction as well, only at a later time point. This indicated a general pain reduction as the natural course of the used OA model, as found before [106]. This is also described by Adaes *et al.,* who found a maximum of pain sensation 1 week after OA induction by collagenase in a rat model[107]. This pain sensation gradually decreased in a period of 4 to 6 weeks after induction. Clinically, OA-related pain is correlated to the radiological presence of synovial inflammation as well as bone marrow lesions, as seen by magnetic resonance imaging [108]. In the CIOA model, both synovial inflammation and dynamic subchondral bone changes are present [109] [109] Osteochondral angiogenesis is shown in OA, in which neural growth factor expression and sensory nerve growth may be the links to perceived pain [110]. Since cartilage itself is an aneural tissue, this is a plausible mechanistic explanation for pain perception in OA. Subchondral bone changes are biphasic during OA: an initial atrophic phase leads to a decreased subchondral bone volume, after which a hypertrophic phase initiates the increase in bone volume [111]. Botter *et al.* find initial thinning of the subchondral bone plate 2 weeks after OA induction in a mouse CIOA model, after which, at 10 weeks, subchondral bone thickness returns to levels comparable to before OA induction[109]. Clinically, fully eroded joint regions display a thickened subchondral bone region, whereas partially eroded areas show a thinner subchondral bone plate as compared to non-eroded regions [110] . Regarding the effect of mesenchymal cells on subchondral bone, Parrilli *et al.* show that injection of adipose-derived stromal cells counteracted accelerated bone turnover in a rabbit OA model[112]. A trend towards

a decrease in bone volume was observed in the used CIOA model, but no effects of the different treatments nor a correlation between pain reduction and subchondral bone volume were found. The discrepancy in the absence of an MSC effect in the present study could possibly be due to the fact that subchondral bone volume was calculated on histological slides instead of on true 3D volumetric or densitometric bone measurements by micro-computed tomography (µCT).

The first phase after collagenase injection in the CIOA model is an inflammatory phase, leading to synovial thickening and infiltration with inflammatory cells within 1 week. Cartilage damage and other pathological OA-related changes become more pronounced after 2 to 4 weeks, with marked OA changes found after 6 weeks[107, 113]. Although a clear pain reduction in MSC-secretome- and MSC-treated animals was observed 1 week after treatment – which is 2 weeks after OA induction – no treatment effects on synovial thickness or synovial macrophage phenotype were found at that time point nor at a later stage. In fact, a trend towards a larger presence of iNOS+ cells was observed in MSC-treated knees, which could indicate a more pro-inflammatory phenotype. Synovial inflammation most likely played a role in pain perception, partly given the fact that pain and synovial inflammation both diminished in time. Nevertheless, it was not possible to relate the early analgesic effect of MSC secretome or MSCs to this OA characteristic. Ter Huurne *et al.* observe a clear anti-inflammatory effect after injection of adipose-derived stem cells in a mouse collagenase model [31]. The discrepancy between this report and the present study's findings could possibly be explained by the use, in the present study, of human cells in an immunocompetent mice strain. Other groups describe that although immuno-privileged, MSCs maintain a degree of immunogenicity [58]. A trend towards increased synovial inflammation is observed after injection of allogeneic rat MSCs in a rat mono-iodoacetate (MIA) model of OA [85]. This increased synovial inflammation is significant when using xenogeneic human MSCs [32], further pointing towards the maintenance of the MSC immunogenicity. In this aspect, the use of the MSC secretome is likely to be safer, because the concentration of immune complexes – possibly present on the extracellular vesicles – in the secretome is lower than with cells, causing a weaker host inflammatory response [57]. Although there is the possibility that some factors in the human MSC secretome might not cross react with the mouse immune system. Therefore, it is not possible to conclude that the secretome showed its full potential. Furthermore, the secretome could contain components causing an adverse effect. Additional proteomic studies are needed to examine the exact components of the secretome, to further elucidate its working mechanism.

In conclusion, human MSC secretome from patients with end-stage OA was shown to diminish pain and structural OA-related changes in a mouse CIOA model. These effects were at least as effective as injection of MSCs themselves. The use of MSC secreted factors instead of the cells themselves provides options to enhance standardisation, affordability and efficacy of this therapeutic approach. The study's results encourage further development of this strategy towards cell-based treatments as a true disease-modifying anti-osteoarthritic drug with wide clinical availability.

CHAPTER 4

Intra-articular allogenic MSC secretome reduces inflammation in an equine model

Published as

Effects of intra-articular allogenic mesenchymal stem cell secretome in an equine model of joint inflammation

Clodagh M. Kearney, Sohrab Khatab, Gerben M. van Buul, Saskia G. M. Plomp, Nicoline M. Korthagen, Margot C. Labberté, Laurie R. Goodrich, John D. Kisiday, P. R. Van Weeren, Gerjo J. V. M. van Osch and Pieter A. J. Brama

in Frontiers in Veterinary Science, 2022

Sohrab Khatab helped design and prepared the injections for the experiments (production of MSC and MSC secretome), drafted part of the manuscript, edited and reviewed the complete manuscript.

Abstract

Background: Allogenic mesenchymal stem cell (MSC) secretome is a novel intra articular therapeutic that has shown promise in in vitro and small animal models and warrants further investigation.

Objectives: To investigate if intra-articular allogenic MSC-secretome has anti inflammatory effects using an equine model of joint inflammation.

Study Design: Randomized positively and negatively controlled experimental study.

Method: In phase 1, joint inflammation was induced bilaterally in radiocarpal joints of eight horses by injecting 0.25 ng lipopolysaccharide (LPS). After 2h, the secretome of INFy and TNFα stimulated allogeneic equine MSCs was injected in one randomly assigned joint, while the contralateral joint was injected with medium (negative control). Clinical parameters (composite welfare scores, joint effusion, joint circumference) were recorded, and synovial fluid samples were analyzed for biomarkers (total protein, WBCC; eicosanoid mediators,CCL2;TNFα;MMP;GAGs;C2C;CPII)at fixed post-injection hours (PIH 0, 8, 24, 72, and 168h). The effects of time and treatment on clinical and synovial fluid parameters and the presence of time-treatment interactions were evaluated. For phase 2, allogeneic MSC-secretome vs. allogeneic equine MSCs (positive control) was tested using a similar methodology.

Results: In phase 1, the joint circumference was significantly ($p < 0.05$) lower in the MSC-secretome treated group compared to the medium control group at PIH 24, and significantly higher peak synovial GAG values were noted at PIH 24 ($p < 0.001$). In phase 2, no significant differences were noted between the treatment effects of MSC-secretome and MSCs.

Main Limitations: This study is a controlled experimental study and therefore cannot fully reflect natural joint disease. In phase 2, two therapeutics are directly compared and there is no negative control.

Conclusions: In this model of joint inflammation, intra-articular MSC-secretome injection had some clinical anti-inflammatory effects. An effect on cartilage metabolism, evident as a rise in GAG levels was also noted, although it is unclear whether this could be considered a beneficial or detrimental effect. When directly comparing MSC-secretome to MSCs in this model results were comparable, indicating that MSC-secretome could be a viable off-the-shelf alternative to MSC treatment.

Introduction

Osteoarthritis (OA) is a common debilitating disease in horses and humans [114]. Given the fact that chronic and intermittent inflammation plays a predominant role in the prolonged disruption of joint homeostasis characteristic of OA, inflammation appears to be a logical target for novel therapeutics.

Mesenchymal stem cells (MSCs) are increasingly considered to be a promising biological treatment option for OA in horses and humans, and recently much focus has been on the use of allogenic MSCs [115]. While there is still some discussion regarding the safety and efficacy of allogenic MSCs, more recent studies have shown that allogenic MSCs show similar effects to autologous MSCs in normal and inflamed joints [116], and a recent review concluded from accumulating evidence in studies to date in horses that allogenic MSCs are safe [115]. Recently an allogenic mesenchymal stem cell product became the first stem cell-based veterinary medicine approved by the European Medicine Agency [117].

There is mounting evidence that the anti-inflammatory effects of MSCs result from their capacity to influence their micro-environment through the secretion of trophic factors [26, 34-38]. These secreted factors, known as secretomes are a cocktail of mediators and extracellular vesicles involved in many processes including inflammation and regeneration. Beneficial therapeutic effects of stem cell secretome were first described in the cardiovascular field, where a group investigating the potential therapeutic effects of MSCs on cardiomyocytes after exposure to hypoxia demonstrated *in vivo* that myocardial protection could also be afforded by concentrations of paracrine factors secreted by MSCs [99]. The potential of these secreted factors to exert paracrine effects was naturally of interest in orthopedic research. While early experimental work with MSCs focused on exploring their capacity for differentiation and repair or regeneration of damaged joint tissues, the ability of MSCs to locally embed and replace damaged tissue is now known to be low [29, 118]. Similar to the work with cardiomyocytes it has now been hypothesized that much of the therapeutic effectiveness of MSCS in joint disease is due to their release of paracrine factors which could counteract inflammatory and catabolic processes and foment endogenous repair [36, 38, 45]. This has led researchers to investigate these secreted factors themselves as novel therapeutics rather than the parent MSCs. Our group and others have previously shown beneficial effects of MSC-secretome in *in vitro* and small animal *in vivo* OA models where an earlier reduction in pain and protective effects on cartilage were noted [45, 79, 102]. If it would be possible to use the secretome as a therapeutic treatment instead of the cells themselves, it would provide opportunities to optimize the composition and concentration of these components *in*

vitro. This would allow for an off-the-shelf cell-free treatment option with the potential to be widely available and affordable.

To the best of our knowledge, intra-articular administration of MSC-secretome has not previously been studied *in vivo* in the horse, although reports of its use in other areas have recently emerged Mocchi (18). A research group from Cornell University has investigated various applications with regard to wound healing and found that conditioned medium from equine mesenchymal stem cells had both positive effects in an equine *in vitro* wound healing model [119] and also that equine MSC-secretome inhibits biofilm formation and mature biofilms of various bacteria [120]. Lange-Consigilio *et al.* investigated conditioned medium from amniotic membrane-derived MSCs (AMC-CM) as an intralesional treatment in horses and ponies with naturally occurring tendon or ligament injuries and reported no adverse effects and favorable clinical outcomes [121]. Those promising findings further supported our aim of investigating MSC-secretome in an equine model of joint disease.

In the presented study, we use a bilateral low dose LPS-induced inflammatory joint model in horses to first investigate the potential anti-inflammatory effects of allogenic MSC-secretome on clinical parameters and various biological markers in synovial fluid related to inflammation and cartilage turnover, compared to a control consisting of carrier medium only (negative control). Next, we compared the efficacy of intra-articular MSC-secretome to allogenic MSCs from the same cell lines the secretome was derived from (positive control). We hypothesized that intra-articularly injected MSC-secretome would demonstrate anti-inflammatory effects in this equine model of joint inflammation, and that intra-articularly injected MSC-secretome would be as effective as MSCs in reducing inflammation.

Materials and Methods

Study Design

A complete overview of the study design is shown in Figure 1. In preparation for the experimental phase of the study, bone marrow-derived MSCs previously collected and stored at the Colorado State University Veterinary Teaching Hospital under the approval of the Institutional Animal Care and Use Committee of Colorado State University (15-5810A) were transported to the Erasmus Medical Center in Rotterdam. Using these cells MSC Secretome was prepared using techniques previously described for the production of secretome from Human bone marrow MSCs [79]. Control medium was also prepared as a negative control, this product being the same formulation used to transport the MSC secretome but just not having been exposed to MSCs. Cells from the same cell lines as used for the MSC preparation were also transported to Dublin, where the final preparatory steps and viability assessment were performed immediately prior to their use in Phase 2 of the experiment.

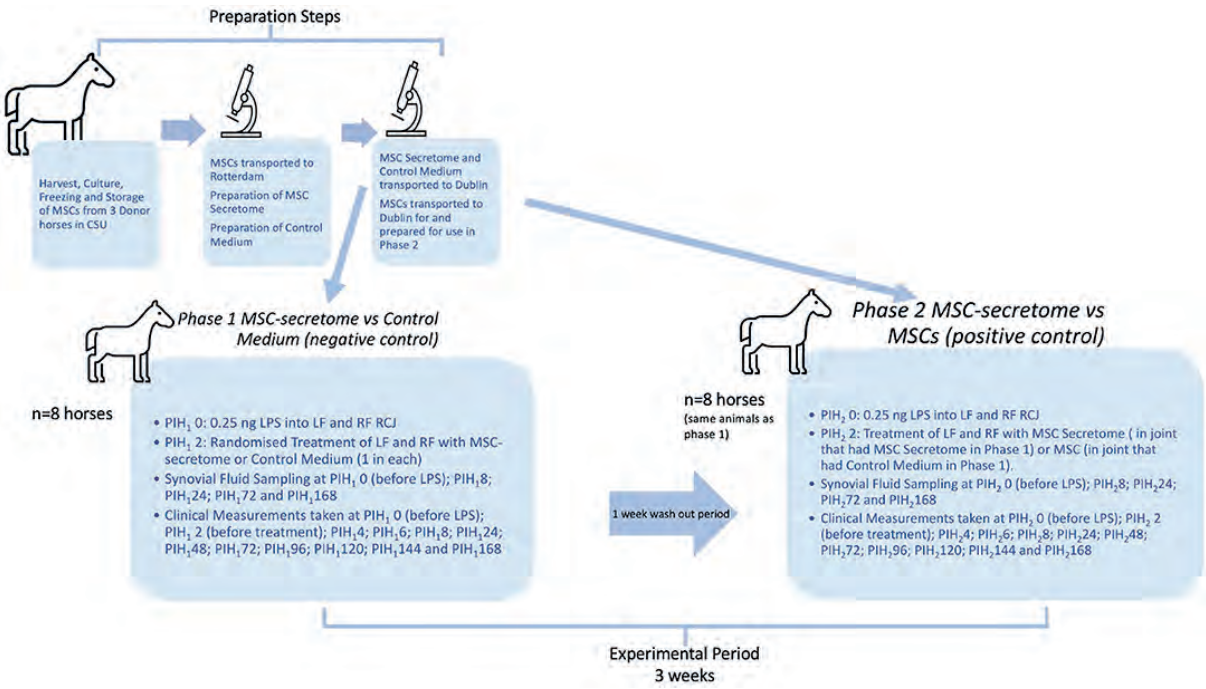

Figure 1. Overview of study design. The preparation steps were carried out in advance of the experimental period. Bone marrow derived mesenchymal stem cells (MSCs) were harvested from donor horses in Colorado State University (CSU) Veterinary Teaching Hospital and cultured, frozen and stored according to their standard protocols. Later, MSCs were transported, still frozen, to Erasmus MC in Rotterdam, where they were thawed and cultured and then used to prepare Mesenchymal stem cell secretome (MSC-secretome) treatments. Cells from the same cell lines as used for the MSC preparation were also transported to Dublin, where the final preparatory steps and viability assessment were performed immediately prior to their use in Phase 2 of the experiment. The experimental period represents 3 weeks in total. PIH (Post Induction Hour) indicates time in hours after induction of inflammation with intra-articular injection of 0.25 ng of lipopolysaccharide (LPS) in each radiocarpal joint (RCJ) of 8 horses. At $PIH_{1}2$, one randomly selected RCJ of each horse was injected with intra-articular mesenchymal stem cell secretome and the contralateral joint was injected with medium (negative control). Following $PIH_{1}168$, horses had a washout period (7 days) during which they were on pasture rest. At $PIH_{2}2$, the RCJ that had previously been treated with intra-articular mesenchymal stem cell secretome was again treated with intra-articular mesenchymal stem cell secretome and the contralateral joint was injected with mesenchymal stem cells (positive control).

For the experimental phase of the study 8 horses from the research herd of University College Dublin Lyons Research Farm were used following approval of the University College Dublin Animal Research Ethical Committee (AREC-16-29-Brama) and the Irish Health Products Regulatory Authority (AE18982-P105), in compliance with Irish legislation on experimental animal use. At the start of phase 1 both radiocarpal joints of each horse were injected with lipopolysaccharide (LPS) to induce joint inflammation. Two hours later one randomly selected radiocarpal joint of each horse was injected with intra-articular MSC secretome and the contralateral joint injected with control medium. Over the following week clinical parameters were measured and recorded, and serial synovial fluid samples were also taken during this period to determine the effect of each treatment on the joints involved. All investigators were unaware of the treatment assignment with the exception of the first author.

The same eight horses were used in both Phase 1 and Phase 2 of the study in an effort to reduce the numbers of experimental animals used so that each animal could act as its own control. Following a wash out period of 1 week after the last sampling, and 2 weeks after the first induction of inflammation with LPS Phase 2 of the study was initiated when inflammation was again induced in both radiocarpal joints of each horse with intra-articular injections of 0.25 ng of LPS. From previous work using the same dose of LPS intra-articularly, it was expected that all clinical and synovial markers of inflammation would be returned to baseline levels by this time [122]. In this phase, the radiocarpal joint that had previously been treated with intra-articular MSC-secretome was again treated with intra-articular MSC-secretome and the contralateral joint was injected with mesenchymal stem cells. Clinical measurements and synovial fluid samples were taken as before. Specific detail regarding each step of the study is documented in the following sections.

Collection and Expansion of MSCs

Equine bone marrow-derived MSCs from three donors were collected at the Colorado State University Veterinary Teaching Hospital. The procedure of harvesting and culturing MSCs is previously described [123]. Specific characterization of these MSCs was not performed, however, previously published reports from this laboratory can give us some indication of the likely behavior of these cells. In respect of specific criteria set out in a recent position paper in this journal in this journal [124] these cells should demonstrate plastic adherence [123], chondrogenic and osteogenic potential [125-127], high CD 90, and low to negligible MHCII expression [125, 128]. The MSCs were cryopreserved in a freeze media comprised of 95% fetal bovine serum (FBS) and 5% dimethyl sulfoxide (DMSO) and stored at −80°C prior to being shipped to Rotterdam. There the MSCs were cultured using previously described procedures [79]. Briefly, MSCs were thawed, counted, and plated at 50,000 cells/cm^2 and, after 24 h, the flasks

were rinsed to remove the non-adherent cells. When 70% confluency was achieved, MSC were trypsinized [0.25% trypsin/ethylenediaminetetraacetic acid (EDTA) solution (Life Technologies)] and seeded in cell culturing flasks at a density of 2,300 cells/cm^{2}in expansion medium consisting of minimal essential medium alpha (αMEM; Gibco), 10% heat inactivated fetal calf serum (FCS; Gibco), 1.5 µg/ml fungizone (Invitrogen), 50 µg/ml gentamicin (Invitrogen), 25 µg/ml ascorbic acid-2-phosphate (Sigma-Aldrich) and 1 ng/mL fibroblast growth factor 2 (FGF2; AbD Serotec, Oxford, UK). Cells were cultured in an incubator at 37°C, 5% CO_2, and 90% humidity. The medium was refreshed 2 times a week. MSCs were passaged at ~70% confluency. The cells were passaged three times in a monolayer prior to being used in the experimental protocols.

Preparation of MSC-Secretome and Control Medium

The dose of secretome per joint was planned to be the secretome equivalent of 10×10^6 MSCs. To produce the MSC-secretome, passage 3 MSCs were plated at a density of 3.5×10^4 cells/cm^2 and cultured for 24 h in an expansion medium. After 24 h, cells were activated to secrete immunomodulatory factors by culturing for 24 h in stimulating medium van [45, 79]. This stimulating medium consisted of αMEM supplemented with 1.5 µg/ml fungizone, 50 µg/ml gentamicin, 1% insulin–transferrin–selenium (ITS; Biosciences), 50 ng/ml equine interferon gamma (Recombinant Equine IFN-gamma Protein, R&D) and 50 ng/ml equine tumor necrosis factor alpha (Recombinant Equine TNF-alpha Protein, R&D). After 24 h of stimulation, MSCs were washed five times with phosphate-buffered saline (PBS; Gibco). To collect the paracrine factors, a collecting medium was added, consisting of only αMEM (MEM α, nucleosides, no phenol red, ThermoFisher) with 0.05% equine serum albumin (ESA; Rocky Mountain Biologicals Inc.)—to stabilize the secreted factors and as an adhesive for smaller molecules to bind to and to be retained after the concentration step—and without phenol red that can mimic estrogen and therefore influence cell behavior *in vivo*. About 1 ml of collecting medium was added per 2.0×10^5 MSCs. MSC-secretome was collected after 24 h and centrifuged at 700 × g for 8 min to remove cell debris. To achieve the desired concentration (secretome equivalent of 10×10^6 MSCs) in an end volume of 3 ml, suitable for intra-articular injection, the MSC-secretome was concentrated, according to a previously developed protocol by our lab [79]. Briefly, this was done by loading MSC-secretome on a 3 kDa cut-off filter (Merck Millipore Centricon Plus-70 device, 3K) and spinning down for 20 min at 4,000 ×g. Molecules above 3 kDa were retained. The concentrated equine MSC-secretome was collected, aliquoted, and stored at −80°C for further use. For each injection concentrated MSC-secretome from each of the three donors was pooled to give aliquots of a final volume of 3 ml, representing the secretome of 10×10^6 MSC.

Control medium was prepared by subjecting the collecting medium used for the MSC-Secretome—αMEM (with no phenol red) and 0.05% equine serum albumin—to the same handling as the MSC-secretome, including 24 h incubation and concentration step, but not including exposure to the MSCs, and then stored at −80°C until required.

Both the MSC-secretome and the control medium were thawed on ice immediately prior to injection.

Preparation of MSC Injections

Circa 24 h prior to injection the culture flasks containing MSCs from the same cell lines as used for the production of MSC-secretome, were washed five times with phosphate-buffered saline (PBS; Gibco). Whereafter the same collecting medium as in the MSC-secretome preparation was added, consisting of only αMEM w/o phenol red with 0.05% equine serum albumin (ESA; Rocky Mountain Biologicals Inc.). Unlike the cells used for the MSC-secretome production, these MSCs were not stimulated with equine interferon gamma and equine tumor necrosis factor alpha as it was considered they would be exposed to an inflammatory environment in the LPS-inflamed joints. After 24 h, the MSCs were trypsinized and the MSCs were collected. The viability of the MSCs was evaluated after trypsinization: <5% of the cells were dead, as indicated by visual assessment following trypan blue positive staining. For each intra-articular injection, cells were pooled from each donor to give a total of 10×10^6 MSC collected in a volume of 3 ml of control medium. The cells were injected within 2–4 h of trypsinization and evaluation.

Experimental Animals

Eight horses (16 joints) were selected to participate in a randomized controlled experiment. The animals of various breeds (six mares and two geldings) (mean ± SD age 14.6 ± 2.4 years, bodyweight 370.4 ± 27.6 kg) were from the University research herd. There was no known history of forelimb lameness in any of the animals. Each animal was examined clinically by 2 ECVS boarded surgeons, and was found to have no sign of forelimb lameness. On clinical and radiographic examinations their carpal joints were found to be within normal limits. While individual animals were previously used in other experimental studies the radiocarpal joints of these animals had not previously been injected or treated in any way. During the sampling phases of the experiment, the animals were stabled individually in single boxes (4 m × 4 m) on wood shavings. Horses received concentrates once daily, with regular hay and water provided *ad libitum*. Following the week of sampling and measurements during which the horses were stabled, they were then turned out to pasture in a familiar group for a week. They were brought back in on the morning of the second induction of LPS and were again stabled under the same conditions during this second week of sampling

and measurements. Before commencement of Phase 2 of the study, each animal was again examined by two ECVS boarded surgeons and was found to be free of any forelimb lameness and of any clinical signs of inflammation of the radiocarpal joints (joint effusion, heat, or pain on palpation or flexion).

Experimental Protocol

Induction of Inflammation

At post induction time (PIH) 0, both carpi of each horse were clipped and prepared for dorsal arthrocentesis. Lipopolysaccharide from *Escherichia coli* O55:B5 (catalog number L5418; Sigma-Aldrich Ireland Ltd., Arklow, Co. Wicklow Ireland) was diluted to a final concentration of 0.25 ng/ml in sterile lactated Ringer›s solution. Horses were sedated with xylazine (0.2–0.5 mg/kg intravenously, Chanazine 10%® Chanelle, Ireland) and butorphanol (0.01–0.02 mg/kg intravenously; Alvegesic vet 10®, ALVETRA u. WERFFT GmbH, Vienna, Austria). Synoviocentesis was performed in each limb with a 20 G × 40 mm needle and 1 ml LPS solution (0.25 ng LPS) was delivered aseptically into each radiocarpal joint after withdrawal of the PIH 0 synovial fluid (SF) sample.

Treatments

Phase 1 MSC-Secretome vs. Medium (Negative Control)

In the first phase of the experiment, 2 h following induction of inflammation with LPS ($PIH_1 2$), following preparation of the regions as before, one randomly assigned radiocarpal joint of each horse was injected with 3 ml of allogeneic MSC-secretome (treatment), and the opposite radiocarpal joint was injected with the same volume of control medium (negative control).

Phase 2 MSC-Secretome vs. MSCs (Positive Control)

Following a wash-out period of 1 week after the last sampling, and 2 weeks after the first induction of inflammation with LPS, the same group of horses was used for Phase 2 of the study. From previous work using the same dose of LPS intra-articularly, it was expected that all clinical and synovial markers of inflammation would be returned to baseline levels by this time [122]. In this second phase of the experiment, 2 h following induction of inflammation with LPS ($PIH_2 2$), following preparation of the regions as before, the same radiocarpal joint as had been treated with allogeneic MSC-secretome in the previous phase was injected with secretome (treatment), and the opposite radiocarpal joint was injected with allogeneic MSCs (positive control).

Clinical Evaluations

Welfare Monitoring

Before synoviocentesis and induction of inflammation and again every 2 h until PIH 8, and thereafter daily until PIH 168 a Composite Welfare Score (CWS) was assigned by an experienced vet. The CWS is the sum of scores for each of the following categories: food and water intake; clinical parameters (temperature, pulse, and respiratory rate); natural behavior; and provoked behavior. Each of the categories is scored on a scale of 0–4, so the total range of scores is 0–16. This scoring system has been designed by our group for this bilateral equine LPS model to monitor welfare and to fulfill institutional and national ethical regulatory requirements (scoresheet available in supporting information).

Clinical Measurements

In each induction, before synoviocentesis at PIH 0, every 2 h until PIH 8, and thereafter daily until PIH 168, radiocarpal joint effusion was graded on a subjective scale as previously described [129]. An experienced clinician carefully palpated the joints and assigned a score ranging from 0 to 4; a score of 1, 2, or 3 denoting mild, moderate, or severe radiocarpal joint effusion, respectively, and 4 indicating severe swelling of the entire carpal region. In addition, joint circumference was measured at a fixed anatomical landmark at the level of the accessory carpal bone with a tape measure in mm. At the start of each phase, a mark was drawn on the skin over the accessory carpal bone to use as a reference point so that all measurements would be taken at the same level. All clinical measurements were performed by the first author and therefore cannot be considered to be blinded.

Synovial Fluid Analysis

At fixed time points (PIH 0, 8, 24, 72, and 168), synoviocentesis of each radiocarpal joint was performed under sedation as described above and a 4–5 ml sample of synovial fluid was collected. About 1.3 ml of this synovial fluid was placed in ethylenediamine tetra-acetic acid (EDTA) for manual white blood cell count (WBC) and total protein (TP) measurement (refractometer). The remainder was immediately centrifuged in plain tubes for 15 min at 4°C at 10,000 rpm and then aliquoted and stored at −80°C until further analysis.

Synovial Fluid Molecular Biomarker Analysis

Seven assays were performed on each synovial fluid sample.

Eicosanoid inflammatory mediators—Prostaglandin F2α (PGF2α), Prostaglandin E_2(PGE_2), Prostaglandin E_1 (PGE_1), Leukotriene B_4 ($LTB_{4)}$, and 11-hydroxyeicosatetraenoic acid (11-HETE)—concentrations were determined by high-performance liquid chromatography (HPLC)–tandem mass spectrometry (MS/MS) analysis using previously validated methods [130]. Briefly, measurements were made using a 4000 Q TRAP mass spectrometer with electrospray ionization (EPI) interface (Sciex, Toronto, ON), operated in multiple-reaction monitoring (MRM) mode at unit mass resolution. The mobile phases consisted of 10 mM ammonium acetate pH 3.5 in water, and 10 mM ammonium acetate pH 3.5 in methanol. Peaks were identified by comparison of retention time and mass spectra of standards using Analyst software version 1.6.2 (Applied Biosystems, Nieuwerkerk a/d IJssel, The Netherlands).

General matrix metalloproteinase (MMP) activity was measured using cleavage of fluorogenic substrate FS-6i (Calbiochem, San Diego, CA, USA) as previously described [131, 132]. Briefly, samples were first diluted 20-fold in MMP buffer [0.1 mol/L Tris, 0.1 mol/l NaCl, 10 mmol/L $CaCl_2$, 0.05% (w/v) Triton X-100, 0.1% (w/v) PEG6000, pH 7.5 and 5 mmol/L FS-6]. Samples were subsequently added in triplicate to a black 384-well microplate and the fluorescent signal was monitored continuously for 45 min at 37°C using a CLARIOstar microplate reader. The slope of the resultant linear curve [relative fluorescence units/s (RFU/s)] was then calculated as a measure of general MMP activity. A quantity of 5 mmol/L EDTA was used as a negative control.

Synovial fluid samples were evaluated for glycosaminoglycan (GAG) concentrations using a modified 1,9-dimethylmethyleneblue assay adapted for use in microtitre plates, as previously described [133].

C–C motif chemokine ligand 2 (CCL2) and tumor necrosis factor-α (TNF-α) concentrations were quantified using commercial equine-specific ELISA kits (DIY0694E-003 Kingfisher Biotech, Minnesota USA and #ESS0017, Thermo Fisher Scientific, Massachusetts, USA) using an adapted protocol as previously described [122]. The coating buffer consisted of carbonate/bicarbonate buffer (pH 9.6) and the blocking/dilution buffer was PBS with 1% w/w bovine serum albumin (BSA) (Sigma Aldrich, Saint Louis, USA). Samples were diluted 1:1 in PBS/1% BSA/0.1% (v/v) Tween-20, and results were calculated to a standard curve plotted on four parameters logistic curve fit. Values equal to, or below the blank were set to zero.

Commercial ELISA kits were used to determine concentrations of collagen-cleavage neoepitope of type II collagen (C2C), and carboxypropeptide of type II collagen epitope (CPII) (IBEX Technologies, Quebec, Canada), following the manufacturer's recommendations. Samples for C2C were 1:1 diluted and for CPII were 1:10 diluted, both in buffer III, and results were calculated to a standard curve plotted on four parameter logistic curve fit. Values equal to, or below the blank were set to zero.

GAGs, CCL2, TNF-α, C2C, CPII, GAG were all quantified on a VersaMax™ ELISA microplate reader. GAGs were measured at 525 and 595 nm and all the ELISAs were measured according to the manufacturer's recommendations.

Statistical Analysis

An a priori power analysis was performed. The power calculation was based on previous similar studies using the LPS model with described differences in synovial fluid biomarkers indicating joint inflammation [131, 134, 135]. The power calculation suggested that eight horses would give a power of 0.8 and an alpha error rate of 0.05. Data are presented as the mean ± standard deviation (SD).

For each phase, a linear mixed effects model for repeated measures was fitted, with the horse as a random effect and time, treatment, and their interaction as fixed effects. An Independent variance-covariance structure was used in the model. Planned univariate contrasts (Wald tests) were performed between marker concentrations in MSC-secretome (treatment) and medium (negative control) (Phase 1), or MSC-secretome (treatment) and MSC (positive control) (Phase 2) treated joints at specific time points following observation of an overall significant effect of treatment, using Bonferroni's correction for multiple comparisons, with each phase considered as a separate experiment. Normality was assessed by visual inspection of plots of standardized residuals. The suitability of the mixed effects model over a linear model was assessed by AIC, BIC, and Likelihood Ratio Test. Computer software was used (*Stata Statistical Software: Release 15*. StataCorp LLC, College Station, TX) and the level of significance was set at $p < 0.05$ for all statistical analyses ($p < 0.025$ with Bonferroni correction).

Results

Phase 1: MSC-Secretome (Treatment) vs. Medium (Negative Control)

Validation of Inflammatory Response

In both control and treated limbs, clear inflammatory responses, in the form of the expected peaks and subsequent falls in total protein and synovial white blood cell counts were seen after administration of LPS (Figures 2A,B).

Welfare Monitoring

For those horses that had slight Composite Welfare Score (CWS) increases in the early stages of the period of inflammation, their scores had returned to the normal range by 24 h post induction (Supplementary Table S2).

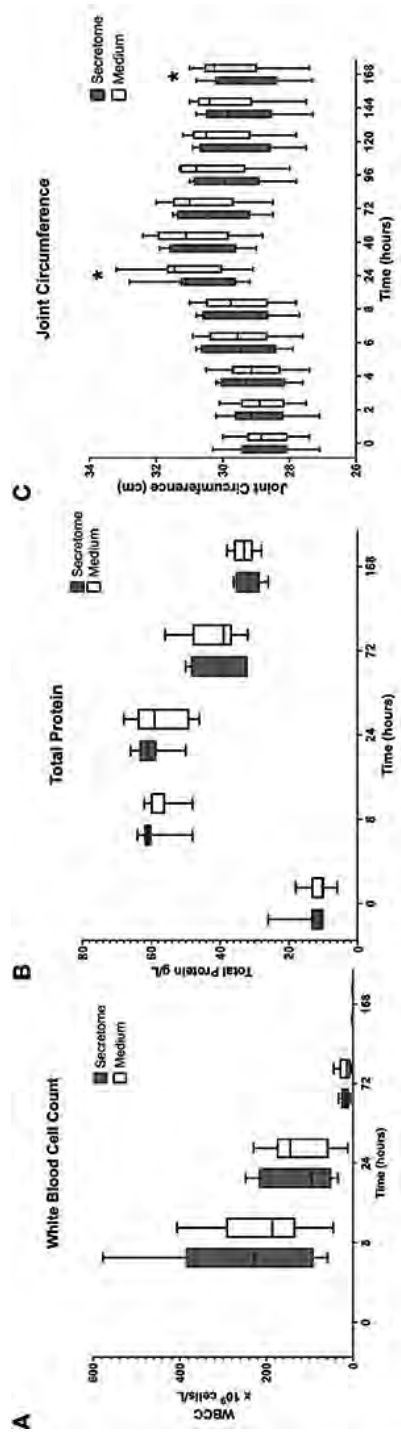

Figure 2. Phase 1 synovial white blood cell counts, total protein, and joint circumference. **(A)** Synovial White Blood Cell Count, **(B)** Synovial Fluid Total Protein, and **(C)** Joint Circumference over time following induction of inflammation with intra-articular injection of 0.25 ng of LPS in the left and right radiocarpal joints of horses at PIH_1 0 (n = 8 horses). Joints were treated with either intra-articular mesenchymal stem cell (MSC) secretome or medium (negative control) at $PIH_1$2. Boxes depict median and interquartile ranges; whiskers denote minimum and maximum values. For the Synovial White Blood Cell Count, the box and whiskers for the first timepoint are not visible on the graph as the values for these were very low with each measurement recorded being < 1 × 10^9 cells/L. *p< 0.05, indicating time points where there are significant treatment effects.

Clinical Monitoring

For the primary research question investigating the effects of intra-articular administration of secretome on joint circumference a statistically significant treatment effect was seen with a reduction in joint circumference in the MSC-secretome treated group compared to the control treated group at PIH 24 (−0.33125 cm, $p = 0.0247$) and at PIH 168 (−0.45 cm, $p = 0.0012$) (Figure 2C). From the data in Supplementary Table S3 it appears that joint circumference in both treatment groups remains above baseline levels at PIH 168, although it is not known whether these are significant differences as contrasts comparing each timepoint in each treatment group to baseline values were not performed. As joint effusion scores were on an ordinal scale, after consideration of the repeated measures design, in particular in conjunction with the small sample size ($n = 8$), formal statistical methods such as ordinal logistic regression were considered inappropriate. No appreciable differences were apparent from simple observation between treatment groups. Results are summarized in Supplementary Table S3.

Synovial Fluid Molecular Biomarker Monitoring

The results for all synovial fluid parameters are summarized in Supplementary Table S4, which also includes where available our laboratory's baseline ranges for each synovial fluid biomarker.

Regarding the effects of intra-articular administration of secretome on synovial concentrations of biomarkers, results indicate a difference in treatment effect with increases in GAG concentrations in the MSC-secretome treated group compared to the control treated group in the first phase at PIH 24 (+201.29 µ/ml, $p = 0.00067$) (Figure 3A). For the other biomarkers, treatment effects are not evident, as illustrated for selected markers in Figures 3B,C.

Summarizing the results of the comparison between MSC-secretome and medium indicated that MSC-secretome reduces joint circumference and influences GAG release, but not other synovial fluid cartilage turnover or inflammation markers.

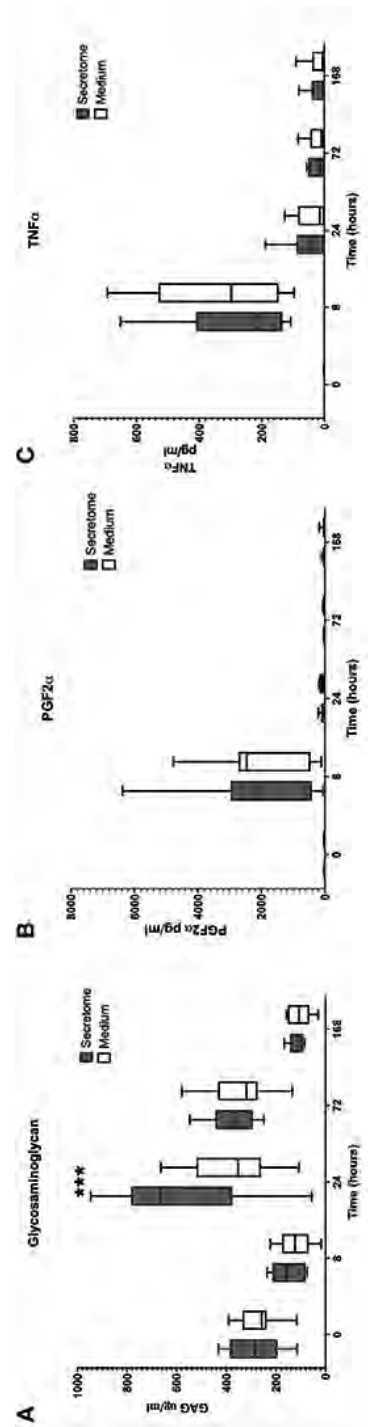

Figure 3. Phase 1 synovial fluid glycosaminoglycan, prostaglandin F2α and tumor Necrosis Factor α concentrations in synovial fluid over time following induction of radiocarpal joints of horses at PIH_1 0 ($n = 8$ horses). Joints were treated with either intra-articular mesenchymal stem cell (MSC)-secretome or medium (negative control) at $PIH_1$2. Boxes depict median and interquartile ranges; whiskers denote minimum and maximum values. ***$p < 0.001$, indicating timepoints where there are significant treatment effects.

Phase 2: MSC-Secretome (Treatment) vs. MSCs (Positive Control)

Validation of Inflammatory Response

In both groups (MSC and MSC-secretome treated joints) clear inflammatory responses in the form of the expected peaks and subsequent falls in synovial white blood cell counts and total protein were seen after administration of LPS (Figures 4A,B).

Welfare Monitoring

As in Phase 1 for horses that had slight CWS increases in the early stages of the period of inflammation, their scores had returned to the normal range by 24 h post induction (Supplementary Table S2).

Clinical Monitoring

A potentially confounding finding was that from Supplementary Tables S3, S5 it can be seen that for both treatment groups the joint circumference was slightly higher at Timepoint 0 of Phase 2 than at Timepoint 168 of Phase 1. This was unexpected as the measurements had been decreasing toward the end of Phase 1 and the horses were carefully checked at the start of Phase 2 and no evidence of joint effusion was recorded at Timepoint 0. This apparent discrepancy would seem to be due to some inconsistency in the placement of the marks drawn on the skin over the accessory carpal bone meaning that measurements were taken at slightly different levels between groups.

For joint circumference, while from PIH 24 onwards the values of the MSC-secretome treated group appeared lower than those of the MSC treated group these differences were not found to be significant (Figure 4C). For joint effusion scores, as in Phase 1, no appreciable differences were observed between treatment groups. Results are summarized in Supplementary Table S5.

Synovial Fluid Molecular Biomarker Monitoring

The results for all synovial fluid parameters are summarized in Supplementary Table S6. No significant differences between the MSC-secretome treated and MSC treated joints were noted for any clinical or synovial fluid biomarker as illustrated for selected markers in Figure 5. For synovial GAG, the peak value of the MSC-secretome treated group was higher than the peak value of the MSC treated group at PIH 24 but this did not reach significance ($p = 0.029$) (Figure 5B).

In summary, the comparison between MSC-secretome and MSCs revealed no significant difference in treatment effect.

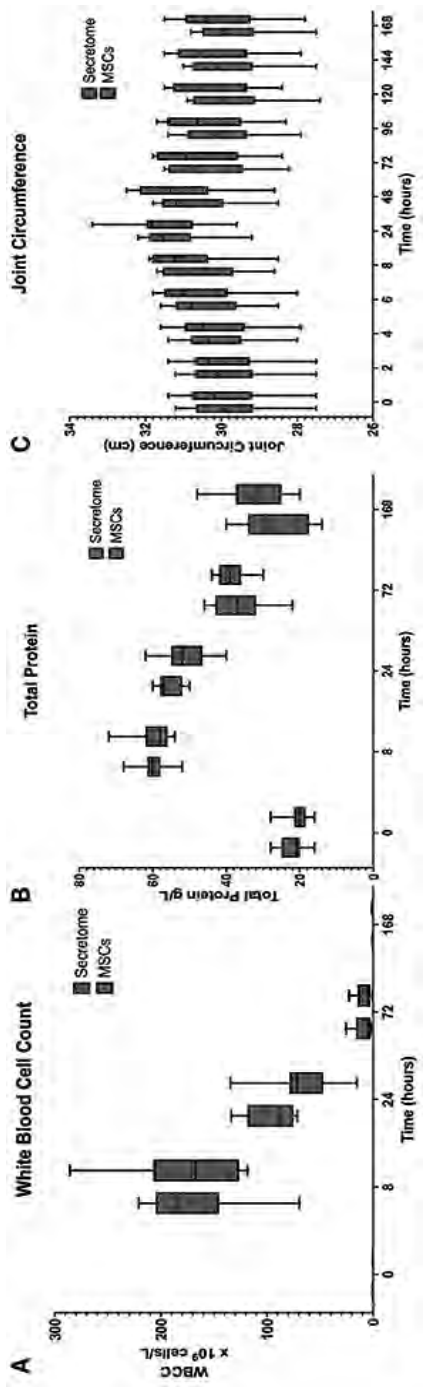

Figure 4. Phase 2 synovial white blood cell counts, total protein and joint circumference. **(A)** Synovial White Blood Cell Count, **(B)** Synovial Fluid Total Protein, and **(C)** Joint Circumference over time following induction of inflammation with intra-articular injection of 0.25 ng of LPS in the left and right radiocarpal joints of horses at PIH_2 0 ($n = 8$ horses). Joints were treated with either intra-articular mesenchymal stem cell (MSC)-secretome of mesenchymal stem cells (MSCs) (positive control) at PIH_2. Boxes depict median and interquartile ranges; whiskers denote minimum and maximum values. For the Synovial White Blood Cell Count the box and whiskers for the first timepoint are not visible on the graph as the values for these were very low with each measurement recorded is $< 1 \times 10^9$ cells/L.

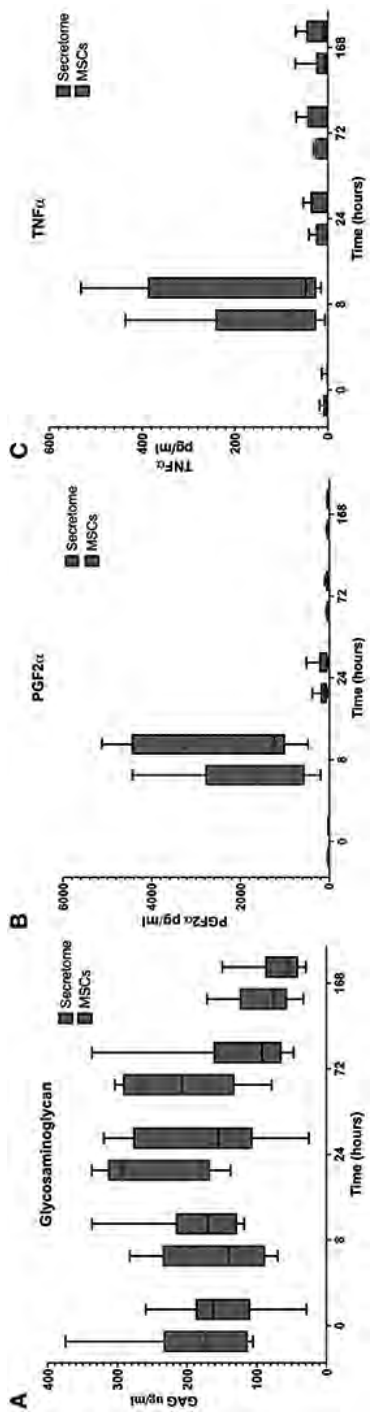

Figure 5. Phase 2 synovial fluid glycosaminoglycan, prostaglandin f2α and tumor necrosis factor α. **(A)** Glycosaminoglycan, **(B)** Prostaglandin F2α, and **(C)** Tumor Necrosis Factor α concentrations in synovial fluid over time following induction of inflammation with intra-articular injection of 0.25 ng of LPS in the left and right radiocarpal joints of horses at PIH_2 0 (n = 8 horses). Joints were treated with either intra-articular mesenchymal stem cell (MSC)-secretome of mesenchymal stem cells (MSCs) (positive control) at $PIH_2$2. Boxes depict median and interquartile ranges; whiskers denote minimum and maximum values.

Discussion

In this study, we compared the effect of intra-articular allogenic MSC-secretome in an equine within-animal-controlled model of joint inflammation to negative control (medium) and positive control (allogenic MSCs). We report two main findings. First, when compared to negative control, intra-articular allogenic MSC-secretome reduces joint circumference and increases GAG release at the 24-h timepoint (PIH 24) in an equine model of LPS induced synovial inflammation. Second, when compared in the same equine LPS model of synovial inflammation, no significant differences in treatment effects of intra-articular allogenic MSC-secretome vs. allogeneic MSCs were detected.

In our previous *in vivo* study assessing the effects of MSC-secretome injection in a murine OA model, clinical benefits such as an early reduction in pain as determined by increased weight bearing were seen [79]. In the present study, clinical benefit seen as a significant reduction in carpal circumference in the group of horses treated with MSC-secretome was noted, corroborating what was found in the earlier mouse model.

The previous *in vitro* work also demonstrated anti-inflammatory and matrix turnover altering effects of MSC secretome on human osteoarthritic cartilage and synovium [99]. In addition, we found a reduction in cartilage damage after MSC-secretome injection in our murine OA model study [45, 79]. Other groups have shown protective effects of MSC-secretome in an inflammatory *in vitro* chondrocyte model [102] and beneficial effects of MSC-derived extracellular vesicles in various pre-clinical OA models *in vivo* [136, 137]. In the present study, we demonstrated a significant increase in levels of GAGs in the synovial fluid of secretome-treated joints compared to the control (medium treated) joints. In previous studies using GAG levels as outcome assessments when investigating intra-articular therapeutics increases in GAG levels [138, 139] have been varyingly explained as either a catabolic response due to an increased breakdown of GAGs already present in the cartilage, or as an anabolic response reflected by an increase in GAG production of the cartilage being exposed to an inflammatory environment. From our results, we cannot definitively assess whether the increased GAG concentration found in secretome treated joints was caused by a catabolic or an anabolic response, but the inclusion of further biomarkers such as the CS 846 epitope which has been found to be useful as a marker of aggrecan synthesis [140] could help to clarify this in future studies.

MSCs have been studied as a potential form of cell therapy for equine joint disease in both experimental and clinical settings [141, 142]. Currently, in Europe, there are two approved veterinary stem cell-based products, namely allogenic blood or umbilical cord-derived mesenchymal stem cells, which lend credibility to their therapeutic potential. For this study, we chose allogenic bone marrow-derived MSCs as our positive

control—given similar expected effects and based on the experience of our group with bone marrow-derived MSCs. In the second phase of this study, we report that there were no significant differences in treatment effects of intra-articular allogenic MSC-secretome and allogenic MSCs in this model of joint inflammation. We consider this to be a positive finding, considering that the allogenic MSCs are now generally accepted to be safe for use in equine joints [143], and safety and efficacy have been further validated by European Medicine Agency authorizations [117]. We also observe in our study that a second dose of secretome did not result in increased inflammatory responses when compared to MSCs injection. However, it is challenging to compare our results to other studies investigating the effects of allogenic MSCs in equine joints, given the differences in MSC sources, experimental models, and outcome measures reported. As we did not directly test the efficacy of allogenic MSCs by comparing them to a negative control while we can conclude that in the second phase of our study the efficacy of MSCs and MSC-secretome are equivocal the possibility that neither are effective in this model of inflammation cannot be ruled out. It must be acknowledged that the effect on clinical measurements seen in the first phase of this study while significant is quite small, and it is unclear whether these would translate to clinical benefit. This finding is perhaps disappointing, particularly compared to the more positive results reported by Williams *et al.* for their umbilical derived MSCs [144]. However, there are many differences between the models used, not least the source of MSCs, the dose of LPS and the timing of treatment. We believe that our results do support the overall conclusions from other studies [116] [144, 145], that allogenic MSCs but also allogenic MSC-secretome are safe for use and warrant further investigation.

A significant weakness in this study is the limited characterization of the therapeutic treatments investigated. While we have previously used the techniques described to produce MSC secretome from human MSCs [79], it would have been useful to further characterize the therapeutic produced here from equine MSCs. In the absence of further evaluation of the product, it is difficult to predict what therapeutic effects it could be expected to have, and it is clear that species differences can be expected. For example, in the study by Khatab *et al.* investigation of human MSC-derived secretome, indoleamine 2,3-dioxygenase (IDO) activity was measured to confirm the anti-inflammatory potential of donors but such assay was not even possible for the equine donors as equine MSCs do not produce IDO [146]. Further evaluation of the equine MSC-secretome produced using the described techniques, which at the minimum should involve measurement of some expected inflammatory cytokines in the product should be included in any future studies. Similarly, we would consider it essential in future studies to include further characterization of the MSCs used. While previously published studies and other studies using MSCs isolated and cultured using these methods can give us some insight into the expected traits of these cells for

this study [123, 125-128] specific characterization of the pooled MSCs used for the current study was regrettably not performed. Future work should include at least the suggested minimal definitions for equine MSCs as set out in a recent position study [124]. This would not only allow for better standardization of the MSCs used and therefore of the secretome obtained, but also allow for easier comparison of these with MSCs and MSC-based products investigated by other research groups. The limited amount of characterization in the current study means that the previously mentioned disappointing comparison with other studies or reported success in clinical cases is perhaps then not surprising, as we cannot be sure that we are comparing similar products.

The horse is a particularly interesting experimental model for joint research, being both a target species for novel therapeutics and a suitable translational model [147, 148]. Based on *in vitro* findings regarding differences in the behavior of MSCs in inflammatory environments it appears that testing the safety and potential efficacy of allogeneic MSCs using experimental models of inflammation may be particularly important [143]. Previous studies examining the effects of MSCs in an *in vivo* inflammatory joint environment have each used different models of joint inflammation. Williams *et al.* reported a significant reduction in inflammation when allogenic umbilical cord blood-derived MSCs were administered into joints inflamed with a 0.5 ng dose of LPS [144]. Using the more severe amphotericin-B model of joint inflammation, to examine the effects of allogenic bone marrow derived stem cells Barrachina *et al.* reported that clinical and synovial inflammatory parameters were significantly reduced, and also that the second injection of allogeneic cells yielded no adverse reactions [145]. A further study reported by Colbath *et al.* looking at the effects of allogenic and autogenous bone marrow-derived stem cells in an rIL-1β model of synovial inflammation did not find either type of MSCs to be effective in reducing inflammation [116]. While no experimental model will exactly replicate naturally occurring disease, we have chosen to focus on the equine intra-articular LPS synovitis model as our group has extensive experience with this model and it has now been widely used for testing potential therapeutics [131, 132, 134, 135, 144]. We have demonstrated that sub nano doses of LPS elicit marked, reliable yet transient effects on certain synovial fluid inflammatory biomarkers, MMP activity, and some markers of cartilage turnover [149]. Additionally, synovial fluid biomarkers in horses have been extensively studied [140] and changes in synovial fluid concentrations of the same have been used as outcomes measures in studies investigating the effects of various interventions and therapeutics [135, 150].

One of the main limitations of large animal models, in general, is the inherent variability in biological responses between animals. Within animal controlled models are effective in counteracting this limitation. In addition, bilateral orthopedic models

have been proven to significantly enhance statistical power [151]. We recently refined our model to ethically allow for animal controlled testing of therapeutics in a bilateral low dose LPS induced inflammation model by using a lower dose of LPS (0.25 ng) [122, 132]. A disadvantage of this low dose bilateral model is that it precludes the use of unilateral lameness measurements as an outcomes measure. Lameness assessment is inherently reliant on the ability to detect asymmetry of movement between limbs, which may be absent when bilateral lameness is present [152]. We do not believe that any described lameness grading systems are suitable for application to bilateral lameness. Indeed, assigning grades in bilateral lameness is thought by some experts to be potentially misleading [152]. Furthermore, while it does produce reliable intra-articular inflammation, it is accepted that doses of <0.5 ng LPS give variable, inconsistent levels of lameness [153]. Hence lameness levels in our study, while monitored and recorded as part of the overall composite welfare scores, were not considered to be valid outcome measures in this study and therefore were not evaluated or reported as such.

We believe allogenic MSC-secretome as a treatment of joint inflammation could offer many clinical and logistical advantages over MSCs themselves. The use of allogenic stem cells has previously been acknowledged to have potential medical advantages over autologous cells [115]. Allogenic cells may be screened and characterized prior to administration leading to a more consistent, higher quality end product. Ongoing production processes rather than the logistical restraints of multiplying cells from the target animal allow for wider availability and cost effectiveness, which is of particular importance in veterinary medicine [146]. In addition to wider accessibility, the off-the-shelf nature of the potential end-product could also allow for more appropriate timing of treatment and repeated treatments where necessary. There is a further potential benefit to MSC-secretome being a cell-free product as it is known that MSCs maintain a certain degree of immunogenicity, particularly after stimulation which is performed to optimize their trophic effects [45, 55, 58]. It is expected that the concentration of immune complexes in the secretome is lower than with cells, causing a weaker host inflammatory response [57]. MSC-secretome could therefore also be a more attractive product due to the potential risk of immunological reactions to foreign MHC antigens expressed by [154].

Work outlining the importance of MSC extracellular vesicles and other secreted factors is ongoing [155]. As these components become further characterized, we may be better able to direct toward the production of certain trophic factors with the use of specific priming techniques. In addition, optimal dosages and timings need to be determined. In the future we could have the ability to produce more targeted treatments for specific conditions, and stages of the disease. While this study is an important first step to establishing the safety and potential efficacy of MSC-secretome

as an intra-articular therapeutic, clearly further investigations are needed. Equally, in the absence of an ideal experimental model for joint inflammation, and as we know different inflammatory environments can stimulate MSCs in different ways, it would be interesting to compare the effects of MSCs and MSC-secretome in different models of intra-articular disease, and even more relevantly in cases of naturally occurring disease.

Limitations

A number of limitations to this experimental model must be acknowledged. While this low dose intra-articular LPS model certainly produces a reliable intra-articular inflammation, the transient and self-limiting nature of this inflammation is of course not completely reflective of natural disease states, where recurrent episodes of inflammation play a crucial role in development and progression of OA.

A further limitation is that only markers of cartilage metabolism were investigated, and the cartilage in these joints was not directly examined either before (by means of direct arthroscopic visualization and/or biopsy) or after (arthroscopic visualization or post mortem examination) the experimental treatments were administered. It would have been interesting to compare the findings in our biomarkers to any changes in the structure of the cartilage or synovium. Histopathological evaluation of the cartilage for example have helped elucidate the reasons for the differences in GAG levels between treatment groups. However, such examinations were outside of the scope of this study.

The use of the same joints for both phases of the study could also be considered a limitation. Based on our previous work examining the effects of LPS induction and repeated inductions of LPS [122] [149] we know that outcomes measures return to baseline values around 7 days post LPS induction. Therefore, we were confident that leaving 14 days between LPS inductions would be a sufficient period. The return to within or close to baseline ranges seen for the majority of biomarkers by timepoint 168 in Phase 1 would appear to support this. While the minimal effects seen in Phase 1 of the study suggest it is unlikely that there are sustained effects in this joint as we do not know what the duration of effect (if any) of MSC-secretome is, we cannot fully exclude the possibility that in Phase 2 we are seeing the cumulative effect of two doses of MSC-secretome. An Advantage from a safety point of view was that this approach provided the opportunity to evaluate a repeated dose of the MSC-secretome, to assess if there was any obvious evidence of sensitization.

A further limitation to consider with this model is that we have not isolated the potential inflammatory effect of repeated arthrocentesis, which has been previously reported [150, 156]. Therefore, it is not possible to determine to what degree the physical insults of arthrocentesis and fluid aspiration may be contributing to the articular inflammatory reaction described, and how much of the reaction is a response

to the LPS itself. While this was not addressed here, an earlier study where responses in saline injected control joints were studied showed that while increases in gross markers of inflammation such as total protein and white blood cell counts were seen in control joints [157], these responses were substantially less than the increases noted here. Further studies comparing the effects of absolute controls (saline) to the effects of LPS found that there were substantially greater responses in the LPS injected joints across a range of markers such as prostaglandin E2 and tumor necrosis factor-α [158, 159]. Given this evidence and considering the principles of 3 R, we believe that using more animals as controls was not justified, particularly as in this bilateral model each joint undergoes the same degree of "insult" or inflammation induced from the LPS plus the physical effects of sampling across the same timeline and therefore it is the effects of the therapeutics being investigated on the sum of this inflammation that is of interest.

Conclusions

In conclusion, we have found indications for a small beneficial effect of allogenic MSC-secretome on clinically assessed inflammation as well as an effect on matrix turnover dynamics evaluated by biological markers. Additionally, while further investigations comparing the two both to each other and to negative controls are clearly needed our findings suggest that the treatment effects of allogenic MSC-secretome in this model are comparable to those of intra-articular allogenic MSCs. These results encourage further development of secretome-based strategies for therapeutic use as a durable and off-the-shelf disease modifying anti-osteoarthritic drug.

Supplementary Material

Table S1: Composite Welfare Score Sheet for the Equine LPS Model

Parameter	**Animal ID**	**Score**	**Date/Time**
Food and water intake	Normal	0	
	Moderate	1	
	Low	2	
	No food or water intake	4	
Clinical parameters	Normal temperature (T), cardiac (C) and respiratory (R)rates	0	
	Slight changes	1	
	T ± 1°C, C/R rates increase more than 30 %	2	
	T ± 2°C, C/R rates increase more than 50 %	4	
Natural behaviour	Normal	0	
	Minor changes in behaviour including mobility - increase in lameness	1	
	Less mobile and alert	2	
	Restless or still	4	
Provoked behaviour	Normal	0	
	Minor depression or exaggerated response	1	
	Moderate change in expected behaviour	2	
	Reacts violently, or very weak	4	
	Total	**0-16**	

Score	**Action**
0-3	Normal, no action to be taken
4-8	Monitor carefully, consider analgesics
9-12	Seek second opinion from named animal care and welfare officer and/or named veterinary surgeon. Consider euthanasia.
13-16	Indicates severe pain. Seek immediate second opinion from named veterinary surgeon. Animal withdrawn from project. Based on advice from named veterinary surgeon, initiate appropriate treatment and analgesia. If animal's symptoms cannot be alleviated, again in consultation with the named veterinary surgeon, consider euthanasia.

Table S2 Composite Welfare Scores

		Timepoint											
Phase		**0**	**2**	**4**	**6**	**8**	**24**	**48**	**72**	**96**	**120**	**144**	**168**
1 (MSC- secretome vs Medium)		0	0	0	4	2	0	0	0	0	0	0	0
2 (MSC-secretome vs MSCs)		0	0	0	2	2	0	0	0	0	0	0	0

Table S2 Composite Welfare Score: This score is a total of scores for each of the following categories: food and water intake; clinical parameters; natural behaviour; and provoked behaviour, over time following induction of inflammation with intra-articular injection of 0.25ng of LPS in the radiocarpal joints of horses at PIH 0. Each of the categories is scored from 0-4, so the total range of scores is 0-16. In Phase 1 joints were treated with either MSC-secretome or a similar volume of medium (control) at PIH 2 and in Phase 2 joints were treated with either MSC-secretome or MSCs at PIH 2. Data correspond to the mode (n = 8 joints for each treatment group).

Table S3 Clinical Parameters MSC Secretome vs Medium (control)

	Treatment	**Timepoint**											
		0	**2**	**4**	**6**	**8**	**24**	**48**	**72**	**96**	**120**	**144**	**168**
Joint Effusion Score	MSC-secretome	0	0	1	1	1	2	2	1	1	0	0	0
	Medium (control)	0	0	1	2	1	3	2	1	1	0	0	0
Joint Circumference (cm)	MSC-secretome	28.81 ± 0.98	28.94 ± 0.99	29.15 ± 0.99	29.48 ± 1.09	29.58 ± 1.10	30.84 ± 1.18	30.63 ± 1.05	30.29 ± 1.12	29.83 ± 1.13	31.30 ± 1.21	29.54 ± 1.20	29.35 ± 1.17
	Medium (control)	28.75 ± 0.82	28.85 ± 0.83	29.05 ± 0.97	29.49 ± 1.07	29.61 ± 1.09	31.15 ± 1.27	30.91 ± 1.23	30.65 ± 1.17	30.34 ± 1.22	30.09 ± 1.17	29.98 ± 1.22	29.80 ± 1.18

Table S3: Clinical Parameters MSC Secretome vs Medium (control)
Joint Effusion is a score (scale 0-4) for observed/palpated joint effusion recorded over time following induction of inflammation with intra-articular injection of 0.25ng of LPS in the radiocarpal joints of horses at PIH 0. Joints were treated with either MSC-secretome or a similar volume of medium (control) at PIH 2. n = 8 joints for each treatment group. Data correspond to the mode.
Joint Circumference is the joint circumference measurement at each time-point following induction of inflammation with intra-articular injection of 0.25ng of LPS in the radiocarpal joints of horses at PIH 0. Joints were treated with either MSC-secretome or a similar volume of medium (control) at PIH 2. n = 8 joints for each treatment group. Data correspond to the mean ± standard deviation of the mean.

Table S4 Synovial Fluid Analysis MSC Secretome vs Medium (negative control)

	Treatment	Timepoint				
		0	**8**	**24**	**72**	**168**
Total Protein (g/L)	MSC-secretome	13.13 ± 5.49	59.75 ± 4.95	60.25 ± 4.83	41 ± 10.02	31.75 ± 3.62
	Medium (control)	11.25 ± 3.54	57.75 ± 4.46	57.5 ± 8.47	41.5 ± 7.84	33.25 ± 3.37
WBCC Cells x 10^9/L	MSC-secretome	0.02 ± 0.03	253.31 ± 177.64	124.60 ± 84.10	17.88 ± 9.85	0.79 ± 0.77
	Medium (control)	0.00 ± 0.01	212.23 ± 113.53	122.19 ± 77.83	17.88 ± 14.53	0.69 ± 0.45
PGF2α (pg/mL)	MSC-secretome	17.33 ± 4.36	2203.08 ± 2000.12	91.50 ± 61.72	36.33 ± 13.37	43.64 ± 25.03
	Medium (control)	20.64 ± 6.99	1994.70 ± 1625.36	108.19 ± 66.95	39.99 ± 18.27	53.76 ± 51.53
PGE_2 (pg/mL)	MSC-secretome	21.01 ± 6.42	13872.95 ± 13725.05	602 ± 470.77	91.93 ± 42.86	56.01 ± 21.66
	Medium (control)	22.55 ± 6.07	10744.44 ± 10225.28	921.89 ± 1023.54	101.75 ± 53.69	168.36 ± 331.17
PGE_1 (pg/mL)	MSC-secretome	179.53 ± 101.9	10246.5 ± 6788.65	712.18 ± 403.4	198.21 ± 78.72	270.99 ± 56.62
	Medium (control)	206.43 ± 108.71	10538.5 ± 7401.15	844.12 ± 636.73	337.78 ± 110.48	556.92 ± 781.05
LTB_4 (pg/mL)	MSC-secretome	16.93 ± 7.75	61 ± 29.96	70.28 ± 31.09	53.77 ± 31.52	45.62 ± 29.73
	Medium (control)	27.38 ± 24.02	83.68 ± 63	63.2 ± 39.69	76.29 ± 78.64	57.94 ± 58.81
11-HETE (pg/mL)	MSC-secretome	121.15 ± 51.51	914.28 ± 1053.64	250.1 ± 205.54	124.71 ± 53.84	149.43 ± 64.05
	Medium (control)	113.76 ± 57.93	546.46 ± 300.14	166.23 ± 53.06	144.89 ± 68.14	121.53 ± 69.85
CCL2 (pg/mL)	MSC-secretome	102.13 ± 116.77	71368.13 ± 97017.17	702.63 ± 458.69	238.63 ± 203.88	167.63 ± 190.44
	Medium (control)	111.38 ± 104.82	43989.38 ± 42342.12	651.50 ± 683.74	235.00 ± 185.23	252.38 ± 259.89
TNF-α (pg/mL)	MSC-secretome	0.00 ± 0.00	273.21 ± 191.60	55.44 ± 66.07	22.58 ± 25.15	17.78 ± 31.38
	Medium (control)	0.28 ± 0.78	341.53 ± 223.52	36.15 ± 49.87	24.16 ± 31.03	22.29 ± 32.24
MMP (RFU/s)	MSC-secretome	29.98 ± 11.48	121.94 ± 89.45	114.95 ± 47.49	141.79 ± 29.87	95.21 ± 39.90
	Medium (control)	23.95 ± 12.65	129.51 ± 89.13	140.56 ± 61.25	146.44 ± 53.84	116.66 ± 40.97
GAG (µ/mL)	MSC-secretome	285.94 ± 110.53	149.68 ± 65.83	577.34 ± 283.50	375.73 ± 95.94	117.46 ± 29.89
	Medium (control)	269.61 ± 82.98	120.73 ± 67.70	376.05± 174.10	340.45 ± 132.58	106.44 ± 46.22
C2C (ng/mL)	MSC-secretome	233.19 ± 96.08	219.44 ± 45.81	423.25 ± 187.34	372.93 ± 162.88	367.19 ± 114.00
	Medium (control)	202.91 ± 54.45	210.94 ± 32.53	466.36 ± 166.72	384.16 ± 109.22	323.38 ± 160.81
CPII (ng/mL)	MSC-secretome	2094.57 ± 1939.07	2040.35 ± 1112.75	3457.83 ± 3721.16	3830.93 ± 4319.92	3152.11 ± 2472.29
	Medium (control)	1653.74 ± 888.17	1888.55 ± 485.17	2078.10 ± 2313.17	3744.100 ± 4516.21	2787.14 ± 3298.96

Table S4: Synovial Fluid Analysis MSC Secretome vs Medium (negative control)
Comparison of Synovial Fluid Total Protein (TP), White Blood Cell Count (WBCC), Prostaglandin F2α (PGF2α), Prostaglandin E_2 (PGE_2), Prostaglandin E_1 (PGE_1), Leukotriene B_4 (LTB_4) and 11-hydroxyeicosatetraenoic acid (11-HETE), CCL2, Tumour necrosis factor-α (TNF-α), general matrix metalloproteinase activity (MMP), Glycosaminoglycan (GAG), collagen-cleavage neoepitope of type II collagen (C2C) and carboxypropeptide of type II collagen epitope (CPII) over time following induction of inflammation with intra-articular injection of 0.25ng of LPS in the radiocarpal joints of horses at PIH 0. Joints were treated with either MSC-secretome or a similar volume of medium (control) at PIH 2. n = 8 joints for each treatment group. Data correspond to the mean ± standard deviation of the mean.

Table S5 Clinical Parameters MSC Secretome vs MSCs (positive control)

	Treatment	Timepoint										
		0	**2**	**4**	**6**	**8**	**24**	**48**	**72**	**96**	**120**	**144**	**168**
Joint Effusion Score	MSC-secretome	0	0	1	1	1	2	1	0	0	0	0	0
	MSCs	0	0	1	1	1	1	1	0	0	0	0	0
Joint Circumference (cm)	MSC-secretome	29.80 ± 1.15	29.85 ± 1.16	30.10 ± 1.05	30.46 ± 1.05	30.66 ± 1.12	31.26 ± 0.96	30.78 ± 1.13	30.36 ± 1.18	30.04 ± 1.13	29.76 ± 1.17	29.85 ± 1.16	29.73 ± 1.07
	MSCs	29.93 ± 1.21	29.98 ± 1.21	30.21 ± 1.18	30.61 ± 1.27	30.91 ± 1.13	31.58 ± 1.12	31.13 ± 1.27	30.58 ± 1.23	30.36 ± 1.16	30.26 ± 1.11	30.18 ± 1.21	30.05 ± 1.21

Table S5: Clinical Parameters
Joint Effusion is a score (scale 0-4) for observed/palpated joint effusion recorded over time following induction of inflammation with intra-articular injection of 0.25ng of LPS in the radiocarpal joints of horses at PIH 0. n = 8 joints for each treatment group. Data correspond to the mode.
Joint Circumference is expressed the joint circumference measurement at each time-point following induction of inflammation with intra-articular injection of 0.25ng of LPS in the radiocarpal joints of horses at PIH 0. Joints were treated with either MSC secretome or MSCs at PIH 2. n = 8 joints for each treatment group. Data correspond to the mean ± standard deviation of the mean.

Table S6 Synovial Fluid Analysis MSC Secretome vs MSCs (positive control)

	Treatment	Timepoint				
		0	**8**	**24**	**72**	**168**
Total Protein (g/L)	MSC-secretome	21.71 ± 4.07	59.75 ± 4.46	55.50 ± 3.66	36.25 ± 7.67	27.75 ± 9.35
	MSCs	20.50 ± 3.51	59.75 ± 3.66	51 ±6.59	38.5 ± 4.50	32.25 ± 8.71
WBCC Cells x 10^9/L	MSC-secretome	0.33 ± 0.20	171.39 ± 48.53	95.16 ± 23.28	8.77 ± 8.79	0.31 ± 0.31
	MSCs	0.24 ± 0.11	174.73 ± 55.31	69.57 ± 34.20	7.94 ± 7.70	0.44 ± 0.52
PGF2α (pg/mL)	MSC-secretome	18.36 ± 4.63	1854.66± 1403.21	136.01 ± 117.00	42.58 ± 15.06	38.24 ± 13.53
	MSCs	18.65 ± 5.26	2285.08 ± 1867.87	146.10 ± 167.22	50.79 ± 24.13	37.16 ± 7.91
PGE_2 (pg/mL)	MSC-secretome	22.74 ± 5.98	17855.36 ± 14443.44	1072.33 ± 714.85	98.24 ± 28.84	74.94 ± 60.38
	MSCs	23.41 ± 4.45	12028.09 ± 3779.02	1117.37 ± 1027.89	148.41 ± 99.71	80.58 ± 51.65
PGE_1 (pg/mL)	MSC-secretome	152.4 ± 41.18	8908.47 ± 7085.39	821.5 ± 492.9	289.35 ± 94.17	280.84 ± 54.57
	MSCs	165.79 ± 55.8	10860.7 ± 7321.25	836.07 ± 632.13	350.13 ± 158.13	306.31 ± 64.07
LTB_4 (pg/mL)	MSC-secretome	28 ± 23.59	92.51 ± 39.1	70.14 ± 47.93	81.85 ± 71.59	58.13 ± 41.37
	MSCs	27.6 ± 14.52	86.23 ± 36.59	67.57 ± 12.45	87.31 ± 61.64	41.31 ± 15.27
11-HETE (pg/mL)	MSC-secretome	91.3 ± 51.5	530.44 ± 723.12	181.71 ± 56.43	98.87 ± 35.31	121.08 ± 60.06
	MSCs	134.27 ± 35.59	617.06 ± 471.63	172.77 ± 115.87	127.75 ± 150.27	133.26 ± 53.12
CCL2 (pg/mL)	MSC-secretome	163.86 ± 153.91	3966.25 ± 2699.64	219.88 ± 228.39	217.63 ± 136.48	241.00 ± 187.18
	MSCs	197.00 ± 135.12	4472.14 ± 3619.39	282.75 ± 362.16	261.50 ± 253.18	303.63 ± 227.81

Table S6 Synovial Fluid Analysis MSC Secretome vs MSCs (positive control) *(continued)*

	Treatment	Timepoint				
		0	**8**	**24**	**72**	**168**
TNF-α (pg/mL)	MSC-secretome	5.41 ± 7.18	136.28 ± 148.52	9.31 ± 17.33	10.39 ± 14.32	16.06 ± 24.12
	MSCs	1.69 ± 4.77	166.73 ± 209.69	13.30 ± 23.10	16.53 ± 28.67	20.70 ± 126.46
MMP (RFU/s)	MSC-secretome	75.90 ± 35.32	173.60 ± 61.93	153.39 ± 56.12	142.03 ± 50.08	104.20 ± 41.89
	MSCs	63.63 ± 32.14	201.69 ± 54.80	144.93 ± 26.63	144.18 ± 55.34	127.58 ± 61.26
GAG (µ/mL)	MSC-secretome	189.91 ± 89.00	158.88 ± 77.87	252.15 ± 80.14	204.16 ± 83.53	89.06 ± 44.96
	MSCs	154.16 ± 68.42	182.81 ± 71.64	176.34 ± 100.06	125.95 ± 94.18	67.15 ± 39.31
C2C (ng/mL)	MSC-secretome	344.71 ± 92.93	254.09 ± 105.92	472.66 ± 100.69	382.46 ± 115.01	369.58 ± 122.76
	MSCs	307.74 ± 85.91	250.60 ± 93.67	484.69 ± 187.97	454.31± 250.23	394.89 ± 106.56
CPII (ng/mL)	MSC-secretome	2273.41 ± 1599.60	2467.06 ± 1091.01	6328.89 ± 3517.10	2951.61± 1749.63	4892.72 ± 5420.77
	MSCs	3743.85 ± 4276.55	2875.11 ± 1829.41	4510.74 ± 1866.50	2911.80± 2152.44	2645.51 ± 1790.07

Table S6: Synovial Fluid Analysis MSC Secretome vs MSCs (positive control)
Comparison of Synovial Fluid Total Protein (TP), White Blood Cell Count (WBCC), Prostaglandin F2α (PGF2α), Prostaglandin E_2 (PGE_2), Prostaglandin E_1 (PGE_1), Leukotriene B_4 ($LTB_{4)}$ and 11-hydroxyeicosatetraenoic acid (11-HETE), CCL2, Tumour necrosis factor-α (TNF-α), general matrix metalloproteinase activity (MMP), Glycosaminoglycans (GAG), collagen-cleavage neoepitope of type II collagen (C2C) and carboxypropeptide of type II collagen epitope (CPII) over time following induction of inflammation with intra-articular injection of 0.25ng of LPS in the radiocarpal joints of horses at PIH 0. Joints were treated with either MSC-secretome or MSCs at PIH 2. n = 8 joints for each treatment group. Data correspond to the mean ± standard deviation of the mean.

CHAPTER 5

Intra-articular injections of PRPr reduce pain and synovial inflammation in a murine OA model

Published as

Intra-articular injections of platelet-rich plasma releasate reduce pain and synovial inflammation in a mouse model of osteoarthritis

Sohrab Khatab, Gerben M. van Buul, Nicole Kops, Yvonne M. Bastiaansen-Jenniskens, P. Koen Bos, Jan A. Verhaar and Gerjo J. van Osch

in The American Journal of Sports medicine, 2018

Sohrab Khatab designed and conducted the experiments, performed data collection and analysis and drafted, edited and reviewed the manuscript.

Abstract

Background: Osteoarthritis (OA) is a degenerative joint disease leading to pain and disability for which no curative treatment currently exists. A promising biological treatment for OA is intra-articular administration of platelet rich plasma (PRP). PRP injections in OA joints can relieve pain, although the exact working mechanism is unclear.

Purpose: To examine the effects of PRP on pain, cartilage damage and synovial inflammation in a mouse OA model.

Study design: Controlled laboratory study.

Methods: OA was induced unilaterally in the knees of male mice (n=36) by two intra-articular injections of collagenase at days -7 and -5. At day 0, pain was measured by registering weight distribution on the hind limbs; after which mice were randomly divided in two groups. Mice received three intra-articular injections of PRP-releasate (PRPr) or saline in the affected knee. Seven mice per group were euthanized at day 5 to assess early synovial inflammation. Pain in the remaining mice was registered a total of three weeks. These mice were euthanized at day 21 to assess cartilage damage and synovial inflammation on histology. Antibodies against iNOS, CD163 and CD206 were used to identify different subtypes of macrophages in the synovial membrane.

Results: Mice in the PRPr group increased the distribution of weight on the affected joint in two consecutive weeks after start of the treatment ($p<0.05$), whereas mice in the saline group did not. At day 21, PRPr injected knees had a thinner synovial membrane ($p<0.05$), and a trend towards less cartilage damage in the lateral joint compartment ($p=0.053$) than saline injected knees. OA knees treated with saline had less anti-inflammatory (CD206+ and CD163+) cells at day 5 than healthy knees, an observation which was not made in the PRPr-treated group. A higher level of pain at day 7 was associated with a thicker synovial membrane at day 21. The presence of CD206+ cells was negatively associated with synovial membrane thickness

Conclusions: In a murine OA model, multiple PRPr injections reduced pain and synovial thickness, possibly through modulation of macrophage subtypes.

Clinical relevance: PRPr injections shortly after joint trauma can reduce pain and, synovial inflammation and may inhibit OA development in patients.

Introduction

OA is a degenerative joint disease, characterized by loss of cartilage integrity, changes in subchondral bone, formation of osteophytes and inflammation of the synovial membrane. This process results in pain and disability. Current treatments focus on pain reduction, exercise therapy and – in end-stage OA – joint replacement. To this day no curative treatment exists for OA. Since joint arthroplasties have a limited life-span, the need for disease-modifying drugs or therapies is high. Ideally such a therapy would inhibit or repair damage to the joint tissues and reduce pain and disability. A biological therapy for tissue injury that has emerged in recent years is treatment with platelet-rich plasma (PRP). PRP is a plasma product extracted from whole blood that contains at least 1.0×10^6 platelets per microliter [59]. The platelets undergo degranulation after which they release growth factors and cytokines such as transforming growth factor beta (TGFβ) and platelet-derived growth factor (PDGF)[59-61], two important factors in tissue healing.

Several clinical trials in OA have concluded that multiple PRP injections are safe and have a beneficial effect on OA symptoms such as pain, for up to 12 months [70, 71, 160-163]. Evidence is accumulating from both in vitro and in vivo studies for PRP's potential in the treatment of OA. From preclinical research we know that PRP promotes the proliferation of cells derived from human synovium and cartilage [164, 165], and that PRP-treated chondrocytes repair cartilage better than non-treated chondrocytes [63]. These cells in turn produce more superficial zone protein (SZP), which functions as a boundary lubricant that helps to reduce friction and wear [64, 164, 166]. PRP itself was also shown to reduce friction in bovine articular cartilage explants [164]. The anti-inflammatory effects of PRP have been demonstrated both in a co-culture system of osteoarthritic cartilage and synovium[164] and in human osteoarthritic chondrocytes, where it reduced multiple pro-inflammatory effects induced by IL-1β [66]. Furthermore, in a canine OA model, multiple PRP injections were shown to have beneficial effects on pain and functional impairment, but no effect on the severity of radiographic OA [167].

However, while the use of PRP products seems promising for the treatment of OA, the wide variability in outcome parameters evaluated, in models used and in PRP and PRP releasate (PRPr) production protocols makes interpretation of results between studies difficult [76, 77, 168]. This difficultly in comparing the results of PRP research may be one of the reasons why the exact working mechanisms of intra-articular injected PRP products are not fully understood. Unravelling this mechanism could provide an opportunity to further improve therapeutic PRP efficacy.

In this study we assessed the effect of human PRPr compared to saline in a murine model of collagenase-induced OA (CIOA). We studied the effects of PRPr on several OA related processes in the joint: pain, cartilage damage and synovial inflammation and

evaluated correlations between these parameters. We payed particular attention to effects on different macrophage phenotypes in the synovium. Our hypothesis is that multiple intra-articular injections of PRPr will reduce pain, have a protective effect on cartilage and inhibit synovial inflammation.

Materials Methods

Platelet rich plasma releasate preparation

Human PRP was acquired from the national blood bank (Sanquin, Amsterdam, The Netherlands) with a platelet count of 8.5 x 10^8/ml. This PRP product is produced by pooling buffy coats of 5 different donors in plasma. After centrifugation, the platelets are filtered out to produce the PRP. The blood samples had identical ABO and Rh(D) compatible blood type, and were pathogen free. PRP was activated by adding 10% v/v 228 mM $CaCl_2$ and incubated on a rotating device at 37°C [66]. After one hour of incubation a clot was formed and the supernatant was harvested. This supernatant contains the released factors of the activated platelets and hence is called the PRP releasate (PRPr). Whereas erythrocytes could be detected in the PRP, they were no longer detected after the activation of the PRP by a clinical cytometer (Model xn1000, Sysmex Netherlands BV, Etten-Leur, Netherlands). Leukocytes were not detectable in the PRP or the PRPr. After harvesting the PRPr the samples were stored at -80°C and used within a week for in vivo experiments. The concentration of PDGF-BB in the cryopreserved samples was 1.2 x 10^4 pg/ml, measured by ELISA**.**

Animal model of injury and treatment

All animal experiments were performed on 36 male C57/Bl6 mice age 12 weeks (blinded), with approval of the animal ethical committee (blinded 116-14-03). The mice were housed in groups of three or four mice per cage, under 12 hours light-dark cycle at a temperature of 24°C degrees Celsius, and had access to water and food ad libitum at the animal testing facilities.

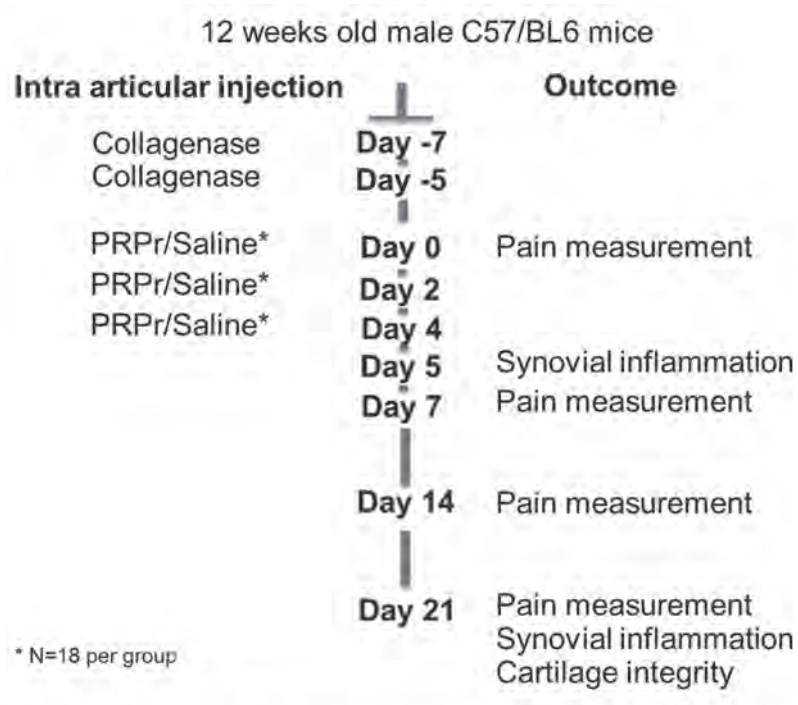

Figure 1. Experimental set up of the in vivo experiment. On the left the intra-articular injections at different time points. On the right the outcome measurements. At day 5 a group of 14 mice were euthanized (n= 7 per group) to assess the early effects of PRPr on synovial inflammation. Another group of 22 mice was used to assess the presence of pain up to 3 weeks and to assess synovial inflammation and cartilage damage at end point.

Before starting the experiments, mice were allowed to acclimatize for a week. In all mice, OA was induced unilaterally by two intra-articular injections of 6 µl of 3 units collagenase type VII (Sigma-Aldrich) at days -7 and -5. Collagenase induced OA is an established model for joint instability in mice [80, 113, 169-171]. All intra-articular injections were applied under 2.5% isoflurane anesthesia, with a 50 µL glass syringe (Hamilton Company, Ghiroda, Romania) using a 30G needle (Becton, Dickinson and Company, New Jersey, USA). The contralateral control knees were kept naïve and were not injected with any substance. Mice were randomly assigned to either the treatment group with 6 µl PRPr (n=11 mice) or the control group (n=11 mice) with 6 µl saline. Both groups received three consecutive PRPr or saline injections; the first injection was given 7 days after the first collagenase injection (referred to as day 0) and repeated with consecutive injections at day 2 and 4 (Figure 1).

Weight distribution over the left and right hind limbs was evaluated as an indicator of pain at day 0 and hereafter once weekly for 3 weeks.

During the whole experiment the animals were capable to move around freely and could reach the food pellets and drink nozzle on the top for their cage. Animals were euthanized at day 21 and knee joints were harvested for histological analysis.

To assess the early effects of PRPr on synovial inflammation, an additional group of animals was used containing 7 mice in each group. These animals underwent identical OA induction and treatment protocols. They were euthanized at day 5 after the start of PRPr treatment and knee joints were prepared for histological evaluation.

Measurement of hind limb weight distribution

Hind limb weight distribution was registered with an incapacitance tester [85] (Linton Instrumentation, Norfolk, UK) as an indicator of pain. It is a static method to measure pain, which is validated in mouse, rats and other animal models [85, 167, 172-175]. Mice were positioned on the incapacitance meter with each hind limb resting on a separate force plate. Measurements were performed at day 0, just before therapy administration and hereafter at day 7, 14 and 21. The observer was blinded to the pressures measured during the test. Therefore afterwards, measurements with a registration of below 3 grams (<10% of total bodyweight) per hind limb or less than 10 grams (<30% of total bodyweight) in total over both hind limbs were excluded. On average 15 measurements per time point per animal were available. For each time point per mouse, the average of these measurements was used to calculate the percentage of weight on the affected limb as an indication of pain in the affected limb. A single value per measurement time point was used for statistical analyses.

Histological analyses

Knees were fixed in formalin 4% (v/v) for one week, decalcified in 10% EDTA for 2 weeks and embedded in paraffin. Coronal sections of 6 µm were cut for analysis of synovial inflammation and cartilage damage.

Structural integrity

Cartilage damage was evaluated on thionin-stained sections by two observers blinded to the treatment groups with a scoring system described by Glasson *et al.*[96]. Briefly this score ranges from 0 for normal cartilage, to 6 for cartilage with clefts and erosion to the calcified cartilage in >75% of articular surface. For each knee the cartilage quality in the lateral and medial compartment of the knee was scored on 3 sections with 180 µm interval between the sections. The maximum score of the 3 sections, for each compartment was taken for analyses [96].

Synovial inflammation

For synovial inflammation assessment, sections were stained with hematoxylin eosin. Images were acquired using the NanoZoomer Digital Pathology program (Hamamatsu Photonics, Ammersee, Germany). Synovial thickness was measured from the capsule to the superficial layer of the synovial membrane in the parapatellar recesses at the medial and the lateral side at three positions per section, based on a previously described method [80]. These measurements were done on three sections per knee, with 180 µm between the sections. In total we obtained 18 synovium thickness measurements per knee, which were averaged to obtain a single value per knee joint.

Macrophage staining

To evaluate the macrophage subtypes in the synovial membrane, inducible nitric oxide (iNOS) was used as a marker for pro-inflammatory macrophages, cluster of differentiation 163 (CD163) as a marker for anti-inflammatory macrophages, and CD206 as a marker for tissue repair macrophages. For this purpose, sections were deparaffinized, washed and heat-mediated antigen retrieval was performed for CD163 and CD206, by placing the slides in 95°C citrate buffer (pH 6) for 20 minutes. Antigen retrieval for iNOS was performed in by placing the slides in 95°C Tris-EDTA buffer (pH 9) for 20 minutes. Blocking of aspecific binding was done with 10% goat serum (Southern Biotech, Birmingham, USA) for 30 minutes. Hereafter, sections were incubated with the primary antibodies iNOS (2.0 µg/ml #15323, Abcam, Cambridge, UK), CD163 (0.34 µg/ml, #182422, Abcam, Cambridge, UK), and CD206 (2.5 µg/ml,#64693, Abcam, Cambridge, UK) for 1 hour, followed by 30 minutes incubation with a biotinylated anti-rabbit Ig link (Biogenex, HK-326-UR, Fremont, USA), diluted 1:50 in PBS/1%BSA. Thereafter, sections were incubated with an alkaline phosphatase-conjugated streptavidin (Biogenex, HK-321-UK) label diluted 1:50 in PBS/1%BSA. To reduce background, endogenous alkine phosphatase activity was inhibited with levamisole (Sigma-Aldrich Chemie N.V. Zwijndrecht, The Netherlands). Neu Fuchsin (Fisher Scientific, Vienna, Austria) and Napthol AS-MX phosphate (Sigma-Aldrich Chemie N.V. Zwijndrecht, The Netherlands) substrate was used for color development and counterstained with hematoxylin. As a negative control Rabbit IgG antibody (Dako Cytomation, Glostrup, Denmark) was used. The sections were ranked from weakest to strongest staining for either iNOS, CD163, or CD206, by two observers blinded for the treatment group. The maximum rank was based on the total number of joints scored for the individual staining. When multiple sections had similar strength of staining, the mean of the rank numbers was given to each section. Per section the mean rank of both observers was used for analyses.

Statistical Analysis

For the late time point and pain reduction we consider a decrease in pain of 20% in the therapy groups to be relevant in our study. According to a power calculation of the sample size (using a standard deviation of 20%), with a statistical power level (1-β) of 0.8 and significance level (α) of 0.05, our sample size per group for a one tailed hypothesis test will be 10 mice. For the short term we considered a 25% decrease of synovial thickness as relevant for our study. According to a power calculation of the sample size (using a standard deviation of 20%), with a statistical power level (1-β) of 0.8 and significance level (α) of 0.05, our sample size per group for a one tailed hypothesis test will be 6 mice. An additional mice per group gives us n=11 for late time point and n=7 mice for the early time point. Giving a total of n=18 mice per treatment group and 36 mice in total. Data was analyzed with IBM SPSS statistics 21 *(SPSS, Chicago, IL)*. For the effect on weight distribution, normality was confirmed with a Shapiro Wilk test. Two-tailed paired t-tests were conducted to evaluate differences between time points within each group and two tailed unpaired t-tests were conducted to evaluate differences between treatment groups at each time point. Statistic testing on synovial thickness measurements where conducted using a Welch t-test, after normality was confirmed with a Shapiro-Wilk test for knees at both day 5 and day 21. To compare the maximum OA scores between saline and PRPr treated groups, a Mann-Whitney U test was performed. A Kruskal-Wallis test was performed for the ranked macrophage data between the healthy control, saline and PRPr group. For all tests, P values < 0.05 were considered statistically significant.

Correlation analysis was performed by means of a Spearman's rho test. All data collected was categorized per animal. In this way we can look for correlations between the pain measurements at different time points and the corresponding histological findings at day 21. For the interpretation of the correlation coefficient we used the absolute value of r_s, dividing the correlations in weak (<0.5), moderate (0.40-0.59), strong (0.60-0.79) and very strong (>0.80). Correlations were significant if P values < 0.05.

Results

Multiple PRPr injections reduce pain

We determined the weight distribution over the hind limbs as an indicator of pain (Figure 2A). Seven days after induction of OA, 43.1 ± 9.6% of weight was distributed on the affected limb, indicating pain (Figure 2B). Mice in the PRPr group significantly increased the weight on the affected joint on day 7 (P=0.041) and 14 (P=0.034) compared to day 0, indicating a reduction in pain. The mice that received saline injections did not significantly change the weight distribution on any of the time points, compared to the start of treatment, albeit a trend for improvement over time was visible. The biggest difference between PRPr and Saline was seen at day 7, although it did not reach statistical significance.

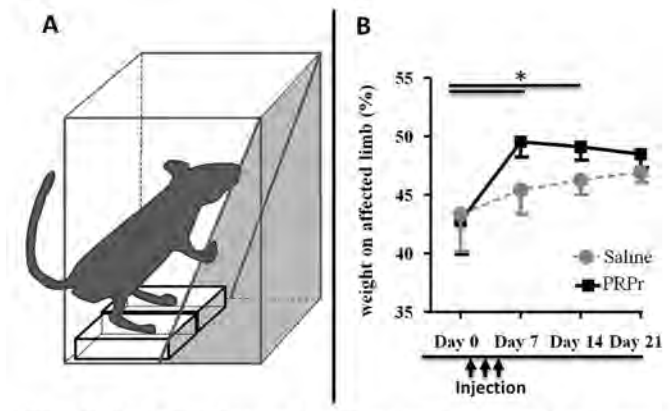

Figure 2. Weight distributed on the affected limb in mice with collagenase-induced osteoarthritis treated with PRP releasate. In panel A the position of the hind limbs on the two pressure plates of the incapacitance tester. In panel B the weight distribution on the effected limb in time. In black the PRP releasate (PRPr) group versus in gray (dotted line) the saline group. Treatment started at day 0, 7 days after the first collagenase injection; the arrows depict the time of injection of PRP releasate or saline (day 0, 2 and 4). Mean + SEM of 11 mice per group per time point are presented. * = p<0.05

Multiple PRPr injections have no effect on cartilage

Collagenase injected knees that were treated with saline (control group) had more cartilage damage than the healthy controls at the endpoint of the study, in particular in the lateral joint compartment, confirming development of OA (Figure 3A, P=0.025). Whereas the PRPr group was not significantly different from healthy group. This suggests a protective effect of the PRPr on cartilage. Although there was no significant difference in cartilage damage between saline and PRPr groups. Cartilage damage

in the medial compartment was less after PRPr treatment than in the saline injected knees, albeit this did not reach statistical significance (P=0.053).

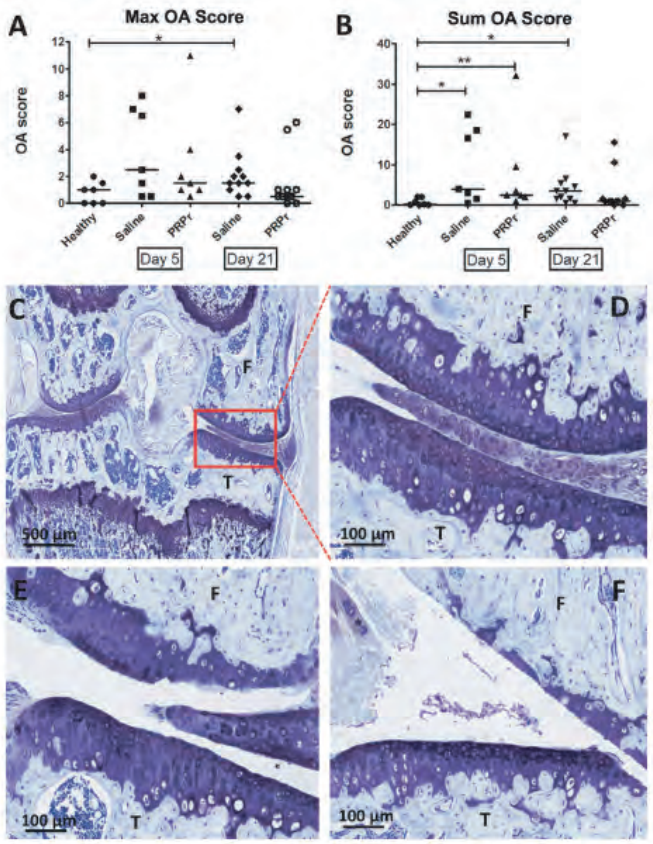

Figure 3. The (A) maximum and (B) sum osteoarthritis (OA) score per knee of the lateral (femoral condyle and tibial plateau) compartment of each knee. Bars represent the median of each group. n = 7 mice per group for Healthy group and day 5 time point; n = 11 mice per group for day 21 time point. *$P < .05$; **$P < .01$. (C) Overview of thionin staining of the mouse knee joint and typical examples of (D) OA score 1-2, (E) OA score 3-4, and (F) OA score 5-6 of the femoral condyle. OA score ranges from 0 to 12 per compartment. F, femur; PRPr, platelet-rich plasma releasate; T, tibia.

Multiple PRPr injections reduce synovial membrane thickening

Collagenase injected knees displayed a significantly thickened synovial membrane compared to healthy knees. Although the synovial membrane thickness was not statistically different between PRPr and saline injected groups 5 days after start of treatment, synovial membrane thickness at day 21 was significantly less in the PRPr group than in the saline control group (Figure 4A, P=0.041). Overall, synovial membrane thickness was largely reduced over time between day 21 and day 5 (P<0.001).

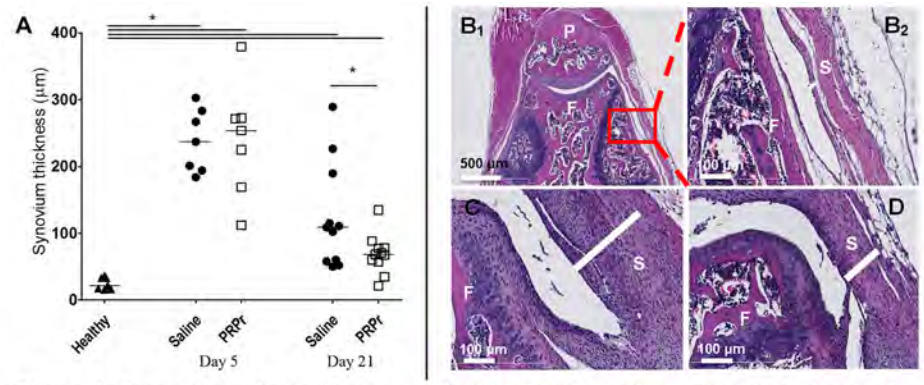

Figure 4. Synovial membrane thickness in healthy controls and in osteoarthritic knees after treatment with PRP releasate (PRPr) or saline. In panel **A** the average synovial thickness at day 5 and day 21 after treatment. Bars represent the means of each group. Day 5, n= 7 mice per group. Day 21, n=11 mice per group. * = p<0.05. Right panel **(B-D)** an overview of the patellofemoral joint and representative examples of a healthy knee **(B1, B2)**, example of osteoarthritic knee injected with saline **(C)** and osteoarthritic knee injected with PRPr **(D)**, with different thickness of the synovial membrane at the parapatellar recesses. S= Synovial membrane, F=Femur and P= patella.

Multiple PRPr injections maintain the CD206 and CD163 positive macrophages

To further analyze the synovial inflammation process, we assessed the presence of different macrophage subtypes. We examined the presence of iNOS, CD206 and CD163 positive macrophages by ranking healthy, collagenase injected saline control and collagenase injected PRPr treated knees at day 5 and day 21. The presence of iNOS positive macrophages, indicating a pro-inflammatory response, was higher in collagenase injected knees than in healthy control knees at both day 5 (saline P=0.004; PRPr P=0.006) and day 21 (saline P=0.016; PRPr P=0.046), independent of treatment (Figure 5A). Although no significant differences were observed in the presence of iNOS positive macrophages between treatment groups, PRPr injected knees did show a trend towards less iNOS positive macrophages than in the saline injected knees at day 5 (p = 0.109). We furthermore determined the presence of macrophages related to tissue repair (CD206+) and anti-inflammatory macrophages (CD163+). In the collagenase injected saline control group, the presence of CD163 and CD206 positive macrophages was significantly lower than in the healthy knees, at day 5 (Figure 5B-C, P=0.024 and P=0.042 respectively). The presence of CD206 and CD163 positive macrophages in the PRPr treated knees did not differ from that of healthy knees, both at day 5 and day 21). At day 21, in the same group, the presence of CD206, but not CD163, was significantly increased (P=0.023 and P=0.185 respectively).

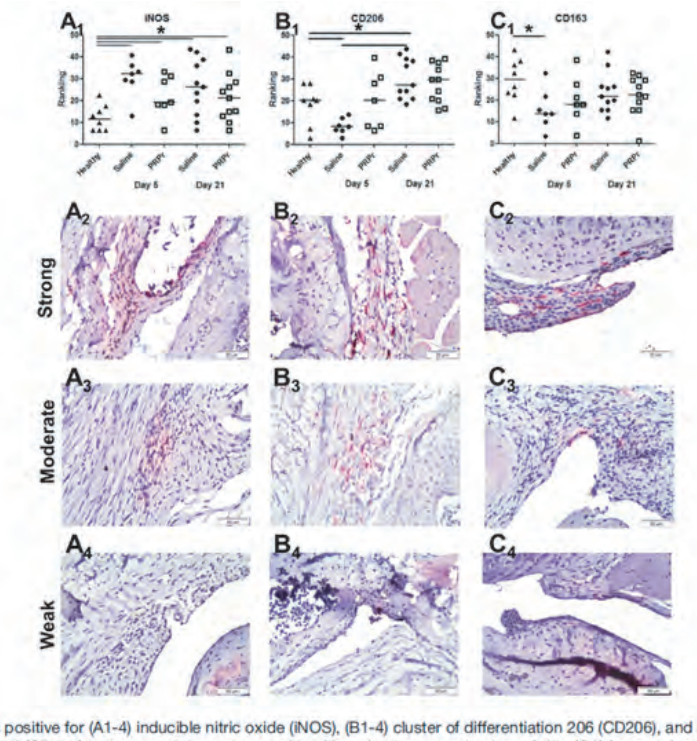

Figure 5. Cells positive for (A1-4) inducible nitric oxide (iNOS), (B1-4) cluster of differentiation 206 (CD206), and (C1-4) cluster of differentiation 163 (CD163) in the synovial membrane of healthy mice knees and osteoarthritic (OA) knees injected with platelet-rich plasma releasate (PRPr) or saline. Knees are ranked based on the presence of the marker of interest. Bars represent the median of each group. Day 5, n = 7 mice per group. Day 21, n = 11 mice per group. *$P < .05$.

Pain reduction is associated with a thinner synovial membrane

Interestingly, reduction of pain at day 7 was strongly associated with a thinner synovial membrane at day 21 (Table 1, P=0.002). There was no significant correlation between pain reduction at day 21 and synovial thickness at day 21, possibly due to the overall pain reduction seen in all animals. Furthermore, the presence of iNOS+ macrophages was moderately associated with lateral OA damage (P=0.02). No significant associations were found between iNOS+ macrophages and pain or synovial thickness between treatment groups. The presence of repair macrophages (CD206+) was associated with a thinner synovial membrane (P=0.007) and anti-inflammatory macrophages (CD163+, P<0.001).

Table 1
Selection of correlations coefficients between the parameters tested.

Spearmans Rho		Correlation Coefficient	Strength	P-value	Interpretation
Pain reduction day 7	Synovial thickness day 21	-0.622	Strong	0.002	Less pain at day 7 associated with less synovial inflammation at day 21[a]
Pain reduction day 21	Synovial thickness day 21	-0.098	Very Weak	0.670	No association between pain day 21 and synovial inflammation day 21
CD206 macrophage marker	Synovial thickness	-0.440	Moderate	0.007	More CD206+ is associated with thinner synovial membrane
CD206 macrophage marker	CD163 macrophage marker	0.560	Moderate	0.000	Precense of CD163+ and CD206+ subtypes associated with each other
iNOS macrophage marker	Lateral OA score	0.492	Moderate	0.020	Presence of iNOS+ is associated with more cartilage damage lateral compartment

[a] Weight distribution on the affected limb was measured as indicator of pain; the higher the percentage of weight on the affected limb the less pain, thus giving a negative association with synovial thickness.
The correlations involving macrophage data and synovial thickness are based on day 5 and 21 histology data.
The correlation involving OA score is based on day 21 histology data.

Discussion

The results of this study suggest that multiple intra-articular injections of PRPr in a collagenase induced OA (CIOA) mouse model reduce synovial inflammation and have a protective effect on cartilage, while at the same time reducing pain. The strongest effect on pain reduction was seen in the period shortly after start of treatment. Next to pain reduction, multiple PRPr injections inhibited synovial inflammation, as demonstrated by a thinner synovial membrane compared to the saline control. Furthermore, PRPr injections had an effect on the balance between inflammatory and anti-inflammatory macrophages in the synovial membrane, in particular by preventing the early decrease in anti-inflammatory macrophages seen after induction of CIOA. We also noted that, although the association was not significant, PRPr-injected knees tended to have fewer pro-inflammatory iNOS+ macrophages than saline-injected knees.

Collagenase injections induce joint inflammation, in particular in the first two weeks, making this model suitable for testing potential anti-inflammatory therapies. For example, others have shown that intra-articular injection of adipose-derived stem cells (ASC) in this model reduces synovial inflammation at day 42, when ASCs are injected one week after induction of CIOA [80]. This demonstrates the possibility to interfere with inflammation using biological treatments in this model. Our results confirm that early intervention in this model can have beneficial effects.

PRPr injections reduced pain for two consecutive weeks. Mice with high pain levels at day 7 were very likely to have thicker synovial membranes two weeks later.

The pathway by which PRPr reduces pain may involve inhibition of the production of prostaglandin E2 (PGE2). PGE2 is a lipid mediator of inflammatory pain that causes pain hypersensitivity via nociceptor sensitization [176]. In an inflammatory environment, the main contributors to PGE2 release are thought to be tissue-resident macrophages [176]. Our data suggest that PRPr-injected knees may have fewer pro-inflammatory and more anti-inflammatory macrophages, possible resulting in lower PGE2 production. It is known that PRP can promote the differentiation of monocytes towards repair and anti-inflammatory CD206 and CD163-positive macrophages [177]. This is supported by the finding in a rabbit knee osteoarthritis model that intra-articular injections of leucocyte-poor PRP reduced PGE2 concentrations.[178] Moreover, PRPr has been reported to contain high levels of interleukin 1 receptor antagonist (IL-1Ra)[179] that can inhibit acute inflammation caused by IL1 and promote macrophage polarization towards an M2 phenotype [180]. Our finding that animals in neither the treated nor the untreated group appeared to experience any pain at three weeks may be partly due to the fact that acute inflammation weakens in time after collagenase injection, thereby reducing nociceptive input to the central nervous system. Less nociceptive input can be preceded by desensitization of the mice nervous system for pain. In the latter case, the threshold for the activation of the joint nociceptors is reduced, and thus a bigger stimulus is needed to register pain [181].

Besides synovial inflammation, cartilage damage is an important hallmark of OA. In this study, 28 days after OA induction, cartilage damage in the lateral joint compartment after multiple PRPr injections was not different from the healthy knees. The severity of the cartilage damage, however, was significantly increased in the lateral compartment of the CIOA joints treated with saline. The mild cartilage damage we observed in our study made it difficult to detect differences between PRPr and saline groups. The absence of a difference between PRPr treated CIOA mice and healthy mice could be an indication of a chondroprotective effect of PRPr injections. No correlation between pain and cartilage damage at any time point was found, confirming previous findings in the field [182].

We used a commercially available human derived PRP, which was pooled from 5 healthy human donors. Pooling PRP donors can reduce the inter donor variability described previously [183, 184]. This PRP is poor in leucocytes and in this study was activated prior to injection in mice. In contrast, others inject non-activated PRP and rely on activation *in vivo* [185-188]. We choose to activate the PRP product prior to injection because firstly, it is hard to control the activation of PRP *in vivo*, and thus hard to draw conclusions about the working mechanism of PRP without knowing the level of activation [62]. Some of the disappointing results from other studies might be attributed to less than optimal activation. Secondly, activating PRP with $CaCl_2$ leads to higher levels of PDGF-AA and BB than other activation methods such as freeze-thaw

[189]. Thirdly, the activation of PRP results in the formation of a so-called cloth, which catches any remaining erythrocytes and leucocytes, making the end product low in cells and high in growth factors. Although possible positive effects of a PRP product rich in leucocytes is still being debated [190], a product depleted from allogenic or in this case xenogeneic cells will cause less immunoreaction. Lastly, by having a PRP product low in leucocytes and short storage before activation, we can reduce the catabolic factors in PRPr [191]. Since leucocytes are the main contributors to TNFα levels in PRP - but also to levels of interleukins 6 and 8 - these levels might increase further in the period during which leucocyte-rich PRP is stored [192, 193]. Although the working mechanism of PRP is not fully understood, the current knowledge about its active components is improving. This will likely help the PRPr product to be optimized by filtering out components, such as TNFα and vascular endothelial growth factor (VEGF), or increasing the concentrations of other components such as PDGF. Others have reported that freeze drying of PRP increases its efficacy. Freeze drying could also prolong the lifetime of the PRP product, making it an off-the-shelf product with a longer lifetime [194, 195]. We could therefore reduce the levels of catabolic factors in PRPr by selecting a PRP product low in leucocytes and minimizing the duration of storage before activation [191].

Here we have demonstrated in an OA model that multiple PRPr injections reduce pain and synovial membrane thickness, and that PRPr appears to modulate the phenotype of synovial macrophages. We believe that PRPr injections are a more potent therapy for early stage intervention after trauma and early OA, rather than a treatment for end-stage OA. The latter is confirmed in a few clinical trials, where PRP injections did not affect patients with end-stage OA [196]. This knowledge can be used in future experiments to determine the best time point for intra-articular PRPr injections after trauma, and to further evaluate and confirm the chondroprotective effects of PRPr in the long term. Together with improvements of the PRPr product itself, could help to make PRPr a suitable treatment shorty after joint trauma or for patients with low grade OA, both for pain relief and the inhibition of OA pathophysiology.

CHAPTER 6

General discussion

Effect of biological therapeutics on cartilage and subchondral bone

Cartilage damage, and in its extension the occurrence of changes in the subchondral bone, such as the formation of sclerosis, is an important hallmark of OA. Ultimately, this is what we aim to repair or - even better -to prevent.

Focusing first on MSC. Several (pre)clinical studies show promising results for intra-articular injection of MSC as a treatment for OA. For this purpose, different MSC sources are being used [94, 197, 198]. As described previously, MSC often are no longer detectable three weeks after intra-articular [39, 40]. We aimed to improve the therapeutic efficacy by prolonging the presence of MSC within the joint, such that there is a continuous interplay between the diseased joint and the MSC. To this end, we encapsulated the MSC in alginate. Our first experiments, using subcutaneous implantation, showed a more prolonged presence of the Fluc-MSC even 5 weeks after implantation. The encapsulated MSC remained viable with immunomodulating capacity in both High M and High G alginate. The next step was to test this in an MIA-induced OA model in rats, where we demonstrated that we could track viable cells and the alginate constructs for a minimum of 8 weeks after intra-articular administration. Unfortunately, we did not see any effect of either free or encapsulated MSC on cartilage damage. Due to the very mild osteoarthritic changes in all groups, it was not easy to detect differences between treatment groups. Possibly, a concentration of 300 **µ**g MIA was too low in our model to have profound effects, in comparison, others have reported used of up to 1 gr of MIA to induce OA [94]. By trying to prevent a fully degenerative joint that would be beyond the repair capacity of cellular therapies, we possibly prevented significant cartilage damage and had a very low window of effect for treatment.

The MSC trophic capacities provide the exciting option of possibly basing future therapies on the secreted factors rather than the MSC themselves. Although the longevity of the secreted factors is expected to be even lower than that of the MSC, they do have an effect *in vivo*. This prompted us to work towards a cell-free approach. Our results of using the MSC secretome in a murine CIOA and horse LPS models underscores this. Although the overall development of OA was low in our CIOA model, more knees developed OA in the control group. OA development was prevented in knees treated with MSC secretome or MSC, with no significant difference found in the MSC (secretome) injected CIOA knees compared to healthy knees. Unfortunately, we observed no therapy effect on the subchondral bone. Here, we demonstrated that the MSC secretome, a cell-free product, is as effective as injecting the MSC themselves since there were no differences in cartilage or subchondral bone when injecting the MSC secretome versus the MSC themselves. This is confirmed in our findings in the

equine LPS model, in which MSC and MSC secretome seemed to have a protective effect on cartilage turnover, but no differences were seen between both treatment groups. Our findings in the equine study are in line with the work of Barrachina *et al.* [145], In their equine study, they describe the inhibition of cartilage degradation by MSC in an early OA stage. Similarly, they used primed allogenic bone marrow-derived MSC, analogous to ours. In conclusion, MSC-secreted factors appear to be a promising, cell-free therapy option for OA, with comparable, albeit limited, effects comparable to the MSC themselves.

Next, we explored the therapeutic effects of sequential intra-articular PRP releasate (PRPr) injections. This other potential DMOAD, PRPr, is a cell-free, injectable, biological treatment. PRPr has been shown to stimulate chondrocyte proliferation and promote extracellular matrix synthesis in *in vitro* studies. Findings from *in vivo* studies suggest that PRP could delay cartilage degeneration and even contribute to cartilage repair in early OA. Moreover, intra-articularly injected PRP was shown to positively affect clinical outcomes and less cartilage damage as seen on imaging in patients with knee osteoarthritis. However, clinical studies present variable results regarding pain relief and joint function [70, 199, 200]. This may partly be due to the heterogeneity of PRP preparations, as the platelet concentration, white blood cell content, and activation method can affect biological properties. Moreover, like the MSC secretome, PRPr is also a black box mixture of biologically active factors, the exact working mechanisms of which are unknown. Our results from the CIOA murine model suggest that PRPr injections might have a chondroprotective effect. This is based on the absence of a difference between PRPr-treated CIOA and healthy mice knees. No correlations were seen between cartilage damage and other outcomes.

Summarizing, our research has demonstrated the potential beneficial effects of MSC and PRP-based cell-free therapies on cartilage but no effect on subchondral bone. We have demonstrated that encapsulation of MSC can prolong their presence within the joint but did not translate to enhanced therapeutic efficacy in a mild OA model. The MSC secretome exhibited comparable therapeutic efficacy to the MSC itself. PRP demonstrated a chondroprotective effect. These findings suggest that the secreted factors from these cell-based therapies may be the key drivers of their therapeutic potential.

Effect of biological therapies on synovial inflammation.

Injury to articular cartilage, whether due to trauma or degenerative processes, modifies the joint's load-bearing surface area. These mechanical alterations can precipitate abnormal joint loading, leading to the production of pro-inflammatory cytokines and joint inflammation. Consequently, inflammation can lead to even more

cartilage damage [201]. Thus, since inflammation is an important hallmark of OA, joint inflammation is a logical target for DMOADs.

In **Chapter 2**, the immunomodulatory abilities of encapsulated MSC were demonstrated *in vitro;* they produced IL-6 and displayed IDO activity. Furthermore, they inhibited the proliferation of CD4+ and CD8+ T lymphocytes in a dose-dependent manner comparable to when using MSC in monolayer. Nevertheless, encapsulated MSC in our *in vivo* MIA model did not significantly affect inflammation. Instead, we noticed a trend towards increased synovial thickening and bead encapsulation in the synovial membrane compared to free MSC injection. Empty alginate bead injection in a rat joint caused a similar synovial thickening. This might indicate a foreign body reaction on alginate even when it is clinical-grade alginate. However, this foreign body reaction was very limited in our subcutaneous experiments. Thus, the synovial inflammation may be caused by the local joint environment due to chemical, mechanical, or cellular damage to the alginate constructs, prompting host immune cells to recognize the donor MSC as a threat and attempt to neutralize them—either way, an undesirable reaction was observed. These processes could have masked the possible positive effects of MSC on inflammation in our model.

Injection of MSC or MSC secretome in the CIOA model demonstrated a moderate association with the presence of anti-inflammatory macrophages (CD163+) and a thinner synovial membrane. A similar observation was made for the association between the presence of CD163+ cells and experienced pain. Thus, the more abundant these CD163+ cells were present, the less pain and synovial thickness were observed. Nevertheless, no direct relationship was found between pain and synovial thickness. MSC-treated knees showed a trend towards a more prominent presence of the more inflammatory subtype iNOS+ macrophages, possibly a reaction to xenogenic MSC.

Ter Huurne *et al.* observed a stronger anti-inflammatory effect, compared to our results, after injecting allogeneic ASC in a CIOA model [31]. Similarly, Choi *et al.* demonstrated that intra-articulair injection of microencapsulated allogeneic ASC significantly decreased the progression and extent of OA, in a rabbit OA model, although, in that study, no cell or construct tracking was performed [50]. The discrepancy in efficacy between these reports and our findings may be attributed to the use of human cells in immunocompetent mice and rat strains in our studies. Using xenogeneic cells may present two potential disadvantages. Firstly, major histocompatibility complex class II (MHC-II) molecules may be present on stimulated MSC and potentially on extracellular vesicles present within the MSC secretome, which could trigger a host-versus-graft reaction. Secondly, xenogeneic MSC could lead to issues where crucial factors and cytokines are not conserved across species, potentially resulting in ineffective communication between the xenogeneic MSC and the diseased joint environment *in vivo*.

When using allogeneic MCS in our equine experiments, intra-articular treatment with eqMSC secretome did appear to have a clinical anti-inflammatory effect, leading to significantly less joint effusion. Free eqMSC injections did not demonstrate a superior treatment effect to eqMSC secretome in this joint inflammation model. In line with our finding related to cartilage and subchondral bone, this indicates that MSC secretome could be a viable alternative to MSC treatment when allogenic MSC are used.

MSC or MSC secretome administration in inflamed joints has shown promising effects in clinical trials. Although numerous clinical studies have been performed, most of them have yet to investigate the role of MSC on inflammation within their study. At best, they state that since there is a positive effect on clinical outcomes such as pain and function, there should also be an anti-inflammatory effect [202-204]. *Chahal et al.* included inflammation testing in their recent clinical trial. They demonstrated that a high dose of MSC resulted in a notable reduction in MRI-assessed synovitis. Additionally, there was a decrease in pro-inflammatory macrophages within the synovial fluid, further underlining MSC's effect on clinical symptoms and its correlation with inflammation [205].

Even more, clinical trials and animal studies investigating the efficacy of PRP in reducing inflammation and improving outcomes in OA patients, showed promising results. In our studies we also found that PRPr injections inhibited synovial inflammation *in vivo*. This potential of PRPr was further confirmed in > 40 other animal studies, as reviewed by *Boffa et al.* [206]. Our study provided insight into the possible mechanism of action for this effect by showing that PRPr affected the balance between inflammatory and anti-inflammatory macrophages in the synovial membrane in a murine model. Furthermore, we demonstrated that an early pain reduction after PRPr injections was associated with thinner synovial membrane at end of the experiments. Moreover, less inflammation was positively associated with more anti-inflammatory macrophages. We could conclude that pre-clinical studies using animal models have provided additional insights into PRP's anti-inflammatory and disease-modifying effects, thus paving the way to developing and improving PRP products to become true DMOAD.

While animal models can help elude the working mechanisms of different biological therapeutic approaches, confirming their positive results in clinical studies is crucial. Like MSC clinical trials, most PRP clinical trials do not focus primarily on inflammation. Multiple trials have demonstrated decreased VAS scores, improved functionality, and WOMAC scores after intra-articular PRP injection(s). Since there is a clinical improvement, these studies state that there must have been an anti-inflammatory effect while not having investigated the inflammation in their respective studies. Fortunately, others have done just that and demonstrated a lower concentration of

pro-inflammatory cytokines such as IL-1β and TNF-α in the synovial fluid of PRP-treated patients with knee OA or even in the blood plasma of patients [207]. This resulted in a notable reduction in joint inflammation and further cartilage destruction after administration [208]. Therefore, we hypothesize that PRPr injections are more effective when applied as a therapeutic intervention after trauma and early OA, to counter the early pro-inflammatory conditions to prevent cartilage damage, rather than as a treatment for end-stage OA.

To recapitulate our inflammation related results, we show that MSC and the MSC secretome have multiple immunomodulatory effects in the CIOA model, accentuating the importance of synovial inflammation and its associations with other pathophysiological OA-related processes. However, the anti-inflammatory effects remained relatively modest, emphasizing the need for further studies to improve the MSC efficacy. Although we demonstrated anti-inflammatory effects in our *in vitro* experiments with encapsulated allogenic rat MSC, we could not translate this to our *in vivo* OA experiments, using xenogeneic MSC in rats. While we demonstrated that encapsulated MSC do reside for a prolonged time *in vivo*, we did not see inhibitory effects on inflammation. Possibly the foreign body reaction to the alginate masked the paracrine effect of MSC or using xenogenic MSC was the reason for a mild anti-inflammatory response of the encapsulated MSC. One could use the secretome of allogeneic MSC improve the transability of our cell free product, as we demonstrated in the equine experiments in which an anti-inflammatory effect was seen. Furthermore, our findings suggest that PRP is a promising therapeutic option for OA, with significant potential to reduce inflammation.

Effect of biological therapies on pain

Pain is an important clinical feature of osteoarthritis, significantly impacting the quality of life for those affected. Pain and discomfort are the main reasons patients seek help and present themselves at the doctor's office. This pain is a massive burden on patients; it has adverse effects on sleep, mood and even memory and cognitive dysfunction [209]. While analgesics such as NSAIDs and corticosteroids, administered systemically or locally, can be used to address pain, their effects are temporary. These interventions aim for symptom relief and do not demonstrate actual disease-modifying effects [210]. Pain in osteoarthritis is a complex phenomenon involving multiple pathways, including mechanical, inflammatory, and neuropathic mechanisms [211]. Synovial inflammation causes pain by sensitizing peripheral nociceptors and promoting the release of inflammatory mediators that activate and sensitize the nociceptive system [212, 213]. Subchondral bone changes, such as bone marrow lesions and microfractures, combined with its rich innervation, also play a significant role in osteoarthritic pain

[214]. All this could be of great importance for understanding possible pain pathways in OA. In this context, cell-based therapies using MSC, or cell-free options such as PRP, are promising approaches to address the underlying pathophysiological mechanisms of osteoarthritis, with the potential to provide sustained pain relief if they modulate the disease process.

In various pre-clinical studies using MSC, their effect on pain was observed. Intra-articular administration of adipose derived MSC significantly improved lameness scores and reduced pain in hip OA in dogs [215], synovial derived MSC gave similar results in surgery induced OA in beagles [216] and using MSC in MIA model in rats [217]. Several factors could explain the pain reduction by MSC based on their biological properties. In a prior study by van *Buul et al.* utilizing the rat MIA OA model, our group demonstrated that treatment with MSC exhibited a significant increase in weight-bearing on the affected limb four weeks after treatment, suggesting a pain-relieving effect of MSC therapy [32]. However, due to the high variability in withdrawal threshold measurements over time in the rat MIA OA model described in this thesis, we deemed these results inconclusive. In the murine CIOA model, pain, we observed a reduction in pain in both the MSC and MSC secretome groups 1 week after treatment and lasted for the entire experiment. When using the same CIOA model, PRPr injections significantly reduced pain for two consecutive weeks. Interestingly, in both experiments, the control group also showed a pain reduction, albeit this started at a later time. This indicates a general pain reduction as the natural course of the used CIOA model, as previously described by Adaes *et al.* [107]. Synovial inflammation most likely played a role in pain perception, partly because pain and synovial inflammation is known to diminish in time [113]. Nevertheless, in the MSC experiments, we could not correlate pain with other OA characteristics. However, in the PRPr experiments, we demonstrated that mice with higher pain levels on day 7 were more likely to develop thicker synovial membranes two weeks later. The PRPr-treated knees in our study likely contain fewer pro-inflammatory and more anti-inflammatory macrophages, leading to reduced production of PGE2, a key mediator of inflammatory pain and hypersensitivity. This suggests a correlation between pain levels, synovial inflammation, and macrophage activity._msocom_2_This aligns with findings of another group in a rabbit knee OA model, where leukocyte-poor PRP injections reduced PGE2 levels [218].

Although animal models are valuable for investigating pathogenesis, their translational value is limited by various factors, such as joint anatomy, including joint size and cartilage thickness, and the inherent healing potential of the species used [219]. Next to this, one must consider that animals behave differently to pain. For animals such as mice, rats, and even horses, as possible prey animals, it is better not to appear weak and therefore to hide their pain [12, 15]. This underscores the importance of clinical research, with a growing number of trials focused on evaluating the effects

of biologicals on pain. A pilot study of MSC therapy in OA indicated significant pain relief following a year after intra-articular injections of MSC when compared to hyaluronic acid (HA) [220]. As described in the review by de *Carvalho Carneiro et al.* multiple clinical studies demonstrated similar results, showing pain mitigation and recovery of physical activities without serious adverse effects [221]. *Lamo-Espinosa et al.* demonstrated that the administration of MSC led to significant long-lasting alleviation of pain symptoms [28]. Likewise, intra-articular PRP injections have reduced pain and improved function in patients with knee OA more effectively than hyaluronic acid or steroid injections [222, 223]. In contrast, others have demonstrated that multiple PRP injections in patients with symptomatic mild to moderate radiographic knee OA, did not significantly differ in symptoms or joint structure compared to placebo [200, 224]. However, a disadvantage of these studies is that they are often small in scale or need more randomization. Additionally, the focus is not always on pain outcomes but on patient-reported outcome measures.

Summarizing our pain related outcomes, we demonstrated that MSC and PRPr can reduce pain in our *in vivo* models. Furthermore, we demonstrated an association between higher pain levels and synovial inflammation, possibly via the presence of fewer pro-inflammatory and more anti-inflammatory macrophages. Nevertheless, while biologics such as MSC and PRPr hold promise, the current evidence is still limited and sometimes inconclusive.

Towards clinical application

MSC and PRP, along with their secreted paracrine factors, have been shown to exert beneficial effects in the treatment of osteoarthritis and other musculoskeletal disorders as mentioned before. In this thesis, we have examined and discussed the effects as well as the potential mechanisms of action of these potential disease-modifying agents in different models. Nevertheless, a number of questions remain unanswered to fully realize the potential of these DMAODs and to work toward their clinical application.

Source and delivery

Selecting the optimal source for MSC and preparing them for clinical use remains a significant challenge. Ideally, one would need an easily accessible, abundant and homogenous source of MSC with the capacity to expand in culture without losing its ability to proliferate, differentiate and, more importantly, secrete high concentrations of anti-inflammatory cytokines and growth factors. Factors such as donor site, donor age and disease status can influence the functional characteristics of isolated MSC, necessitating careful donor screening and characterization [225].

The question is what tissue to use as an MSC source. The different sources of MSC have different advantages; two main ones used in OA research are bone marrow-derived and adipose-derived MSC [226, 227]. BM-derived (BM MSC, or MSC in this work) is the golden standard and is widely studied [227]. At the same time, adipose-derived is more abundant and more accessible to isolate, thereby gaining popularity [226]. No winner has emerged yet. BM MSC may have a stronger innate ability to undergo chondrogenic differentiation, which could be more advantageous for direct cartilage repair strategies than adipose-derived MSC. However, adipose-derived MSC may offer additional regenerative benefits over BM MSC due to their enhanced paracrine signaling, especially regarding inflammatory modulation (bron). A recent meta-analysis demonstrated that MSC from these sources holds promise for treating knee OA, with bone marrow-derived MSC showing superior short- and long-term benefits; however, additional research involving larger clinical samples and longer follow-up is necessary to validate these results [228].

While each MSC donor type presents challenges, allogenic MSC from young, healthy donors offers a more practical and promising option. Their availability and strong regenerative and anti-inflammatory potential make them ideal for developing off-the-shelf therapies, especially when consistency and effectiveness are critical for clinical success. To increase their efficacy we could use encapsulation of MSC to improve the longevity and interaction of the MSC with the diseased joint. To bypass the possible host versus graft reactions on MSC use, one could use MSC secretome instead as we have demonstrated, this is as effective as free or encapsulated MSC products,

offering a promising future for osteoarthritis treatment. In this way, an abundant, consistent and controlled cell product would always be available. This would facilitate easy use, interpretation of clinical study results and, ultimately, regulatory approval

Other important aspects of delivery are dose and timing. The optimal dose and timing of MSC (secretome) administration require careful consideration and significantly impact therapeutic efficacy. While some studies have explored single-dose versus repeated injections, the ideal dosage range and the appropriate interval between injections remain to be determined. Factors such as the specific disease stage/phase, severity, and individual patient characteristics may influence the optimal dosing regimen. Continued research is necessary to better understand the relationship between MSC dose, timing of administration, and the desired therapeutic outcomes in the context of osteoarthritis treatment.

In parallel to the continued research and development efforts focused on optimizing and translating MSC-based therapies for OA, we have also explored the use of PRP, as mentioned before PRP is not a cell free product, but by activating it *in vitro*, this is achievable. In our case the cell free PRPr. PRP is more easily accessible and the components are derived from the patient's blood on the day of administration. However, the challenges of autologous PRP include the lack of standardization, reproducibility and variability in composition between patients [229]. This imposes difficulties when interpreting evidence regarding PRP efficacy, since the intervention details vary dramatically from study to study, making it hard to draw firm conclusions. To circumvent this, we could use a standardised allogeneic batch of PRP, like we used in or work. Another key aspect that influences the therapeutic potential of PRP is the presence of leukocytes, there is still debate on leukocyte rich vs poor PRP [190-193]. PRP containing higher concentrations of leukocytes can be more pro-inflammatory, especially when using an allogenic batch [192, 193]. It may worsen joint damage, whereas PRP with lower leukocyte levels tends to be more anti-inflammatory and promote tissue regeneration. If more standardized preparation protocols of activated PRP with low leukocyte count are developed and used, we could better examine its efficacy and value as a DMOAD in OA. At a later stage, we could use purification strategies to filter the anti-inflammatory cytokines and growth factors, enhancing the therapeutic efficacy of PRPr.

In a more distant future, once the optimal cocktail of anti-inflammatory cytokines and growth factors to counter osteoarthritis is determined, one could utilize an allogeneic MSC or PRP source, characterize it, and even genetically engineer cells to produce these factors in high concentrations. One could even filter out certain factors to the desired concentration, making them ready for intra-articular injection, disregarding less favourable cytokines. Alternatively, bypassing this and bioengineering the effective factors without using MSC or PRP would directly produce

these factors in bulk; this would be a pure pharmaceutical and much more controllable approach. But to be able to do this, we must fully understand the pathophysiology of OA and be sure what cytokines and growth factors to use.

Joint on a chip

Joint on a chip technology holds great promise for advancing our understanding of osteoarthritis by providing more accurate models of human joint mechanics and cellular interactions [230, 231]. In combination with 3D-bioprinting, replicating the tissues, biomechanics, and biochemical status of a native joint, this technique can provide insight into disease pathophysiology and could help with DMOAD development [230, 232, 233], and it offers a potential alternative to animal models. One could test multiple potential combinations of cytokines/growth factors in this system on a larger scale and accelerate the development off new DMOADs. Continued research in this area may lead to innovative approaches for studying and treating osteoarthritis, ultimately improving patient outcomes.

Imaging

A deep understanding of the disease's pathophysiology and progression is central to developing regenerative therapies. With the aid of new imaging techniques and synovial fluid analysis, we are gaining more insight into the different phenotypes and stages of OA. This can be used mainly in clinical research to better understand the progression of disease and to monitor the effects of treatment. While conventional radiography remains the gold standard for OA diagnosis and monitoring in clinical practice, advanced MRI and CT techniques offer a more comprehensive assessment of cartilage and the joint for research purposes. Improvements in quantitative MRI techniques offer a deeper look into cartilage health than traditional MRI by measuring specific properties of cartilage tissue. T2 Mapping can assess the organization and integrity of collagen fibres within cartilage. It can detect early cartilage degeneration before structural changes are visible on conventional MRI. T1rho mapping assesses the interaction between water molecules and their surrounding macromolecules in cartilage. This technique is sensitive to changes in cartilage composition, such as proteoglycan content, which is another early marker of OA. Delayed Gadolinium-Enhanced MRI of Cartilage (dGEMRIC) involves injecting a contrast agent that distributes differently within the cartilage depending on its composition. This technique provides information about cartilage GAG content, a key indicator of cartilage health. Weight-bearing CT (WBCT) is an imaging technique that allows a more realistic representation of joint mechanics during daily activities [234]. This is because weight-bearing can alter joint alignment, cartilage contact points, and overall joint space width compared to non-weight-bearing positions. WBCT can detect subtle

changes in joint space narrowing and cartilage deformation that may not be apparent on conventional CT scans in a non-weight-bearing position. These improved imaging techniques can aid in earlier OA diagnosis, better disease progression monitoring, and more informed treatment decisions.

Biomarkers

Osteoarthritis is a complex disease that involves both structural and biochemical changes in the joint, and the identification of suitable biomarkers has been an area of active research [212]. Biomarkers, in blood or urine can be used to identify patients who may benefit from specific treatments, and in the context of clinical trials, they can be used to monitor the effects of experimental drugs or other therapeutic interventions. Although there is not one ultimate biomarker, some have shown potential as prognostic indicators, meaning they might help monitor disease progression [235]. For example, higher levels of COMP in serum generally correlate with more significant cartilage breakdown. Monitoring COMP levels in serum over time might help track the severity of cartilage damage, although elevated COMP levels in synovial fluid were not confirmed. Hyaluronic acid is a major component of healthy cartilage, and its levels in synovial fluid tend to decrease as OA progresses. Furthermore, inflammatory molecules like IL-1β and TNF-α are involved in OA progression. Monitoring their levels might help assessing the level of inflammation in the joint, which could correlate with disease activity. If we are more interested in the efficacy of our intervention, biomarkers such as C4S related to aggrecan metabolism are interesting. C4S has decreased after IA injections of HA and correlates with pain in knee OA patients [236]. Even white blood cell count in synovial fluid may predict reaction to anti-inflammatory therapy. However, Boffa *et al.* emphasize that more research is needed to confirm the reliability of these biomarkers as predictive tools [235]. Additionally, biomarker levels can vary between individuals, making it essential to establish a baseline for each patient and track changes over time. Using a panel of biomarkers, rather than relying on a single one, might provide a more comprehensive picture of OA progression. Biomarker analysis, alongside clinical evaluation and imaging biomarkers, could enable a more precise understanding of individual disease activity in future clinical studies.

Wearable technology

A recent development in osteoarthritis research, is the use of wearables, examples are mobile apps, smartwatches or pressure sensor inlays. One could use them as an objective measurement of physical activity pre and post MSC/PRP treatment. Or the amount of loading on the affected limb, similar to the our murine experiments in which we measured the percentage of weight distributed on the affected limbs of mice. Studies indicate positive psychosocial impacts next to low technical complexity

and cost, and consistency in the analysis of the data as the most critical facilitators for the feasibility of using wearable technology in a real-world setting. However, the evidence base is still developing, and further research is needed to fully understand the benefits and optimize the use of wearables in osteoarthritis research and management [237-241].

Artificial intelligence

The emerging role of artificial intelligence (AI) in our world could also be of use in selecting the optimal therapy at the specific stage of the disease and potentially tailoring it to the individual patient. In the medical field, AI is already being implemented in radiology departments; AI can automate tasks and improve the diagnostic accuracy of X-rays, CT or MRI. AI can extract quantitative measurements from images, such as cartilage thickness, joint space width, and bone shape. These measurements can provide objective data for OA diagnosis, staging, and monitoring. While still in its early stages, AI algorithms can help streamline analysis and reduce variability between human observers. Researchers are exploring the use of AI to predict future OA progression based on imaging features. This could help identify individuals at higher risk of rapid disease progression and guide personalized treatment strategies. Similarly, AI can be used to analyse a large amount of data from biomarker studies, genomic data, and patient-reported outcomes to gain more significant insights into the complex pathogenesis of OA. Or, one could use a multimodal AI approach to integrate diverse data types like imaging, movement analysis, and biomarker analysis to develop novel predictive models of OA risk and progression. These techniques are still very new and experimental at best, but they hold great promise for improving early OA diagnosis, monitoring disease progression, and evaluating the effectiveness of new therapies.

CHAPTER 7

Summary

Osteoarthritis (OA) is a progressive disabling joint disease, in 2019 there were 528 million people living with osteoarthritis [1]. The prevalence of the diseases is increasing, it already increased by 123.2% in the last 30 years and is projected to double by 2050 [4]. OA is characterized by loss of cartilage integrity, subchondral bone changes, formation of osteophytes and inflammation of the synovial membrane [5]. These processes together .result in pain and functional disability, which are the main reasons for patients to seek medical treatment. However, to this date, no curative treatment for OA exists. The need for disease-modifying drugs or therapies is high. Ideally, such a therapy would inhibit or repair damage to the joint tissues and simultaneously reduce pain and disability. Two promising and potential disease-modifying osteoarthritis drugs (DMOADs) are mesenchymal stem/signalling cells (MSC) and platelet-rich plasma (PRP). This thesis aimed to investigate the use of paracrine factors of mesenchymal stem cells and platelets as early intervention therapy for osteoarthritis.

Summary of the most important results of this thesis

MSC have previously been described to have a beneficial effect in regenerative medicine, both in pre-clinical and some initial clinical studies [36, 42, 44, 99]. MSC were first described by Caplan *et al*, and were found to have osteogenic, adipogenic and chondrogenic capacities [24]. Some initial studies on cartilage regeneration were based on this capacity, and MSC were used to form or restore new cartilage *in vitro* or *in vivo*. Unfortunately, these initial results were relatively modest, and cell tracking studies showed limited long-term engraftment of locally applied cells. Nevertheless, beneficial effects were found in other fields using MSC for systemic applications, such as graft versus host disease. This led Prockop *et al.* and von Bahr *et al.* to postulate the "hit-and-run" mechanism, which proposes that the cells only interact briefly with the microenvironment [36, 42, 44]. In this short period, they could activate local regenerative cells or attract more regional or systemic progenitor cells. Due to their short local viable presence after regional or systemic application, it is hypothesized that the primary working mechanism of these MSC is due to their capacity to secrete a wide variety of anti-inflammatory cytokines and growth factors. These trophic MSC capacities provide an exciting option for possibly basing future therapies on their secreted factors. To develop an allogeneic off-the-shelf therapeutic, we used either an approach in which the cells are encapsulated (**Chapter 2**) or a cell-free approach (**Chapters 3 and 4**). Especially the latter provides excellent options for more comprehensive clinical application by minimizing possible safety and regulatory issues when using allogeneic cell sources.

In **Chapter 2**, we evaluated the efficacy of MCS encapsulated in alginate microbeads using a mono-iodoacetate (MIA) induced rat OA model. The design of this

study was based on the idea that the therapeutic efficacy of MSC could be enhanced by prolonging their local viable presence and, thereby, their secreted factors at the desired location. We compared two clinical grade alginates (High G and High M), and in both MSC remained viable and immunomodulatory active *in vitro*. There were no differences in construct integrity and MSC retention after *in vivo* implantation of encapsulated allogeneic MSC. We could reproducibly produce tiny injectable beads with vital MSC using High G alginate and a micro-encapsulator. Intra-articular injected MSC-alginate beads remained present and metabolically active in the joint for at least 8 weeks *in vivo*. However, encapsulation in alginate did not improve the effect of MSC on pain, cartilage damage, or synovial inflammation in an injected rat knee.

The therapeutic capacity of MSC secretome was examined in **Chapter 3** to develop a true cell-free biological therapeutic. The use of MSC secretome without actual employment of cells originates from the cardiovascular field [99]. This cell-free approach reduces many regulatory and safety issues related to MSC therapy, and *in vitro* cell activation provides opportunities to enhance therapeutic efficacy further. Although the longevity of the secreted factors is expected to be even lower than that of the MSC, they have an effect *in vivo*, possibly by activating a cascade of reactions. We stimulated MSC *in vitro* with pro-inflammatory cytokines to induce the production of paracrine factors. The MSC secretome was injected intra-articularly in a more inflammation-based collagenase-induced murine OA model (CIOA). We used multiple injections to increase possible therapeutic effects further. Injections with MSC secretome resulted in early pain reduction and a protective effect on cartilage damage, albeit no effects were found on subchondral bone remodelling or synovial membrane inflammation.

To further examine the anti-inflammatory effects of MSC secretome, we used equine MSC (eqMSC) secretome in an equine LPS-induced inflammation model in **Chapter 4**. In this experiment, we examined the possible anti-inflammatory capacity of allogeneic MSC secretome, in contrast to the xenogenic MSC secretome used in **Chapter 3**. Secondly, this was a next step in the translatability of the MSC-secretome as a potential DMOAD in a larger animal model. In this model of joint inflammation, intra-articular treatment with eqMSC secretome had a clinical anti-inflammatory effect and affected cartilage metabolism. When directly comparing eqMSC secretome to eqMSCs, eqMSCs did not demonstrate a superior treatment effect in the model, indicating that secretome might be a viable alternative to MSC treatment.

To explore other biological options for encountering OA pathology with a high potential for broad clinical application, we studied platelets as a possible source of paracrine factors. PRP is a plasma product extracted from whole blood that contains at least $1.0 \cdot 10^6$ platelets per microliter. [59]. When the platelets undergo degranulation, they release growth factors and cytokines such as transforming growth factor β (TGF-

β) and platelet-derived growth factor (PDGF), two critical factors in tissue healing [59-61]. The resulting degranulated fluid is denominated PRP releasate (PRPr), and can be harvested for further use. In **Chapter 5**, we studied the therapeutic effect of PRPr in a murine CIOA model. Multiple intra-articular injections of PRPr reduced synovial inflammation and had a protective effect on cartilage while at the same time reducing pain. The most substantial effect on pain reduction was seen shortly after the start of treatment.

Since allogeneic MSC secretome and PRP releasate can be produced in advance, and on a large scale, it could be subjected to quality control testing, and it potentially reduces costs, risks, and regulatory hurdles compared to cell therapies. Ultimately, the ability to classify patient populations and precisely target different stages of OA using personalized therapies like MSC and PRP will be crucial for realizing their full clinical potential as DMOAD.

In conclusion, while MSC and PRP are promising options as off-the-shelf DMOADs, further research is required to fully characterize, optimize, and standardize these therapeutics to ensure their effective clinical translation. Our research has contributed to the future use of cell-free end products by demonstrating similar results of MSC and MSC secretome, and by providing insights in the working mechanisms of MSC secretome and PRP releasate in our animal studies.

CHAPTER 8

Nederlandse samenvatting

Artrose is een progressieve invaliderende gewrichtsziekte die meer dan 10% van de mensen boven de 60 jaar treft, in 2019 waren er 528 miljoen mensen wereldwijd die leefden met artrose. Artrose wordt gekenmerkt door verlies van de integriteit van het kraakbeen, veranderingen in het onderliggende bot, extra botvorming rondom het gewrichtsoppervlak en ontsteking van het slijmvlies aan de binnenzijde van het gewricht. Deze processen leiden samen tot pijn en functionele beperkingen en zijn dus de belangrijkste redenen voor patiënten om medische behandeling te zoeken. Tot op heden bestaat er echter geen genezende behandeling voor artrose en kunnen wij mensen behandelen met adviezen ten aanzien van mobiliteit/fysiotherapie, gewrichtsreductie, pijnstilling en in eind stadium operaties zoals bijvoorbeeld standscorrecties en prothesiologie. De behoefte aan geneesmiddelen of therapieën die de ziekte kunnen remmen of genezen is groot. Idealiter zou een dergelijke behandeling de schade aan het gewrichtsweefsel moeten herstellen en tegelijkertijd de pijn en beperkingen verminderen. Twee veelbelovende middelen waarmee we artrose op deze manier zouden kunnen behandelen zijn mesenchymale stromale/stam (MSC) en (bloed)plaatjes-rijk plasma (PRP). Dit proefschrift had als doel het gebruik van MSC en PRP als vroege interventie-therapie voor artrose te onderzoeken.

Samenvatting van de belangrijkste resultaten van dit proefschrift

Over MSC is al eerder beschreven dat ze een gunstig effect hebben in de regeneratieve geneeskunde, naar aanleiding van studies in in dieren-als mensen. MSC werden voor het eerst beschreven door Caplan *et al.*, hij liet zien dat MSC ook bot, vet en kraakbeenweefsel konden maken, het zogenaamde regeneratiecapaciteit. Enkele eerste studies naar kraakbeenregeneratie waren hierop gebaseerd; MSC werden gebruikt om nieuw kraakbeen te vormen of te herstellen in een kweekschaal of in dieren. Helaas waren deze eerste resultaten relatief bescheiden en lieten deze studies een beperkte lange termijn aanwezigheid zien van lokaal toegepaste cellen. Desondanks werden gunstige effecten gevonden in andere gebieden waarbij MSC voor systemische toepassingen werden gebruikt. Dit leidde ertoe dat Prockop en von Bahr het “hit-and-run”-mechanisme postuleerden, waarin wordt voorgesteld dat de MSC slechts kort interacteren met de micro-omgeving. In deze korte periode kunnen ze lokale regeneratieve cellen activeren of meer regionale of systemische stamcellen aantrekken. Vanwege hun korte lokale aanwezigheid na regionale of systemische toepassing, wordt verondersteld dat het primaire werkingsmechanisme van deze MSC vooral te danken is aan hun vermogen om een breed scala aan ontstekingsremmende stoffen en groeifactoren af te scheiden. Dit wordt ook wel de trofische MSC-capaciteit genoemd en dit biedt een interessante optie om toekomstige therapieën te baseren op de door MSC afgescheiden stoffen in plaats van de MSC zelf. Dit is ook waar we ons

in dit proefschrift mee bezig hebben gehouden. Om een kant-en-klare therapeutische behandeling te ontwikkelen, gebruikten we ofwel een benadering waarbij de cellen zijn ingekapseld **(Hoofdstuk 2)** of een celvrije benadering (**Hoofdstukken 3 en 4**).

In **Hoofdstuk 2** hebben we de werkzaamheid geëvalueerd van MCS ingekapseld in alginaat-microparels in ratten na chemisch geïnduceerde artrose. Het ontwerp van deze studie was gebaseerd op het idee dat de therapeutische werkzaamheid van MSC kan worden verbeterd door hun lokale aanwezigheid en daarmee hun afgescheiden factoren op de gewenste locatie te verlengen. We hebben twee alginaten vergeleken, en in beide bleven de MSC levensvatbaar en actief. Er waren geen verschillen in de integriteit van de constructen en de retentie van MSC na implantatie van ingekapselde allogene MSC. We konden op reproduceerbare wijze kleine injecteerbare parels met vitale MSC produceren. Intra-articulair geïnjecteerde MSC-alginaat parels bleven gedurende ten minste 8 weken aanwezig en metabolisch actief in de rattenknie. Echter zagen we geen positief effect van inkapseling van MSC in alginaat op pijn, kraakbeenschade of synoviale ontsteking in vergelijking tot vrij geïnjecteerde MSC in een rattenknie niet.

De therapeutische capaciteit van het MSC-secretoom, de verzameling van stoffen uitgescheiden door de MSC, werd in **Hoofdstuk 3** onderzocht om een echt celvrij biologisch therapeuticum te ontwikkelen. Het gebruik van alleen MSC-secretoom zonder daadwerkelijke inzet van cellen heeft zijn oorsprong in de hart en vaatziekten. Deze celvrije benadering voorkomt veel regulatoire en veiligheidskwesties die verband houden met MSC-therapie, en door de cellen van te voren in het lab te activeren zouden we de therapeutische werkzaamheid mogelijk nog verder kunnen verbeteren. Hoewel de levensduur van de afgescheiden factoren naar verwachting nog lager zal zijn dan die van de MSC zelf, hebben ze een effect in dierexperimenten, mogelijk door het activeren van een cascade van reacties. We stimuleerden MSC buiten het lichaam met ontstekingsfactoren om de productie van ontstekingsremmende-en groeifactoren te induceren. Het MSC-secretoom werd in het gewricht geïnjecteerd in een artrose model in muizen. We gebruikten meerdere injecties om de mogelijke therapeutische effecten verder te vergroten. Injecties met MSC-secretoom resulteerden in vroege pijnverlichting en hadden een beschermend effect op kraakbeenschade, hoewel er geen effecten werden gevonden op het onderliggende bot of de ontsteking van gewrichtsslijmvlies.

Om de ontstekingsremmende effecten van het MSC-secretoom verder te onderzoeken, gebruikten we paarden MSC-secretoom in een ontstekingsmodel bij paarden in **Hoofdstuk 4**. In dit experiment onderzochten we de mogelijke ontstekingsremmende vermogen van MSC-secretoom van dezelfde diersoort, in tegenstelling tot het MSC-secretoom van andere diersoort dat in Hoofdstuk 3 werd gebruikt. Daarnaast was dit een volgende stap in de vertaalbaarheid van

het MSC-secretoom als potentiële behandeling in een groter dierenmodel. In dit model van gewrichtsontsteking had een intra-articulaire behandeling met paarden MSC-secretoom een klinisch ontstekingsremmend effect en beïnvloedde het de kraakbeenstofwisseling. Bij een rechtstreekse vergelijking van behandeling met paarden MSC-secretoom of met vrij geïnjecteerde paarden MSC vertoonden de vrije MSC geen beter behandelingseffect in het model, wat erop wijst dat secretoom een goed alternatief voor MSC-behandeling kan zijn.

Om andere biologische opties voor de behandeling van artrose te verkennen, hebben we bloedplaatjes bestudeerd als mogelijke bron van werkzame uitgescheiden stoffen, de zogenoemde paracriene factoren. PRP is een plasmaproduct dat wordt geëxtraheerd uit volbloed en ten minste een zesvoudige concentratie bloedplaatjes bevat dan gewoon bloed. Wanneer de bloedplaatjes geactiveerd worden, laten ze groeifactoren en signaleneiwitten vrij, dit zijn cruciale factoren voor weefselherstel. Het resulterende vloeistofpreparaat met alle stofjes erin wordt plaatjes rijk plasma releasate (PRPr) genoemd. In **Hoofdstuk 5** hebben we het therapeutische effect van PRPr in een muis artrose model bestudeerd. Herhaalde intra-articulaire injecties van PRPr verminderde de ontsteking in het gewrichtsslijmvlies en had een beschermend effect op het kraakbeen, terwijl tegelijkertijd de pijn verminderde. Het meest substantiële effect op pijnvermindering werd kort na de start van de behandeling waargenomen. En we zagen een verband tussen minder gewrichtsontsteking en minder pijn.

Aangezien donor MSC-secretoom en PRPr vooraf en op grote schaal geproduceerd kunnen worden, kunnen ze aan kwaliteitscontrole worden onderworpen, en kunnen ze potentieel de kosten, risico's en regelgevende hindernissen verlagen in vergelijking met therapieën waarbij cellen zelf worden ingebracht. Uiteindelijk zal het vermogen om patiëntpopulaties te classificeren en verschillende stadia van artrose nauwkeurig aan te pakken met behulp van gepersonaliseerde therapieën zoals MSC en PRP cruciaal zijn voor het realiseren van hun volledige klinische potentieel.

Concluderend, hoewel MSC en PRP veelbelovende opties zijn als kant-en-klare behandelingen die daadwerkelijk de progressie van artrose kunnen vertragen of terugdraaien, is verder onderzoek nodig om deze therapeutica volledig te karakteriseren, te optimaliseren en te standaardiseren om een effectieve klinische behandeling te waarborgen. Ons onderzoek heeft bijgedragen aan het toekomstige gebruik van celvrije eindproducten door vergelijkbare resultaten van MSC en MSC-secretoom aan te tonen, en door inzichten te geven in de werkingsmechanismen van MSC-secretoom en PRPr in onze dierstudies.

CHAPTER 9

Appendices

PhD portfolio
Curriculum vitae
Dankwoord
References

PhD portfolio

Name PhD student: Sohrab Khatab
Erasmus MC department: Orthopedics and Radiology & Nuclear medicine
Research school: Postgraduate School Molecular Medicine (Mol-Med)
PhD period: November 2014 – December 2018
Promotor: Prof. dr. G.J.V.M. van Osch
Co-promotors: Dr. M.R. Bernsen, Dr. G.M. van Buul

Phd training

	Year	Workload (ECTS)
General courses		
Laboratory Animal Science Art 9	2015	3.0
Academic Integrity & Responsible Research	2015	1.0
Erasmus MC - Biomedical English Writing	2016	2.0
Specific courses (e.g. Research school, Medical training)		
Erasmus MC - Animal Imaging	2015	1.4
Workshops and journal clubs		
Journal clubs (every first Monday of the month)	2014-2018	2.0
Photoshop en illustrator CS6 2013 0.3	2016	0.3
Presentations		
Oral presentations at research meetings		
At the department of Orthopedics, Radiology and Internal medicine	2014-2025	4.0
Oral presentations at ROGO dag	2017-2023	2.0
Oral presentations at research project meetings (NWO)	2017-2018	1.0
Oral presentation Wetenschapsdag Orthopedie	2016-2018	1.0
(Inter)national conferences		
Oral presentation MolMed	2016	1.0
Attending OARSI World Conference, Amsterdam	2016	0.5
Oral presentation annual meeting NBTE, Lunteren	2016	1.0
Poster presentation ICRS Sorrento Italy	2016	0.5
Oral presentation ICRS, Sorrento, Italy	2016	1.0
Oral presentation OARSI Las Vegas	2017	1.0
Poster presentation MolMed Day	2017	1.0

Oral presentation NOV voorjaarsvergadering	2018	1.0
Oral presentation OARSI Liverpool	2018	1.0
Attending ICRS Focus Meeting, Milan	2018	0.5
Oral presentation OARSI World Conference Toronto	2019	1.0

Teaching

Courses		
Omgaan met groepen (BKO)	2016	0.1
Cursus Coaching studenten (BKO)	2015	0.2
Lecturing		
Lecturing minor “Orthopedics Sports Traumatology”	2016-2018	2.0
Histology practical bonepathology for 1st year students	2015-2016	1.0
Supervising		
Supervising MolMed Master research (2016)	2017	4.0
Coaching 5 individual medical students from their 1st till 4th year	2015-2018	3.0
Tutor 1st and 2nd year medical studentgroups	2017	1.0

Other

ICRS Best poster presentation award	2016
OARSI Young Investigator award Las Vegas	2017
OARSI Young Investigator award Liverpool	2018

Curriculum vitae

Sohrab Khatab werd geboren op 1 juni 1986 in Kabul, Afghanistan, en groeide vanaf zijn elfde op in Grubbenvorst in Limburg. Na het behalen van zijn gymnasiumdiploma aan het Blariacum College te Blerick begon hij, in 2006 aan de studie Biomedische Wetenschappen aan de Universiteit Utrecht. In 2007 startte hij de opleiding Geneeskunde aan de Erasmus Universiteit Rotterdam. Door het vooraf-gaande studiejaar in Utrecht miste hij aanvankelijk de gewenste diepgang binnen Geneeskunde. Die vond hij tijdens een masteronderzoek in het levertransplantatielaboratorium van het Erasmus MC, onder begeleiding van prof. dr. L.W.J. van der Laan en dr. J. de Jonge. Daar werkte hij voor het eerst met stamcellen, die in een — mede door hem ontwikkeld — machineperfusiesysteem door geëxplanteerde muizenlevers werden gepompt. Het technische en biomechanische karakter van dit werk beviel hem en legde de basis voor zijn latere onderzoek binnen de orthopedie. Tijdens de coschappen werd namelijk duidelijk dat zijn grootste interesse lag bij de orthopedie en traumatologie. In 2014 behaalde hij zijn artsendiploma en in november van datzelfde jaar startte hij zijn promotieonderzoek, getiteld: *"Towards intra-articular application of biological therapeutics for osteoarthritis"*. Dit promotietraject werd uitgevoerd onder begeleiding van zijn promotor prof. dr. G.J.V.M. van Osch en copromotoren dr. M.R. Bernsen en dr. G.M. van Buul.

Tijdens zijn promotietraject werkte hij onder meer als ANIOS chirurgie in het Franciscus Gasthuis (SFG) te Rotterdam. In 2019 startte hij met de opleiding tot orthopedisch chirurg. Voor zijn vooropleiding heelkunde keerde hij terug naar het SFG, waar hij werkte onder supervisie van dr. T. Klem. In 2020 volgde hij het eerste academische deel van zijn orthopedische opleiding in het Erasmus MC onder leiding van dr. P.K. Bos. Het perifere deel volgde hij in het Elisabeth-TweeSteden Ziekenhuis te Tilburg, onder leiding van dr. T. Gosens en dr. O.J. van der Jagt. In de zomer van 2025 rondde Sohrab zijn opleiding af tot orthopedisch chirurg-traumatoloog in het Erasmus MC. Sindsdien werkt hij in het Admiraal De Ruyter Ziekenhuis in Goes en Vlissingen. Hij woont in Rotterdam met zijn vrouw Judith en hun drie dochters.

Dankwoord

Hoe cliché het ook mag klinken, dit proefschrift was nooit tot stand gekomen zonder de steun van talloze mensen – en, niet te vergeten, proefdieren. Samenwerking, begeleiding en steun brengen ons verder in het leven; dit werk is daar het levende bewijs van.

Hoewel ik onmogelijk iedereen persoonlijk kan bedanken, wil ik hieronder in het bijzonder stilstaan bij degenen die direct of indirect hebben bijgedragen aan het tot stand komen van deze thesis.

Beste **prof. dr. van Osch, beste Gerjo**, ik heb veel bewondering voor je bevlogenheid, analytisch vermogen, integriteit en de wijsheid die je in pacht hebt. Je weet precies hoe je mensen gemotiveerd kunt krijgen en het beste in ze naar boven kunt halen. Ik kwam altijd met veel positieve energie uit onze meetings, zelfs als ik er met "slechte" resultaten inging. Dank voor je begeleiding, je wijze woorden op zowel professioneel als privé vlak. Veel respect hoe jij het lab runt en alle ballen tegelijk in de lucht houdt, zonder dat je oog verliest voor het persoonlijke. Ik vond het erg fijn om met jou samen te werken en ben ook trots dat ik door jou, een topwetenschapper met internationale faam, ben opgeleid tot onderzoeker. Ik heb je geduld wel erg op de proef gesteld, maar eindelijk is het boekje dan af.

Dr. G.M. van Buul, beste Gerben, nadat ik het project van Maarten overnam en mijn onderzoek meer in lijn kwam met dat van jou, werd jij ook meer betrokken bij mijn werk. Dank voor je tomeloze inzet, je brommerritjes uit Delft naar het lab, de e-mails, telefoongesprekken en congresbezoeken om mij te helpen bij mijn PhD. Veel bewondering voor het gemak waarmee jij lastige materie en gedachtes op papier kan krijgen.

Dr. M. R. Bernsen, beste Monique, dank voor je betrokkenheid als co-promotor bij dit project. Jouw (radiologische) kennis en scherpe blik waren van grote waarde. Ik was telkens onder de indruk van hoe je zelfs de kleinste details wist op te merken. Dank voor je betrokkenheid en de essentiële bijdrage vanuit jouw expertise.

Dr. J. Hermans, beste Job, op een mooie augustusweekend in 2013, wist jij mijn interesse voor de orthopedie te wekken. Een jaar later ben ik mede dankzij jou op gesprek geweest bij Gerjo en Prof Verhaar en is daarna mijn carrière binnen de orthopedie begonnen. Daarvoor ben ik je nog steeds erg dankbaar!

Beste **emiritus prof. dr. Verhaar,** dank voor uw steun. Ik heb uw feedback tijdens de "Meet de prof" sessies als waardevol beschouwd. Ik bewonder hoe u ondanks uw drukke agenda oog hield voor jonge onderzoekers zoals ik. Uw feedback en steun hebben een blijvende invloed gehad op mijn ontwikkeling binnen de orthopedie, waarvoor ik u dankbaar ben.

Dr. P.K. Bos, beste Koen, vanaf het begin betrokken bij mijn carrière, dank voor je bijdrage bij de verschillende artikelen en je kritische klinische blik tijdens mijn promotietraject. Bovenal ben ik je erg dankbaar voor het vertrouwen dat je in mij had om mij aan te nemen voor de opleiding tot orthopedisch chirurg. Het was een mooie reis en ik ben trots dat ik, door jou als de "grote" opleider, in onze ROGO ben opgeleid.

Dr. M. Hoogduijn en **prof. dr. F. Jenner** dank voor uw beoordeling van mijn proefschrift en deelname aan de oppositie. **Prof. dr. T. Gosens**, beste Taco, dank dat je naast dat je mijn opleider bent geweest, nu ook deelneemt in de kleine commissie. **Prof. dr. L.J.W. Van der Laan**, beste Luc, dank dat je deel wilt nemen in de oppositie. Mijn eerste ervaring met stamcellen bij jou in het lab gehad, mede daardoor gekozen voor dit onderzoek. **Dr. E.N. Blaney Davidson**, dank voor uw bereidheid om plaats te nemen in de grote commissie.

Nicole Kops, jouw nauwgezette werk in het lab was onmisbaar. Zonder jouw inzet waren veel van de experimenten simpelweg niet gelukt. Dank voor al je hulp, onze gesprekken en het harde gelach. **Wendy en Janneke**, ook dank voor de hulp bij de vele experimenten, het was een fijne samenwerking.

Beste Joost (dr. Haeck), dank voor al je inzet met de imaging, zonder jouw technische kennis en bereidheid om altijd te helpen was een groot deel van deze thesis niet mogelijk geweest. Ook dank aan **Yanto**, voor je hulp bij de BLI/imaging en altijd een glimlach.

I would like to extend my sincere thanks to all **collaborators and co-authors** for their invaluable support. Special gratitude goes to **Prof. Laurie R. Goodrich** (Colorado University) for providing the equine MSC, **Dr. Nicoline Korthagen** (Utrecht University) for her help with the toxicology experiments, **Prof. Danny Kelly** and his team (Trinity College, Dublin) for access to their facilities, and **Prof. Pieter Brama and Dr. Clodagh Kearney** (School of Veterinary Medicine, Dublin) for a wonderful collaboration which resulted in Chapter 4 of this thesis.

Sandra, zonder jou zou een lab ten onder gaan in papierwerk en chaos. Jij zorgde er met flair en humor voor dat alles soepel bleef lopen. Dank voor al je hulp tijdens en nu bij het afronden van dit boekje.

Yvonne, macrophagen wonder, ik herinner me nog de trip naar Las Vegas – waar je nog bijna mijn werk moest presenteren omdat ik een nachtje langer in Salt Lake City moest blijven. **Eric**, de leider van de Ierse clan, altijd in voor bezoek aan de Boudewijn. **Roberto,** koning van de Western Blot, die mij de Italiaanse koffie gewoontes (verbod op cappuccino na 11 uur) en handgebaren bij heeft gebracht. Dank voor jullie steun en gezelligheid.

Maarten Leijs en Wu Wei, onafscheidelijk duo, wat fijn dat ik samen met jullie kon werken. Met uitkijk op het helipad, konden we natuurlijk niet achterblijven met onze eigen radiografisch bestuurbare Trauma heli's: "Get down….get to tha choppahh!". Als ik nu terugdenk voelde het als een soort verlengde studententijd. Maarten uiteindelijk kon ik jouw onderzoek voortzetten en daar hebben we een mooie publicatie aan over gehouden. Dank beide voor de mooie avonturen toen en later ook als AIOS.

I'm grateful to have worked in a lab where colleagues – and eventually friends – came together from different backgrounds and cultures. **Panithi Sukho**, a constant source of kindness and positivity – I have great respect for you. Thanks for teaching us about your culture and especially food. **Andrea**, my "gym bro" — as long as it lasted ;). You're too kind, smart, and a very good Italian chef. Thank you for being a bro. **Shorouk**, my twin but with temperament, thank you for being so true to yourself and morally uncompromising. Respect. With **Mairéad, Caoimhe, Niamh, Callie and Johannes**, there was never a dull moment; you brought so much energy and good vibes into the lab. **Kavitha**, princess of the Tamils – strict but always fair and good sense of humor. **Diego**, I'm glad we didn't scare you away from a career in science! In my last year the international crew got even bigger with **Virginia**, **Yannick, Enrique and Mauri**. Thanks you all, for all the "colour" you have given my time at the lab.

Sabine, dank voor je bijdrage aan dit werk, als master student. Vond het erg leuk om je te begeleiden en het was ook voor mij een leerzaam traject. Mooi om te zien hoe jij je verdere carrière vorm hebt gegeven.

Lizette, de wizzkid van het lab, altijd behulpzaam en tomeloze kennis. Dank ook voor alle hulp. **Mathijs**, de snelheid en efficiëntie waarmee jij op lab werkte was bewonderingswaardig. **Mark en Suus**, dank dat jullie me adopteerden in HS-104, als niet klinische onderzoeker.

Joost Verschueren, naast tegelijk onderzoek doen, ook met je mogen werken als AIOS in EMC en ETZ. Altijd fijn om met iemand te sparren die in zelfde bootje zit (AIOS, PhD afronden, jong gezin) en zelfde interesses deelt. Dat was fijn toen we AIOS waren maar ook nu nog als jonge klare. **Wouter,** mooie vent, dank voor de mooie tijden en gespreken; soms over niks en soms over het leven, het heden en verleden.

Chirurgen, orthopeden, a(n)ios, PA/VS, OK/poli-assistenten en VPK uit SFG, EMC en ETZ, dank voor het bijdragen aan mijn klinische vaardigheden, maar ook voor de mooie tijd die ik heb gehad! **Pieter Druyts** en **Chris van den Broek** veel van jullie geleerd. Niet alleen het opereren, maar ook de "soft-skills" en hoe je met veel plezier geneeskunst kunt beoefenen. Samen klussen op OK blijft toch het mooiste dat er is, mede dankzij het geweldige OK-team (oa **Fanny, Nicole, Hannah, Margot** en **Muriel**). **Olav van der Jagt** en **Jakob van Oldenrijk**, ik heb me altijd verbaasd over jullie onuitputtelijke bron van kennis, beide "opleider" pur sang, ik heb van jullie geleerd dat ook complexe problemen te verklaren en op te lossen zijn door biomechanica, een kritische blik en logisch redeneren. Dank ook voor het stimuleren om buiten mijn comfort zone te werken, om te excelleren.

Ook dank aan mijn nieuwe collega's binnen het Admiraal de Ruyter ziekenhuis. Allereerst voor de kans om in het mooie Zeeland mijn carrière voort te zetten en dat ze me daarbij de ruimte hebben gegeven om de laatste zaken voor dit proefschrift te regelen. Volgens mij gaan we een mooie tijd tegemoet samen.

Buiten het lab en de kliniek waren er nog meer mensen die mij met evenveel toewijding hebben gesteund. Lieve vrienden en familie, dank voor jullie betrokkenheid, steun en oprechte interesse. Jullie zijn er niet alleen geweest tijdens dit traject, maar vormen ook buiten dit alles een belangrijk deel van mijn leven.

In het bijzonder mijn vrienden van vriendengroep **ButeoButeo**, alhoewel ik vaker afwezig dan aanwezig ben de laatste jaren, voelt het altijd als een warm welkom en als vanouds als ik er wél ben. Dankbaar dat ik nog steeds bevriend ben met jullie, vrienden waar ik mee ben opgegroeid en mooie avonturen heb beleefd en nog ga beleven. **De Knots**, lekker primitief, wat een mooie studententijd hebben wij gehad, alles eruit gehaald! Al zijn we verspreid over verschillende steden/landen, een goed feestje slaan we niet gauw over, Awhoeoeoe! Mooi om te zien hoe iedereen zijn eigen pad bewandelt en leven opbouwt. Wij zijn nu de volwassenen…..Hoop jullie allemaal wat vaker te zien!

I also want to thank my **extended family**, spread across the world — from Australia to Canada and everywhere in between. And thank you, **Ama Sai**, **Ama Na**, and **Ama Jaan**, for your love and support throughout my life.

Thanks to my grandparents, without whom I simply would not exist. Though distance kept us apart for much of my life, I always felt their support and their pride.

اگرچه فاصله در بیشترِ سال‌های زندگی‌ام ما را از هم دور نگه داشت، اما همواره پشتیبانی و سربلندیِ شما را احساس کرده‌ام. روحتان شاد

Jacques en **Nelly Verheijen-Coppers** uit Well, waren onze Nederlandse opa en oma in een tijd dat we onze eigen grootouders moesten missen. Zij hebben mijn ouderlijk gezin ongelooflijk veel geholpen, puur uit de goedheid van hun hart, en zo ook indirect bijgedragen aan de totstandkoming van deze thesis.

Theo en Margreet, dank voor jullie steun, adviezen en jullie oprechte interesse in mij en mijn werk. Dank voor het opvangen van de kinderen, als er weer iets tussen kwam. Fijn om jullie als schoonouders te hebben.

Mijn zusje **Sodi** wat ben ik trots op je, je stond altijd al sterk in je schoenen en steunt me al sinds dat je kleuter was. Nu niet alleen een top arts maar ook kunstenares. Dank voor je ontwerp van mijn kaft. **Wida**, mijn kleine zusje met een groot hart, je hebt samen met **Guido**, jullie eigen prachtige gezin opgebouwd en bent een bron van warmte in ons leven. Het voelt als een eer om jullie allebei aan mijn zijde te hebben als paranimfen.

Mijn ouders, **Omar Khatab** en **Laila Nazeri.** Ik ben ongelofelijk trots op jullie. Dertig jaar geleden - met 3 jonge kinderen alles achter moeten laten om een betere toekomst voor ons te creëren. Niet alleen emigreren naar een land met andere gewoontes en taal, maar ook zo snel mogelijk integreren zodat wij geen achterstand zouden hebben. Getraumatiseerd door de oorlog, maar niet laten blijken. Alles zodat wij gewoon kind konden zijn. Jullie hebben mij altijd gestimuleerd om beste uit me naar boven te halen en ik heb me altijd door jullie gesteund gevoeld. Jullie hebben mij, Sodi en Wida gevormd en gelanceerd naar de fijne levens die wij nu hebben. Jullie zijn de sterkste mensen die ik ken en mijn grootste voorbeelden. Niet alleen met jullie weerbaarheid, doorzettingsvermogen en flexibiliteit maar vooral ook met het geven van liefde - aan ons, aan anderen én aan elkaar. Nu ik zelf een jong gezin heb, krijg ik er alleen maar meer respect voor jullie. Ik vind het geweldig om te zien hoeveel energie jullie krijgen van jullie kleinkinderen.

مادر و پدر عزیزم، با تمام وجودم شما را دوست دارم و از همه لطف‌ها و زحماتتان سپاسگزارم

Lieve **Nora, Anne en Merle**, ik ben ontzettend blij en trots op jullie. Jullie zijn onze best gelukte experimentjes. Ik vind het geweldig als ik na een lange dag thuis kom en jullie blij naar de deur rennen om als eerste op mij te springen! Het spijt me dat ik er niet altijd ben om leuke dingen met jullie te doen, omdat papa moest werken of schrijven aan zijn boekje. Papa had al zijn “diploma” gehaald en nu is het boekje ook eindelijk af, dus meer tijd om met jullie te zijn. Papa houdt ongelofelijk veel van jullie!

Lieve **Judith** – dank voor alles. Ik hou van je! Ik overdrijf niet als ik zeg dat dit boekje er zonder jou nooit was gekomen. Je stond aan mijn zijde bij het begin van dit avontuur en nu nog steeds bij het einde. Je hebt me altijd aangemoedigd en zoveel uit handen genomen, zodat ik me volledig kon richten op mijn werk. Je bent een fantastische vrouw -voor mij- en moeder voor onze kinderen en ik ben trots dat ik dit alles met jou mag delen. Op naar nieuwe avonturen met jou!

References

1. Long, H., et al., *Prevalence Trends of Site-Specific Osteoarthritis From 1990 to 2019: Findings From the Global Burden of Disease Study 2019.* Arthritis Rheumatol, 2022. **74**(7): p. 1172-1183.
2. RIVM, *Artrose, Cijfers & Zorgkosten*. 2021, Rijksoverheid.
3. Akker-van Marle, v.d., M.E. and Chorus, A.M.J., *Maatschappelijke kosten en baten van reuma en artrose in Nederland 2011.* TNO Rapport, 2011.
4. Courties, A., et al., *Osteoarthritis year in review 2024: Epidemiology and therapy.* Osteoarthritis Cartilage, 2024. **32**(11): p. 1397-1404.
5. Berenbaum, F., *Osteoarthritis as an inflammatory disease (osteoarthritis is not osteoarthrosis!).* Osteoarthritis Cartilage, 2013. **21**(1): p. 16-21.
6. Houard, X., M.B. Goldring, and F. Berenbaum, *Homeostatic mechanisms in articular cartilage and role of inflammation in osteoarthritis.* Curr Rheumatol Rep, 2013. **15**(11): p. 375.
7. Bondeson, J., et al., *The role of synovial macrophages and macrophage-produced mediators in driving inflammatory and destructive responses in osteoarthritis.* Arthritis Rheum, 2010. **62**(3): p. 647-57.
8. Bigoni, M., et al., *Acute and late changes in intraarticular cytokine levels following anterior cruciate ligament injury.* J Orthop Res, 2013. **31**(2): p. 315-21.
9. Catterall, J.B., et al., *Changes in serum and synovial fluid biomarkers after acute injury (NCT00332254).* Arthritis Res Ther, 2010. **12**(6): p. R229.
10. Lieberthal, J., N. Sambamurthy, and C.R. Scanzello, *Inflammation in joint injury and post-traumatic osteoarthritis.* Osteoarthritis Cartilage, 2015. **23**(11): p. 1825-34.
11. Englund, M., et al., *Meniscal tear in knees without surgery and the development of radiographic osteoarthritis among middle-aged and elderly persons: The Multicenter Osteoarthritis Study.* Arthritis Rheum, 2009. **60**(3): p. 831-9.
12. Wang, L.J., et al., *Post-traumatic osteoarthritis following ACL injury.* Arthritis Res Ther, 2020. **22**(1): p. 57.
13. Carbone, A. and S. Rodeo, *Review of current understanding of post-traumatic osteoarthritis resulting from sports injuries.* J Orthop Res, 2017. **35**(3): p. 397-405.
14. Timur, U.T., et al., *Identification of tissue-dependent proteins in knee OA synovial fluid.* Osteoarthritis Cartilage, 2021. **29**(1): p. 124-133.
15. Benito, M.J., et al., *Synovial tissue inflammation in early and late osteoarthritis.* Ann Rheum Dis, 2005. **64**(9): p. 1263-7.
16. de Lange-Brokaar, B.J., et al., *Synovial inflammation, immune cells and their cytokines in osteoarthritis: a review.* Osteoarthritis Cartilage, 2012. **20**(12): p. 1484-99.
17. Scanzello, C.R. and S.R. Goldring, *The role of synovitis in osteoarthritis pathogenesis.* Bone, 2012. **51**(2): p. 249-57.
18. Griffin, T.M. and C.R. Scanzello, *Innate inflammation and synovial macrophages in osteoarthritis pathophysiology.* Clin Exp Rheumatol, 2019. **37 Suppl 120**(5): p. 57-63.
19. Scanzello, C.R., A. Plaas, and M.K. Crow, *Innate immune system activation in osteoarthritis: is osteoarthritis a chronic wound?* Curr Opin Rheumatol, 2008. **20**(5): p. 565-72.
20. Koh, T.J. and L.A. DiPietro, *Inflammation and wound healing: the role of the macrophage.* Expert Rev Mol Med, 2011. **13**: p. e23.
21. Gallelli, L., et al., *The effects of nonsteroidal anti-inflammatory drugs on clinical outcomes, synovial fluid cytokine concentration and signal transduction pathways in knee osteoarthritis. A randomized open label trial.* Osteoarthritis Cartilage, 2013. **21**(9): p. 1400-8.
22. Klomjit, N. and P. Ungprasert, *Acute kidney injury associated with non-steroidal anti-inflammatory drugs.* Eur J Intern Med, 2022. **101**: p. 21-28.

23. Kompel, A.J., et al., *Intra-articular Corticosteroid Injections in the Hip and Knee: Perhaps Not as Safe as We Thought?* Radiology, 2019. **293**(3): p. 656-663.
24. Caplan, A.I., *Mesenchymal stem cells.* J Orthop Res, 1991. **9**(5): p. 641-50.
25. Caplan, A.I., *What's in a name?* Tissue Eng Part A, 2010. **16**(8): p. 2415-7.
26. Caplan, A.I. and J.E. Dennis, *Mesenchymal stem cells as trophic mediators.* J Cell Biochem, 2006. **98**(5): p. 1076-84.
27. Gupta, P.K., et al., *Efficacy and safety of adult human bone marrow-derived, cultured, pooled, allogeneic mesenchymal stromal cells (Stempeucel(R)): preclinical and clinical trial in osteoarthritis of the knee joint.* Arthritis Res Ther, 2016. **18**(1): p. 301.
28. Lamo-Espinosa, J.M., et al., *Intra-articular injection of two different doses of autologous bone marrow mesenchymal stem cells versus hyaluronic acid in the treatment of knee osteoarthritis: multicenter randomized controlled clinical trial (phase I/II).* J Transl Med, 2016. **14**(1): p. 246.
29. Murphy, J.M., et al., *Stem cell therapy in a caprine model of osteoarthritis.* Arthritis Rheum, 2003. **48**(12): p. 3464-74.
30. Pers, Y.M., et al., *Adipose Mesenchymal Stromal Cell-Based Therapy for Severe Osteoarthritis of the Knee: A Phase I Dose-Escalation Trial.* Stem Cells Transl Med, 2016. **5**(7): p. 847-56.
31. ter Huurne, M., et al., *Antiinflammatory and chondroprotective effects of intraarticular injection of adipose-derived stem cells in experimental osteoarthritis.* Arthritis Rheum, 2012. **64**(11): p. 3604-13.
32. van Buul, G.M., et al., *Mesenchymal stem cells reduce pain but not degenerative changes in a mono-iodoacetate rat model of osteoarthritis.* J Orthop Res, 2014. **32**(9): p. 1167-74.
33. Caplan, A.I., *Mesenchymal Stem Cells: Time to Change the Name!* Stem Cells Transl Med, 2017. **6**(6): p. 1445-1451.
34. Kinnaird, T., et al., *Local delivery of marrow-derived stromal cells augments collateral perfusion through paracrine mechanisms.* Circulation, 2004. **109**(12): p. 1543-9.
35. Le Blanc, K. and D. Mougiakakos, *Multipotent mesenchymal stromal cells and the innate immune system.* Nat Rev Immunol, 2012. **12**(5): p. 383-96.
36. Prockop, D.J., *Repair of tissues by adult stem/progenitor cells (MSCs): controversies, myths, and changing paradigms.* Mol Ther, 2009. **17**(6): p. 939-46.
37. Ren, G., et al., *Mesenchymal stem cell-mediated immunosuppression occurs via concerted action of chemokines and nitric oxide.* Cell Stem Cell, 2008. **2**(2): p. 141-50.
38. Timmers, L., et al., *Human mesenchymal stem cell-conditioned medium improves cardiac function following myocardial infarction.* Stem Cell Res, 2011. **6**(3): p. 206-14.
39. Diekman, B.O., et al., *Intra-articular delivery of purified mesenchymal stem cells from C57BL/6 or MRL/MpJ superhealer mice prevents posttraumatic arthritis.* Cell Transplant, 2013. **22**(8): p. 1395-408.
40. Mak, J., et al., *Intra-articular injection of synovial mesenchymal stem cells improves cartilage repair in a mouse injury model.* Sci Rep, 2016. **6**: p. 23076.
41. Eggenhofer, E., et al., *The life and fate of mesenchymal stem cells.* Front Immunol, 2014. **5**: p. 148.
42. von Bahr, L., et al., *Analysis of tissues following mesenchymal stromal cell therapy in humans indicates limited long-term engraftment and no ectopic tissue formation.* Stem Cells, 2012. **30**(7): p. 1575-8.
43. Estrada, R., et al., *Secretome from mesenchymal stem cells induces angiogenesis via Cyr61.* J Cell Physiol, 2009. **219**(3): p. 563-71.
44. Prockop, D.J. and J.Y. Oh, *Medical therapies with adult stem/progenitor cells (MSCs): a backward journey from dramatic results in vivo to the cellular and molecular explanations.* J Cell Biochem, 2012. **113**(5): p. 1460-9.

45. van Buul, G.M., et al., *Mesenchymal stem cells secrete factors that inhibit inflammatory processes in short-term osteoarthritic synovium and cartilage explant culture.* Osteoarthritis Cartilage, 2012. **20**(10): p. 1186-96.
46. Levit, R.D., et al., *Cellular encapsulation enhances cardiac repair.* J Am Heart Assoc, 2013. **2**(5): p. e000367.
47. Serra, M., et al., *Microencapsulation technology: a powerful tool for integrating expansion and cryopreservation of human embryonic stem cells.* PLoS One, 2011. **6**(8): p. e23212.
48. Sun, J. and H. Tan, *Alginate-Based Biomaterials for Regenerative Medicine Applications.* Materials (Basel), 2013. **6**(4): p. 1285-1309.
49. Lee, K.Y. and D.J. Mooney, *Alginate: properties and biomedical applications.* Prog Polym Sci, 2012. **37**(1): p. 106-126.
50. Choi, S., et al., *Intra-Articular Injection of Alginate-Microencapsulated Adipose Tissue-Derived Mesenchymal Stem Cells for the Treatment of Osteoarthritis in Rabbits.* Stem Cells Int, 2018. **2018**: p. 2791632.
51. Shoichet, M.S., et al., *Stability of hydrogels used in cell encapsulation: An in vitro comparison of alginate and agarose.* Biotechnol Bioeng, 1996. **50**(4): p. 374-81.
52. Leijs, M.J., et al., *Encapsulation of allogeneic mesenchymal stem cells in alginate extends local presence and therapeutic function.* Eur Cell Mater, 2017. **33**: p. 43-58.
53. Duvivier-Kali, V.F., et al., *Complete protection of islets against allorejection and autoimmunity by a simple barium-alginate membrane.* Diabetes, 2001. **50**(8): p. 1698-705.
54. de Vos, P., et al., *Alginate-based microcapsules for immunoisolation of pancreatic islets.* Biomaterials, 2006. **27**(32): p. 5603-17.
55. Barrachina, L., et al., *Priming Equine Bone Marrow-Derived Mesenchymal Stem Cells with Proinflammatory Cytokines: Implications in Immunomodulation-Immunogenicity Balance, Cell Viability, and Differentiation Potential.* Stem Cells Dev, 2017. **26**(1): p. 15-24.
56. Crop, M.J., et al., *Inflammatory conditions affect gene expression and function of human adipose tissue-derived mesenchymal stem cells.* Clin Exp Immunol, 2010. **162**(3): p. 474-86.
57. Rani, S., et al., *Mesenchymal Stem Cell-derived Extracellular Vesicles: Toward Cell-free Therapeutic Applications.* Mol Ther, 2015. **23**(5): p. 812-823.
58. Schu, S., et al., *Immunogenicity of allogeneic mesenchymal stem cells.* J Cell Mol Med, 2012. **16**(9): p. 2094-103.
59. Marx, R.E., *Platelet-rich plasma: evidence to support its use.* J Oral Maxillofac Surg, 2004. **62**(4): p. 489-96.
60. Lacci, K.M. and A. Dardik, *Platelet-rich plasma: support for its use in wound healing.* Yale J Biol Med, 2010. **83**(1): p. 1-9.
61. Nikolidakis, D. and J.A. Jansen, *The biology of platelet-rich plasma and its application in oral surgery: literature review.* Tissue Eng Part B Rev, 2008. **14**(3): p. 249-58.
62. Cavallo, C., et al., *Platelet-Rich Plasma: The Choice of Activation Method Affects the Release of Bioactive Molecules.* Biomed Res Int, 2016. **2016**: p. 6591717.
63. Zhou, Q., et al., *Platelets promote cartilage repair and chondrocyte proliferation via ADP in a rodent model of osteoarthritis.* Platelets, 2016. **27**(3): p. 212-22.
64. Sakata, R. and A.H. Reddi, *Platelet-Rich Plasma Modulates Actions on Articular Cartilage Lubrication and Regeneration.* Tissue Eng Part B Rev, 2016. **22**(5): p. 408-419.
65. Osterman, C., et al., *Platelet-Rich Plasma Increases Anti-inflammatory Markers in a Human Coculture Model for Osteoarthritis.* Am J Sports Med, 2015. **43**(6): p. 1474-84.
66. van Buul, G.M., et al., *Platelet-rich plasma releasate inhibits inflammatory processes in osteoarthritic chondrocytes.* Am J Sports Med, 2011. **39**(11): p. 2362-70.
67. Montanez-Heredia, E., et al., *Intra-Articular Injections of Platelet-Rich Plasma versus Hyaluronic Acid in the Treatment of Osteoarthritic Knee Pain: A Randomized Clinical Trial in the Context of the Spanish National Health Care System.* Int J Mol Sci, 2016. **17**(7).

68. Meheux, C.J., et al., *Efficacy of Intra-articular Platelet-Rich Plasma Injections in Knee Osteoarthritis: A Systematic Review.* Arthroscopy, 2016. **32**(3): p. 495-505.
69. Laudy, A.B., et al., *Efficacy of platelet-rich plasma injections in osteoarthritis of the knee: a systematic review and meta-analysis.* Br J Sports Med, 2015. **49**(10): p. 657-72.
70. Smith, P.A., *Intra-articular Autologous Conditioned Plasma Injections Provide Safe and Efficacious Treatment for Knee Osteoarthritis: An FDA-Sanctioned, Randomized, Double-blind, Placebo-controlled Clinical Trial.* Am J Sports Med, 2016. **44**(4): p. 884-91.
71. Gobbi, A., D. Lad, and G. Karnatzikos, *The effects of repeated intra-articular PRP injections on clinical outcomes of early osteoarthritis of the knee.* Knee Surg Sports Traumatol Arthrosc, 2015. **23**(8): p. 2170-2177.
72. Campbell, K.A., et al., *Does Intra-articular Platelet-Rich Plasma Injection Provide Clinically Superior Outcomes Compared With Other Therapies in the Treatment of Knee Osteoarthritis? A Systematic Review of Overlapping Meta-analyses.* Arthroscopy, 2015. **31**(11): p. 2213-21.
73. Filardo, G., et al., *Platelet-Rich Plasma Intra-articular Knee Injections Show No Superiority Versus Viscosupplementation: A Randomized Controlled Trial.* Am J Sports Med, 2015. **43**(7): p. 1575-82.
74. Filardo, G. and E. Kon, *PRP: Product Rich in Placebo?* Knee Surg Sports Traumatol Arthrosc, 2016. **24**(12): p. 3702-3703.
75. Lai, L.P., et al., *Use of Platelet-Rich Plasma in Intra-Articular Knee Injections for Osteoarthritis: A Systematic Review.* PM R, 2015. **7**(6): p. 637-48.
76. Knop, E., L.E. Paula, and R. Fuller, *Platelet-rich plasma for osteoarthritis treatment.* Rev Bras Reumatol Engl Ed, 2016. **56**(2): p. 152-64.
77. Dohan Ehrenfest, D.M., L. Rasmusson, and T. Albrektsson, *Classification of platelet concentrates: from pure platelet-rich plasma (P-PRP) to leucocyte- and platelet-rich fibrin (L-PRF).* Trends Biotechnol, 2009. **27**(3): p. 158-67.
78. Huang, W.H., et al., *Hypoxic mesenchymal stem cells engraft and ameliorate limb ischaemia in allogeneic recipients.* Cardiovasc Res, 2014. **101**(2): p. 266-76.
79. Khatab, S., et al., *Mesenchymal stem cell secretome reduces pain and prevents cartilage damage in a murine osteoarthritis model.* Eur Cell Mater, 2018. **36**: p. 218-230.
80. Ter Huurne, M., et al., *Antiinflammatory and chondroprotective effects of intraarticular injection of adipose-derived stem cells in experimental osteoarthritis.* Arthritis Rheum, 2012. **64**(11): p. 3604-3613.
81. Gupta, P.K., et al., *Efficacy and safety of adult human bone marrow-derived, cultured, pooled, allogeneic mesenchymal stromal cells (Stempeucel®): Preclinical and clinical trial in osteoarthritis of the knee joint.* Arthritis Res Ther, 2016. **18**(1).
82. Pers, Y.M., et al., *Adipose mesenchymal stromal cell-based therapy for severe osteoarthritis of the knee: A phase I dose-escalation trial.* Stem Cells Transl Med, 2016. **5**(7): p. 847-856.
83. Zhang, Y. and J.M. Jordan, *Epidemiology of osteoarthritis.* Clin Geriatr Med, 2010. **26**(3): p. 355-69.
84. Farrell, E., et al., *A collagen-glycosaminoglycan scaffold supports adult rat mesenchymal stem cell differentiation along osteogenic and chondrogenic routes.* Tissue Eng, 2006. **12**(3): p. 459-68.
85. Van Buul, G.M., et al., *Mesenchymal stem cells reduce pain but not degenerative changes in a mono-iodoacetate rat model of osteoarthritis.* J Orthop Res, 2014. **32**(9): p. 1167-1174.
86. Guenoun, J., et al., *In vivo quantitative assessment of cell viability of gadolinium or iron-labeled cells using MRI and bioluminescence imaging.* Contrast Media Mol Imaging, 2013. **8**(2): p. 165-74.
87. Wong, M., et al., *Development of mechanically stable alginate/chondrocyte constructs: effects of guluronic acid content and matrix synthesis.* J Orthop Res, 2001. **19**(3): p. 493-9.

88. Kang, J.W., et al., *Soluble factors-mediated immunomodulatory effects of canine adipose tissue-derived mesenchymal stem cells.* Stem Cells Dev, 2008. **17**(4): p. 681-93.
89. van Buul, G.M., et al., *Ferumoxides-protamine sulfate is more effective than ferucarbotran for cell labeling: implications for clinically applicable cell tracking using MRI.* Contrast Media Mol Imaging, 2009. **4**(5): p. 230-6.
90. Koda, M., et al., *Delayed granulocyte colony-stimulating factor treatment in rats attenuates mechanical allodynia induced by chronic constriction injury of the sciatic nerve.* Spine (Phila Pa 1976), 2014. **39**(3): p. 192-7.
91. Pritzker, K.P., et al., *Osteoarthritis cartilage histopathology: grading and staging.* Osteoarthritis Cartilage, 2006. **14**(1): p. 13-29.
92. Khatab, S., et al., *Intra-articular Injections of Platelet-Rich Plasma Releasate Reduce Pain and Synovial Inflammation in a Mouse Model of Osteoarthritis.* Am J Sports Med, 2018. **46**(4): p. 977-986.
93. Lux, J. and A.D. Sherry, *Advances in gadolinium-based MRI contrast agent designs for monitoring biological processes in vivo.* Curr Opin Chem Biol, 2018. **45**: p. 121-130.
94. Gupta, P.K., et al., *Efficacy and safety of adult human bone marrow-derived, cultured, pooled, allogeneic mesenchymal stromal cells (Stempeucel®): preclinical and clinical trial in osteoarthritis of the knee joint.* Arthritis Research & Therapy, 2016. **18**(1): p. 301.
95. de Mos, M., et al., *Intrinsic differentiation potential of adolescent human tendon tissue: an in-vitro cell differentiation study.* BMC Musculoskelet Disord, 2007. **8**: p. 16.
96. Glasson, S.S., et al., *The OARSI histopathology initiative - recommendations for histological assessments of osteoarthritis in the mouse.* Osteoarthritis Cartilage, 2010. **18 Suppl 3**: p. S17-23.
97. Park, H.S., et al., *Suppression of LPS-induced NF-kappaB activity in macrophages by the synthetic aurone, (Z)-2-((5-(hydroxymethyl) furan-2-yl) methylene) benzofuran-3(2H)-one.* Int Immunopharmacol, 2017. **43**: p. 116-128.
98. Utomo, L., et al., *Guiding synovial inflammation by macrophage phenotype modulation: an in vitro study towards a therapy for osteoarthritis.* Osteoarthritis Cartilage, 2016. **24**(9): p. 1629-38.
99. Gnecchi, M., et al., *Paracrine action accounts for marked protection of ischemic heart by Akt-modified mesenchymal stem cells.* Nat Med, 2005. **11**(4): p. 367-8.
100. Madrigal, M., K.S. Rao, and N.H. Riordan, *A review of therapeutic effects of mesenchymal stem cell secretions and induction of secretory modification by different culture methods.* J Transl Med, 2014. **12**: p. 260.
101. Konala, V.B., et al., *The current landscape of the mesenchymal stromal cell secretome: A new paradigm for cell-free regeneration.* Cytotherapy, 2016. **18**(1): p. 13-24.
102. Platas, J., et al., *Conditioned media from adipose-tissue-derived mesenchymal stem cells downregulate degradative mediators induced by interleukin-1beta in osteoarthritic chondrocytes.* Mediators Inflamm, 2013. **2013**: p. 357014.
103. Toh, W.S., et al., *MSC exosome as a cell-free MSC therapy for cartilage regeneration: Implications for osteoarthritis treatment.* Semin Cell Dev Biol, 2017. **67**: p. 56-64.
104. Morhayim, J., M. Baroncelli, and J.P. van Leeuwen, *Extracellular vesicles: specialized bone messengers.* Arch Biochem Biophys, 2014. **561**: p. 38-45.
105. Zheng, G., et al., *Mesenchymal stromal cell-derived extracellular vesicles: regenerative and immunomodulatory effects and potential applications in sepsis.* Cell Tissue Res, 2018. **374**(1): p. 1-15.
106. Khatab, S., et al., *Intra-articular Injections of Platelet-Rich Plasma Releasate Reduce Pain and Synovial Inflammation in a Mouse Model of Osteoarthritis.* Am J Sports Med, 2018: p. 363546517750635.

107. Adaes, S., et al., *Intra-articular injection of collagenase in the knee of rats as an alternative model to study nociception associated with osteoarthritis.* Arthritis Res Ther, 2014. **16**(1): p. R10.
108. Carotti, M., et al., *Relationship between magnetic resonance imaging findings, radiological grading, psychological distress and pain in patients with symptomatic knee osteoarthritis.* Radiol Med, 2017. **122**(12): p. 934-943.
109. Botter, S.M., et al., *Osteoarthritis induction leads to early and temporal subchondral plate porosity in the tibial plateau of mice: an in vivo microfocal computed tomography study.* Arthritis Rheum, 2011. **63**(9): p. 2690-9.
110. Mapp, P.I. and D.A. Walsh, *Mechanisms and targets of angiogenesis and nerve growth in osteoarthritis.* Nat Rev Rheumatol, 2012. **8**(7): p. 390-8.
111. Yuan, X.L., et al., *Bone-cartilage interface crosstalk in osteoarthritis: potential pathways and future therapeutic strategies.* Osteoarthritis Cartilage, 2014. **22**(8): p. 1077-89.
112. Parrilli, A., et al., *Subchondral bone response to injected adipose-derived stromal cells for treating osteoarthritis using an experimental rabbit model.* Biotech Histochem, 2017. **92**(3): p. 201-211.
113. van der Kraan, P.M., et al., *Degenerative knee joint lesions in mice after a single intra-articular collagenase injection. A new model of osteoarthritis.* J Exp Pathol (Oxford), 1990. **71**(1): p. 19-31.
114. McIlwraith, C.W., D.D. Frisbie, and C.E. Kawcak, *The horse as a model of naturally occurring osteoarthritis.* Bone & joint research, 2012. **1**(11): p. 297-309.
115. Colbath, A.C., et al., *Mesenchymal stem cells for treatment of musculoskeletal disease in horses: relative merits of allogeneic versus autologous stem cells.* Equine veterinary journal, 2020. **52**(5): p. 654-663.
116. Colbath, A.C., et al., *Single and repeated intra-articular injections in the tarsocrural joint with allogeneic and autologous equine bone marrow-derived mesenchymal stem cells are safe, but did not reduce acute inflammation in an experimental interleukin-1β model of synovitis.* Equine veterinary journal, 2020. **52**(4): p. 601-612.
117. agency, E.m. *First Stem Cell-Based Veterinary Medicine Recommended for Marketing Authorisation.* 2018 [cited 2021 25-05]; Available from: https://www.ema.europa.eu/en/documents/press-release/first-stem-cell-based-veterinary-medicine-recommended-marketing-authorisation_en.pdf.
118. Barry, F. and M. Murphy, *Mesenchymal stem cells in joint disease and repair.* Nature Reviews Rheumatology, 2013. **9**(10): p. 584-594.
119. Bussche, L., et al., *Microencapsulated equine mesenchymal stromal cells promote cutaneous wound healing in vitro.* Stem cell research & therapy, 2015. **6**: p. 1-15.
120. Marx, C., et al., *The mesenchymal stromal cell secretome impairs methicillin-resistant Staphylococcus aureus biofilms via cysteine protease activity in the equine model.* Stem cells translational medicine, 2020. **9**(7): p. 746-757.
121. Lange-Consiglio, A., et al., *Conditioned medium from horse amniotic membrane-derived multipotent progenitor cells: immunomodulatory activity in vitro and first clinical application in tendon and ligament injuries in vivo.* Stem cells and development, 2013. **22**(22): p. 3015-3024.
122. Kearney, C.M., et al., *Treatment effects of intra-articular triamcinolone acetonide in an equine model of recurrent joint inflammation.* Equine veterinary journal, 2021. **53**(6): p. 1277-1286.
123. Kisiday, J.D., et al., *Expansion of mesenchymal stem cells on fibrinogen-rich protein surfaces derived from blood plasma.* Journal of tissue engineering and regenerative medicine, 2011. **5**(8): p. 600-611.

124. Guest, D.J., et al., *Position statement: minimal criteria for reporting veterinary and animal medicine research for mesenchymal stromal/stem cells in orthopedic applications*. Frontiers in Veterinary Science, 2022. **9**: p. 817041.
125. Kisiday, J.D., A.C. Colbath, and S. Tangtrongsup, *Effect of culture duration on chondrogenic preconditioning of equine bone marrow mesenchymal stem cells in self-assembling peptide hydrogel*. Journal of Orthopaedic Research®, 2019. **37**(6): p. 1368-1375.
126. Kisiday, J.D., et al., *Effects of equine bone marrow aspirate volume on isolation, proliferation, and differentiation potential of mesenchymal stem cells.* American journal of veterinary research, 2013. **74**(5): p. 801-807.
127. Kisiday, J.D., et al., *Evaluation of adult equine bone marrow-and adipose-derived progenitor cell chondrogenesis in hydrogel cultures*. Journal of orthopaedic research, 2008. **26**(3): p. 322-331.
128. Colbath, A.C., et al., *Autologous and allogeneic equine mesenchymal stem cells exhibit equivalent immunomodulatory properties in vitro.* Stem cells and development, 2017. **26**(7): p. 503-511.
129. Owens, J.G., et al., *Effects of pretreatment with ketoprofen and phenylbutazone on experimentally induced synovitis in horses.* American journal of veterinary research, 1996. **57**(6): p. 866-874.
130. de Grauw, J.C., C.H.A. van de Lest, and P.R. van Weeren, *A targeted lipidomics approach to the study of eicosanoid release in synovial joints.* Arthritis research & therapy, 2011. **13**: p. 1-12.
131. De Grauw, J.C., et al., *In vivo effects of meloxicam on inflammatory mediators, MMP activity and cartilage biomarkers in equine joints with acute synovitis.* Equine veterinary journal, 2009. **41**(7): p. 693-699.
132. Cokelaere, S.M., et al., *Sustained intra-articular release of celecoxib in an equine repeated LPS synovitis model*. European Journal of Pharmaceutics and Biopharmaceutics, 2018. **128**: p. 327-336.
133. de Grauw, J.C., et al., *Cartilage-derived biomarkers and lipid mediators of inflammation in horses with osteochondritis dissecans of the distal intermediate ridge of the tibia.* American journal of veterinary research, 2006. **67**(7): p. 1156-1162.
134. De Grauw, J.C., et al., *In vivo effects of phenylbutazone on inflammation and cartilage-derived biomarkers in equine joints with acute synovitis*. The Veterinary Journal, 2014. **201**(1): p. 51-56.
135. Sladek, S., et al., *Intra-articular delivery of a nanocomplex comprising salmon calcitonin, hyaluronic acid, and chitosan using an equine model of joint inflammation.* Drug delivery and translational research, 2018. **8**: p. 1421-1435.
136. Toh, W.S., et al., *Advances in mesenchymal stem cell-based strategies for cartilage repair and regeneration.* Stem Cell Reviews and Reports, 2014. **10**: p. 686-696.
137. Zhang, J., et al., *The challenges and promises of allogeneic mesenchymal stem cells for use as a cell-based therapy.* Stem cell research & therapy, 2015. **6**: p. 1-7.
138. Frisbie, D.D., et al., *Effects of triamcinolone acetonide on an in vivo equine osteochondral fragment exercise model.* Equine veterinary journal, 1997. **29**(5): p. 349-359.
139. Céleste, C., et al., *Repeated intraarticular injections of triamcinolone acetonide alter cartilage matrix metabolism measured by biomarkers in synovial fluid*. Journal of orthopaedic research, 2005. **23**(3): p. 602-610.
140. McIlwraith, C.W., *Use of synovial fluid and serum biomarkers in equine bone and joint disease: a review.* 2005.
141. Frisbie, D.D., et al., *Evaluation of adipose-derived stromal vascular fraction or bone marrow-derived mesenchymal stem cells for treatment of osteoarthritis*. Journal of Orthopaedic Research, 2009. **27**(12): p. 1675-1680.

142. Broeckx, S.Y., et al., *Equine allogeneic chondrogenic induced mesenchymal stem cells are an effective treatment for degenerative joint disease in horses.* Stem Cells and Development, 2019. **28**(6): p. 410-422.
143. Colbath, A.C., et al., *Allogeneic vs. autologous intra-articular mesenchymal stem cell injection within normal horses: Clinical and cytological comparisons suggest safety.* Equine veterinary journal, 2020. **52**(1): p. 144-151.
144. Williams, L.B., et al., *Equine allogeneic umbilical cord blood derived mesenchymal stromal cells reduce synovial fluid nucleated cell count and induce mild self-limiting inflammation when evaluated in an lipopolysaccharide induced synovitis model.* Equine veterinary journal, 2016. **48**(5): p. 619-625.
145. Barrachina, L., et al., *Assessment of effectiveness and safety of repeat administration of proinflammatory primed allogeneic mesenchymal stem cells in an equine model of chemically induced osteoarthritis.* BMC Vet Res, 2018. **14**(1): p. 241.
146. Carrade, D.D., et al., *Comparative analysis of the immunomodulatory properties of equine adult-derived mesenchymal stem cells*. Cell medicine, 2012. **4**(1): p. 1-12.
147. Moran, C.J., et al., *The benefits and limitations of animal models for translational research in cartilage repair.* Journal of experimental orthopaedics, 2016. **3**: p. 1-12.
148. Laverty, S., et al., *Synovial fluid levels and serum pharmacokinetics in a large animal model following treatment with oral glucosamine at clinically relevant doses.* Arthritis & Rheumatism: Official Journal of the American College of Rheumatology, 2005. **52**(1): p. 181-191.
149. de Grauw, J.C., C.H.A. van de Lest, and P.R. van Weeren, *Inflammatory mediators and cartilage biomarkers in synovial fluid after a single inflammatory insult: a longitudinal experimental study.* Arthritis research & therapy, 2009. **11**: p. 1-8.
150. Van den Boom, R., et al., *Influence of repeated arthrocentesis and exercise on synovial fluid concentrations of nitric oxide, prostaglandin E2 and glycosaminoglycans in healthy equine joints*. Equine veterinary journal, 2005. **37**(3): p. 250-256.
151. Orth, P., et al., *Reduction of sample size requirements by bilateral versus unilateral research designs in animal models for cartilage tissue engineering.* Tissue Engineering Part C: Methods, 2013. **19**(11): p. 885-891.
152. Dyson, S., *Can lameness be graded reliably?* 2011, Wiley Online Library. p. 379-382.
153. Palmer, J.L., et al., *Biochemical and biomechanical alterations in equine articular cartilage following an experimentally-induced synovitis*. Osteoarthritis and cartilage, 1996. **4**(2): p. 127-137.
154. Hill, J.A., et al., *Antigenicity of mesenchymal stem cells in an inflamed joint environment.* American journal of veterinary research, 2017. **78**(7): p. 867-875.
155. Ragni, E., et al., *Inflammatory priming enhances mesenchymal stromal cell secretome potential as a clinical product for regenerative medicine approaches through secreted factors and EV-miRNAs: the example of joint disease.* Stem cell research & therapy, 2020. **11**(1): p. 165.
156. Van Den Boom, R., et al., *The influence of repeated arthrocentesis and exercise on matrix metalloproteinase and tumour necrosis factor a activities in normal equine joints.* Equine veterinary journal, 2004. **36**(2): p. 155-159.
157. Tulamo, R.M., L.R. Bramlage, and A.A. Gabel, *Sequential clinical and synovial fluid changes associated with acute infectious arthritis in the horse.* Equine veterinary journal, 1989. **21**(5): p. 325-331.
158. Lucia, J.L., et al., *Influence of an intra-articular lipopolysaccharide challenge on markers of inflammation and cartilage metabolism in young horses*. Journal of animal science, 2013. **91**(6): p. 2693-2699.

159. Wang, G., et al., *Changes in synovial fluid inflammatory mediators and cartilage biomarkers after experimental acute equine synovitis.* Journal of Veterinary Research, 2015. **59**(1): p. 129-134.
160. Laudy, A.B., et al., *Efficacy of platelet-rich plasma injections in osteoarthritis of the knee: a systematic review and meta-analysis.* Br J Sports Med, 2015. **49**(10): p. 657-672.
161. Meheux, C.J., et al., *Efficacy of Intra-articular Platelet-Rich Plasma Injections in Knee Osteoarthritis: A Systematic Review.* Arthroscopy J Arthroscopic Relat Surg, 2016. **32**(3): p. 495-505.
162. Montañez-Heredia, E., et al., *Intra-articular injections of platelet-rich plasma versus hyaluronic acid in the treatment of osteoarthritic knee pain: A randomized clinical trial in the context of the Spanish national health care system.* Int J Mol Sci, 2016. **17**(7).
163. Campbell, K.A., et al., *Does Intra-articular Platelet-Rich Plasma Injection Provide Clinically Superior Outcomes Compared with Other Therapies in the Treatment of Knee Osteoarthritis? A Systematic Review of Overlapping Meta-analyses.* Arthroscopy J Arthroscopic Relat Surg, 2015. **31**(11): p. 2213-2221.
164. Sakata, R., et al., *Stimulation of the superficial zone protein and lubrication in the articular cartilage by human platelet-rich plasma.* Am J Sports Med, 2015. **43**(6): p. 1467-1473.
165. Osterman, C., et al., *Platelet-Rich Plasma Increases Anti-inflammatory Markers in a Human Coculture Model for Osteoarthritis.* Am J Sports Med, 2015. **43**(6): p. 1474-1484.
166. Sundman, E.A., et al., *The anti-inflammatory and matrix restorative mechanisms of platelet-rich plasma in osteoarthritis.* Am J Sports Med, 2014. **42**(1): p. 35-41.
167. Cook, J.L., et al., *Multiple injections of leukoreduced platelet rich plasma reduce pain and functional impairment in a canine model of ACL and meniscal deficiency.* J Orthop Res, 2016. **34**(4): p. 607-15.
168. Lai, L.P., et al., *Use of Platelet-Rich Plasma in Intra-Articular Knee Injections for Osteoarthritis: A Systematic Review.* PM R, 2015. **7**(6): p. 637-648.
169. Lorenz, J. and S. Grassel, *Experimental osteoarthritis models in mice.* Methods Mol Biol, 2014. **1194**: p. 401-19.
170. van Osch, G.J., et al., *Laxity characteristics of normal and pathological murine knee joints in vitro.* J Orthop Res, 1995. **13**(5): p. 783-91.
171. Schelbergen, R.F., et al., *Treatment efficacy of adipose-derived stem cells in experimental osteoarthritis is driven by high synovial activation and reflected by S100A8/A9 serum levels.* Osteoarthritis Cartilage, 2014. **22**(8): p. 1158-1166.
172. Dong, J., et al., *Intra-articular delivery of liposomal celecoxib-hyaluronate combination for the treatment of osteoarthritis in rabbit model.* Int J Pharm, 2013. **441**(1-2): p. 285-90.
173. Borbely, E., et al., *Role of capsaicin-sensitive nerves and tachykinins in mast cell tryptase-induced inflammation of murine knees.* Inflamm Res, 2016. **65**(9): p. 725-36.
174. Inglis, J.J., et al., *Regulation of pain sensitivity in experimental osteoarthritis by the endogenous peripheral opioid system.* Arthritis Rheum, 2008. **58**(10): p. 3110-9.
175. Fernihough, J., et al., *Pain related behaviour in two models of osteoarthritis in the rat knee.* Pain, 2004. **112**(1-2): p. 83-93.
176. Ulmann, L., H. Hirbec, and F. Rassendren, *P2X4 receptors mediate PGE2 release by tissue-resident macrophages and initiate inflammatory pain.* EMBO J, 2010. **29**(14): p. 2290-300.
177. Papait, A., et al., *Allogeneic platelet-rich plasma affects monocyte differentiation to dendritic cells causing an anti-inflammatory microenvironment putatively fostering the wound healing.* J Tissue Eng Regen Med, 2016.
178. Yin, W.J., et al., *Advantages of pure platelet-rich plasma compared with leukocyte- and platelet-rich plasma in treating rabbit knee osteoarthritis.* Med Sci Monit, 2016. **22**: p. 1280-1290.

179. Mussano, F., et al., *Cytokine, chemokine, and growth factor profile of platelet-rich plasma.* Platelets, 2016. **27**(5): p. 467-71.
180. Luz-Crawford, P., et al., *Mesenchymal Stem Cell-Derived Interleukin 1 Receptor Antagonist Promotes Macrophage Polarization and Inhibits B Cell Differentiation.* Stem Cells, 2016. **34**(2): p. 483-92.
181. McDougall, J.J., *Arthritis and pain. Neurogenic origin of joint pain.* Arthritis Res Ther, 2006. **8**(6): p. 220.
182. McDougall, J.J. and P. Linton, *Neurophysiology of arthritis pain.* Curr Pain Headache Rep, 2012. **16**(6): p. 485-91.
183. Weibrich, G., et al., *Growth factor levels in platelet-rich plasma and correlations with donor age, sex, and platelet count.* J Craniomaxillofac Surg, 2002. **30**(2): p. 97-102.
184. Mazzocca, A.D., et al., *Platelet-rich plasma differs according to preparation method and human variability.* J Bone Joint Surg Am, 2012. **94**(4): p. 308-16.
185. Radice, F., et al., *Comparison of magnetic resonance imaging findings in anterior cruciate ligament grafts with and without autologous platelet-derived growth factors.* Arthroscopy, 2010. **26**(1): p. 50-7.
186. Castelijns, G., et al., *Evaluation of a filter-prepared platelet concentrate for the treatment of suspensory branch injuries in horses.* Vet Comp Orthop Traumatol, 2011. **24**(5): p. 363-9.
187. de Vos, R.J., et al., *Platelet-rich plasma injection for chronic Achilles tendinopathy: a randomized controlled trial.* JAMA, 2010. **303**(2): p. 144-9.
188. Brossi, P.M., et al., *Platelet-rich plasma in orthopedic therapy: a comparative systematic review of clinical and experimental data in equine and human musculoskeletal lesions.* BMC Vet Res, 2015. **11**: p. 98.
189. Sonker, A. and A. Dubey, *Determining the Effect of Preparation and Storage: An Effort to Streamline Platelet Components as a Source of Growth Factors for Clinical Application.* Transfus Med Hemother, 2015. **42**(3): p. 174-80.
190. Assirelli, E., et al., *Effect of two different preparations of platelet-rich plasma on synoviocytes.* Knee Surg Sports Traumatol Arthrosc, 2015. **23**(9): p. 2690-703.
191. Textor, J.A. and F. Tablin, *Intra-articular use of a platelet-rich product in normal horses: clinical signs and cytologic responses.* Vet Surg, 2013. **42**(5): p. 499-510.
192. Chaudhary, R., et al., *Cytokine generation in stored platelet concentrate: comparison of two methods of preparation.* Indian J Med Res, 2006. **124**(4): p. 427-30.
193. Kobayashi, Y., et al., *Leukocyte concentration and composition in platelet-rich plasma (PRP) influences the growth factor and protease concentrations.* J Orthop Sci, 2016. **21**(5): p. 683-9.
194. Kieb, M., et al., *Platelet-Rich Plasma Powder: A New Preparation Method for the Standardization of Growth Factor Concentrations.* Am J Sports Med, 2016.
195. Nakatani, Y., et al., *Efficacy of freeze-dried platelet-rich plasma in bone engineering.* Arch Oral Biol, 2017. **73**: p. 172-178.
196. Gormeli, G., et al., *Multiple PRP injections are more effective than single injections and hyaluronic acid in knees with early osteoarthritis: a randomized, double-blind, placebo-controlled trial.* Knee Surg Sports Traumatol Arthrosc, 2015.
197. Sato, M., et al., *Direct transplantation of mesenchymal stem cells into the knee joints of Hartley strain guinea pigs with spontaneous osteoarthritis.* Arthritis Res Ther, 2012. **14**(1): p. R31.
198. Friedenstein, A.J., R.K. Chailakhyan, and U.V. Gerasimov, *Bone marrow osteogenic stem cells: in vitro cultivation and transplantation in diffusion chambers.* Cell Tissue Kinet, 1987. **20**(3): p. 263-72.
199. Gormeli, G., et al., *Multiple PRP injections are more effective than single injections and hyaluronic acid in knees with early osteoarthritis: a randomized, double-blind, placebo-controlled trial.* Knee Surg Sports Traumatol Arthrosc, 2017. **25**(3): p. 958-965.

200. Bennell, K.L., et al., *Effect of Intra-articular Platelet-Rich Plasma vs Placebo Injection on Pain and Medial Tibial Cartilage Volume in Patients With Knee Osteoarthritis: The RESTORE Randomized Clinical Trial.* JAMA, 2021. **326**(20): p. 2021-2030.
201. Muthu, S., *Osteoarthritis, an old wine in a new bottle!* World J Orthop, 2023. **14**(1): p. 1-5.
202. Zeng, L., et al., *Efficacy and safety of culture-expanded mesenchymal stromal cell therapy in the treatment of 4 types of inflammatory arthritis: A systematic review and meta-analysis of 36 randomized controlled trials.* Semin Arthritis Rheum, 2024. **68**: p. 152498.
203. Vega, A., et al., *Treatment of Knee Osteoarthritis With Allogeneic Bone Marrow Mesenchymal Stem Cells: A Randomized Controlled Trial.* Transplantation, 2015. **99**(8): p. 1681-90.
204. Matas, J., et al., *Umbilical Cord-Derived Mesenchymal Stromal Cells (MSCs) for Knee Osteoarthritis: Repeated MSC Dosing Is Superior to a Single MSC Dose and to Hyaluronic Acid in a Controlled Randomized Phase I/II Trial.* Stem Cells Transl Med, 2019. **8**(3): p. 215-224.
205. Chahal, J., et al., *Bone Marrow Mesenchymal Stromal Cell Treatment in Patients with Osteoarthritis Results in Overall Improvement in Pain and Symptoms and Reduces Synovial Inflammation.* Stem Cells Transl Med, 2019. **8**(8): p. 746-757.
206. Boffa, A., et al., *Platelet-rich plasma injections induce disease-modifying effects in the treatment of osteoarthritis in animal models.* Knee Surg Sports Traumatol Arthrosc, 2021. **29**(12): p. 4100-4121.
207. Cole, B.J., et al., *Hyaluronic Acid Versus Platelet-Rich Plasma: A Prospective, Double-Blind Randomized Controlled Trial Comparing Clinical Outcomes and Effects on Intra-articular Biology for the Treatment of Knee Osteoarthritis.* Am J Sports Med, 2017. **45**(2): p. 339-346.
208. Huang, G., et al., *Platelet-rich plasma shows beneficial effects for patients with knee osteoarthritis by suppressing inflammatory factors.* Exp Ther Med, 2018. **15**(3): p. 3096-3102.
209. Haddad, F.S., *Unexpected benefits of arthroplasty.* Bone Joint J, 2022. **104-B**(3): p. 309-310.
210. Tonutti, A., et al., *The role of WNT and IL-1 signaling in osteoarthritis: therapeutic implications for platelet-rich plasma therapy.* Front Aging, 2023. **4**: p. 1201019.
211. Copp, G., K.P. Robb, and S. Viswanathan, *Culture-expanded mesenchymal stromal cell therapy: does it work in knee osteoarthritis? A pathway to clinical success.* Cell Mol Immunol, 2023. **20**(6): p. 626-650.
212. Kuyinu, E.L., et al., *Animal models of osteoarthritis: classification, update, and measurement of outcomes.* J Orthop Surg Res, 2016. **11**: p. 19.
213. Mianehsaz, E., et al., *Mesenchymal stem cell-derived exosomes: a new therapeutic approach to osteoarthritis?* Stem Cell Res Ther, 2019. **10**(1): p. 340.
214. Glyn-Jones, S., et al., *Osteoarthritis.* Lancet, 2015. **386**(9991): p. 376-87.
215. Maki, C.B., et al., *Intra-articular Administration of Allogeneic Adipose Derived MSCs Reduces Pain and Lameness in Dogs With Hip Osteoarthritis: A Double Blinded, Randomized, Placebo Controlled Pilot Study.* Front Vet Sci, 2020. **7**: p. 570.
216. Kim, Y.S., Y.I. Kim, and Y.G. Koh, *Intra-articular injection of human synovium-derived mesenchymal stem cells in beagles with surgery-induced osteoarthritis.* Knee, 2021. **28**: p. 159-168.
217. Lee, S.Y., et al., *The Therapeutic Effect of STAT3 Signaling-Suppressed MSC on Pain and Articular Cartilage Damage in a Rat Model of Monosodium Iodoacetate-Induced Osteoarthritis.* Front Immunol, 2018. **9**: p. 2881.
218. Yin, W.J., et al., *Advantages of Pure Platelet-Rich Plasma Compared with Leukocyte- and Platelet-Rich Plasma in Treating Rabbit Knee Osteoarthritis.* Med Sci Monit, 2016. **22**: p. 1280-90.
219. Muthu, S., et al., *Failure of cartilage regeneration: emerging hypotheses and related therapeutic strategies.* Nat Rev Rheumatol, 2023. **19**(7): p. 403-416.

220. Ho, K.K., et al., *Randomized control trial of mesenchymal stem cells versus hyaluronic acid in patients with knee osteoarthritis - A Hong Kong pilot study.* J Orthop Translat, 2022. **37**: p. 69-77.
221. Carneiro, D.C., et al., *Clinical Trials with Mesenchymal Stem Cell Therapies for Osteoarthritis: Challenges in the Regeneration of Articular Cartilage.* Int J Mol Sci, 2023. **24**(12).
222. Szwedowski, D., et al., *Intra-Articular Injection of Platelet-Rich Plasma Is More Effective than Hyaluronic Acid or Steroid Injection in the Treatment of Mild to Moderate Knee Osteoarthritis: A Prospective, Randomized, Triple-Parallel Clinical Trial.* Biomedicines, 2022. **10**(5).
223. McLarnon, M. and N. Heron, *Intra-articular platelet-rich plasma injections versus intra-articular corticosteroid injections for symptomatic management of knee osteoarthritis: systematic review and meta-analysis.* BMC Musculoskelet Disord, 2021. **22**(1): p. 550.
224. Tschopp, M., et al., *A Randomized Trial of Intra-articular Injection Therapy for Knee Osteoarthritis.* Invest Radiol, 2023. **58**(5): p. 355-362.
225. Barreto-Duran, E., et al., *Impact of donor characteristics on the quality of bone marrow as a source of mesenchymal stromal cells.* Am J Stem Cells, 2018. **7**(5): p. 114-120.
226. Perucca Orfei, C., et al., *Cell-based therapies have disease-modifying effects on osteoarthritis in animal models. A systematic review by the ESSKA Orthobiologic Initiative. Part 1: adipose tissue-derived cell-based injectable therapies.* Knee Surg Sports Traumatol Arthrosc, 2023. **31**(2): p. 641-655.
227. Boffa, A., et al., *Cell-based therapies have disease-modifying effects on osteoarthritis in animal models. A systematic review by the ESSKA Orthobiologic Initiative. Part 2: bone marrow-derived cell-based injectable therapies.* Knee Surg Sports Traumatol Arthrosc, 2023. **31**(8): p. 3230-3242.
228. Ding, Q.X., et al., *Comparative Analysis of Short-Term and Long-Term Clinical Efficacy of Mesenchymal Stem Cells from Different Sources in Knee Osteoarthritis: A Network Meta-Analysis.* Stem Cells Int, 2024. **2024**: p. 2741681.
229. Chahla, J., et al., *A Call for Standardization in Platelet-Rich Plasma Preparation Protocols and Composition Reporting: A Systematic Review of the Clinical Orthopaedic Literature.* J Bone Joint Surg Am, 2017. **99**(20): p. 1769-1779.
230. Kimura, H., Y. Sakai, and T. Fujii, *Organ/body-on-a-chip based on microfluidic technology for drug discovery.* Drug Metab Pharmacokinet, 2018. **33**(1): p. 43-48.
231. Petta, D., et al., *A personalized osteoarthritic joint-on-a-chip as a screening platform for biological treatments.* Mater Today Bio, 2024. **26**: p. 101072.
232. Sunildutt, N., et al., *Revolutionizing drug development: harnessing the potential of organ-on-chip technology for disease modeling and drug discovery.* Front Pharmacol, 2023. **14**: p. 1139229.
233. Carvalho, V., et al., *3D Printing Techniques and Their Applications to Organ-on-a-Chip Platforms: A Systematic Review.* Sensors (Basel), 2021. **21**(9).
234. Turmezei, T.D., et al., *Quantitative Three-dimensional Assessment of Knee Joint Space Width from Weight-bearing CT.* Radiology, 2021. **299**(3): p. 649-659.
235. Boffa, A., et al., *Synovial Fluid Biomarkers in Knee Osteoarthritis: A Systematic Review and Quantitative Evaluation Using BIPEDs Criteria.* Cartilage, 2021. **13**(1_suppl): p. 82S-103S.
236. Hasegawa, M., et al., *Changes in biochemical markers and prediction of effectiveness of intra-articular hyaluronan in patients with knee osteoarthritis.* Osteoarthritis Cartilage, 2008. **16**(4): p. 526-9.
237. Cudejko, T., et al., *Applications of Wearable Technology in a Real-Life Setting in People with Knee Osteoarthritis: A Systematic Scoping Review.* J Clin Med, 2021. **10**(23).
238. Belsi, A., E. Papi, and A.H. McGregor, *Impact of wearable technology on psychosocial factors of osteoarthritis management: a qualitative study.* BMJ Open, 2016. **6**(2): p. e010064.

239. Iovanel, G., D. Ayers, and H. Zheng, *The Role of Wearable Technology in Measuring and Supporting Patient Outcomes Following Total Joint Replacement: Review of the Literature*. JMIR Perioper Med, 2023. **6**: p. e39396.
240. Johnson, A.J., et al., *Managing osteoarthritis pain with smart technology: a narrative review.* Rheumatol Adv Pract, 2021. **5**(1): p. rkab021.
241. Grace, S., et al., *The step in time study: A feasibility study of a mobile app for measuring walking ability after massage treatment in patients with osteoarthritis.* BMC Complement Med Ther, 2023. **23**(1): p. 95.